

# Proteomics-based approaches for validation of antibodies against OTR and V1aR

---

**Kuridža, Bojan**

**Master's thesis / Diplomski rad**

**2023**

*Degree Grantor / Ustanova koja je dodijelila akademski / stručni stupanj:* **University of Zagreb, Faculty of Science / Sveučilište u Zagrebu, Prirodoslovno-matematički fakultet**

*Permanent link / Trajna poveznica:* <https://um.nsk.hr/um:nbn:hr:217:185973>

*Rights / Prava:* [In copyright](#)/[Zaštićeno autorskim pravom.](#)

*Download date / Datum preuzimanja:* **2025-02-10**



*Repository / Repozitorij:*

[Repository of the Faculty of Science - University of Zagreb](#)





University of Zagreb  
FACULTY OF SCIENCE  
Department of Chemistry

Bojan Kuridža

# **Proteomics-based approaches for validation of antibodies against OTR and V1aR**

**Diploma Thesis**

submitted to the Department of Chemistry,  
Faculty of Science, University of Zagreb  
for the academic degree of Master in Chemistry

Zagreb, 2023



This Diploma Thesis was performed at the Institute of Biological Chemistry, Faculty of Chemistry, University of Vienna under mentorship of Associate Professor Markus Muttenthaler and under the assistant mentorship of Dr. Predrag Kalaba. The supervisor appointed by the Department of Chemistry was Assistant Professor Marko Močibob.





## Acknowledgments

Firstly, I would like to express my gratitude to A/Prof. Markus Muttenthaler from the University of Vienna for the opportunity to join his research group and for his mentorship for this thesis. I extend my thanks to Asst. Prof. Marko Močibob from the University of Zagreb for agreeing to supervise my work and for trusting the process. I appreciate both professors' constant availability and prompt assistance, which proved especially helpful in handling the ever-present administrative challenges. Special thanks go to Dr. Predrag Kalaba from the University of Vienna, who graciously accepted the role of co-mentor and provided me with invaluable guidance throughout the course of this thesis, and who was always responsive to my concerns and quick in action to address them, despite having many of his own. Thank you for your constant support, and for going above and beyond for me to feel welcome and comfortable in the city of Vienna. I am very thankful for everything I got to learn from and with you. Furthermore, I want to thank Dr. Erik Keimpema from the Medical University of Vienna for generously allowing me to work in his laboratory and for all the clever suggestions provided regarding the experiments. Some more special thanks go to Maja (soon to be Dr.), who in addition to being an exceptional labmate proved to be an even better friend – thank you for everything ♥! I also want to thank the whole Muttenthaler group for creating a warm and welcoming environment and making this all a pleasant experience, especially to Monika and Mia, to whom I owe additional gratitude for their partial contribution to this thesis. And last but not least, I would like to thank Anna from the mass spectrometry centre for her endless patience in handling numerous samples, and for keeping me going with those much-needed cups of coffee as we delved deeper into the field of mass spectrometry.

Additionally, I want to thank all my friends and colleagues who have shared this journey with me over the past few years! Among them, special recognition goes to Matea, Ivan, Saranyarat, Monika, Igor, Tea, and Franjo, who have been with me from the very beginning. Thank you for all the help and support. I would also like to thank everyone else who has been a part of this journey even if only for a moment – some of you had a strong impact and I'm thankful for the pleasure of your company along the way. I am grateful for every single one of you whose paths crossed mine!

I would especially like to thank my family. Thank you all for your unconditional love, trust, and support. I appreciate your patience in putting up with my nonsense day after day, knowing it must not have been easy. ☺ Thank you for standing behind all of my crazy ideas without any reservations, and not standing in the way of my decisions that led me to where I stand today. Your sincere and profound support was a great source of motivation for me to become a better version of myself, it was truly special in its form, implicit but moving!

Also, I want to thank my dear friend Marija, who has been by my side since the very first day of my studies! Knowing that in addition to celebrating all the happy moments and small accomplishments together, I could count on you for support during major challenges, gave me a sense of safety and confidence that is hard to put into words. Thank you, we really grew together!

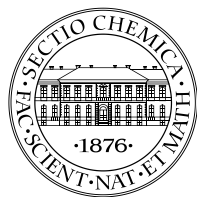
Finally, I would like to use this opportunity to express my gratitude to a special friend, T♥, who I know would have been more than happy to celebrate this occasion with me and hype me up the way no one else ever could.



# Table of Contents

<b>ABSTRACT .....</b>	<b>IX</b>
<b>SAŽETAK.....</b>	<b>XI</b>
<b>PROŠIRENI SAŽETAK.....</b>	<b>XIII</b>
<b>§ 1. INTRODUCTION .....</b>	<b>1</b>
<b>§ 2. LITERATURE REVIEW .....</b>	<b>3</b>
<b>2.1. G protein-coupled receptors.....</b>	<b>3</b>
2.1.1. <i>The overall structure, signaling, and potential of G protein-coupled receptors in drug development.....</i>	<i>3</i>
2.1.2. <i>Oxytocin receptor and vasopressin 1a receptor.....</i>	<i>6</i>
<b>2.2. Oxytocin and vasopressin .....</b>	<b>10</b>
2.2.1. <i>Oxytocin and vasopressin – two structurally similar neuropeptides with significant tasks .....</i>	<i>10</i>
2.2.2. <i>Oxytocin and vasopressin analogs as medications .....</i>	<i>12</i>
<b>2.3. Methods used for validation of antibodies .....</b>	<b>14</b>
2.3.1. <i>Western blot.....</i>	<i>16</i>
2.3.1.1. <i>Membrane protein isolation.....</i>	<i>16</i>
2.3.1.2. <i>Protein quantification methods.....</i>	<i>17</i>
2.3.1.3. <i>Sodium dodecyl sulfate polyacrylamide gel electrophoresis .....</i>	<i>19</i>
2.3.1.4. <i>Protein transfer methods.....</i>	<i>20</i>
2.3.1.5. <i>Washing, blocking, and primary/secondary antibody incubation.....</i>	<i>21</i>
2.3.1.6. <i>Membrane visualization.....</i>	<i>22</i>
2.3.2. <i>Immunoprecipitation coupled with mass spectrometry.....</i>	<i>23</i>
<b>§ 3. EXPERIMENTAL SECTION.....</b>	<b>27</b>
<b>3.1. Materials.....</b>	<b>27</b>
3.1.1. <i>Validated antibodies.....</i>	<i>27</i>
3.1.2. <i>Protein isolation and quantification.....</i>	<i>28</i>
3.1.3. <i>Western blot and protein staining .....</i>	<i>28</i>
3.1.4. <i>Immunoprecipitation .....</i>	<i>29</i>
3.1.5. <i>Instruments .....</i>	<i>29</i>
3.1.6. <i>Software.....</i>	<i>30</i>
<b>3.2. Methods .....</b>	<b>30</b>
3.2.1. <i>Western blot and protein staining .....</i>	<i>30</i>
3.2.1.1. <i>Membrane protein isolation.....</i>	<i>30</i>

3.2.1.2. Protein quantification .....	32
3.2.1.3. Sodium dodecyl sulfate polyacrylamide gel electrophoresis .....	33
3.2.1.4. Transfer and detection .....	37
3.2.2. Immunoprecipitation .....	41
3.2.3. Mass spectrometry.....	44
3.2.3.1. Nano liquid chromatography tandem mass spectrometry Velos method - digested protein.....	44
3.2.3.2. Nano liquid chromatography tandem mass spectrometry Velos method - intact protein.....	45
<b>§ 4. RESULTS .....</b>	<b>47</b>
<b>4.1. Western blot.....</b>	<b>47</b>
4.1.1. Antibodies against vassopresin 1a receptor.....	50
4.1.2. Antibodies against oxytocin receptor.....	58
<b>4.2. Immunoprecipitation .....</b>	<b>64</b>
4.2.1. Antibodies against vassopresin 1a receptor.....	65
4.2.2. Antibodies against oxytocin receptor.....	70
<b>§ 5. DISCUSSION AND CONCLUSION .....</b>	<b>77</b>
<b>5.1. Antibody validation results.....</b>	<b>78</b>
5.1.1. Western blot in validation of antibodies.....	78
5.1.2. Immunoprecipitation coupled with mass spectrometry in antibody validation .....	82
<b>5.2. Limitations and future directions .....</b>	<b>84</b>
<b>5.3. Conclusion.....</b>	<b>85</b>
<b>§ 6. LIST OF ABBREVIATIONS AND SYMBOLS .....</b>	<b>87</b>
<b>§ 7. REFERENCES.....</b>	<b>90</b>
<b>§ 8. APPENDIX.....</b>	<b>XV</b>
<b>§ 9. CURRICULUM VITAE.....</b>	<b>XXVII</b>



University of Zagreb  
Faculty of Science  
**Department of Chemistry**

Diploma Thesis

## ABSTRACT

### PROTEOMICS-BASED APPROACHES FOR VALIDATION OF ANTIBODIES AGAINST OTR AND V1aR

Bojan Kuridža

The oxytocin receptor (OTR) and the vasopressin 1a receptor (V1aR) are two G protein-coupled receptors involved in mediating various physiological processes and social and sexual behaviors. Producing specific antibodies to study these receptors is challenging due to their sequence homology and structure similarity, along with two additional closely related vasopressin receptors. Thus, this thesis aimed to validate ten antibodies to OTR and seven antibodies to V1aR produced against distinctive receptor peptide epitopes, using western blot and immunoprecipitation followed by mass spectrometry. The validation process pointed towards one V1aR antibody (1G1), which showed promising results in both western blot and immunoprecipitation experiments, and needs to be further tested. The best OTR antibody identified in immunoprecipitation experiments (1B2) did not perform well in western blots.

(136 pages, 38 + 20 figures, 13 tables, 219 references, original in English)

Thesis deposited in Central Chemical Library, Faculty of Science, University of Zagreb, Horvatovac 102a, Zagreb, Croatia and in Repository of the Faculty of Science, University of Zagreb

Keywords: antibody validation, G protein-coupled receptor, immunoprecipitation, mass spectrometry, oxytocin receptor, vasopressin 1a receptor, western blot

Mentor: Assoc. Prof. Markus Muttenthaler

Assistant mentor: Dr. Predrag Kalaba

Supervisor (appointed by the Department of Chemistry): Asst. Prof. Marko Močibob

Reviewers:

1. Asst. Prof. Marko Močibob
  2. Assoc. Prof. Ivan Kodrin
  3. Prof. Iva Juranović Cindrić
- Substitute: Assoc. Prof. Đani Škalamera

Date of exam: June 6<sup>th</sup>, 2023





Sveučilište u Zagrebu  
Prirodoslovno-matematički fakultet  
**Kemijski odsjek**

Diplomski rad

## SAŽETAK

### VALIDACIJA ANTITIJELA ZA OTR I V1aR PRISTUPIMA TEMELJENIMA NA PROTEOMICI

Bojan Kuridža

Oksitocinski receptor (OTR) i vazopresinski 1a receptor (V1aR) dva su receptora spregnuta sa G-proteinom uključena u posredovanje raznih fizioloških procesa te društvenog i seksualnog ponašanja. Proizvodnja specifičnih antitijela za proučavanje ovih receptora predstavlja izazov zbog sličnosti njihovog slijeda i strukture, kao i sličnosti dva dodatna blisko povezana vazopresinska receptora. Stoga, cilj je ovog rada bio validirati deset antitijela za OTR i sedam antitijela za V1aR proizvedenih prema karakterističnim peptidnim epitopima receptora, koristeći western blot i imunoprecipitaciju povezanu s masenom spektrometrijom. Jedno antitijelo za V1aR (1G1) u procesu validacije pokazalo je obećavajuće rezultate u eksperimentima western blota i imunoprecipitacije. Najbolje od OTR antitijela identificiranih u eksperimentima imunoprecipitacije (1B2) nije se pokazalo uspješnim u western blotovima.

(136 stranica, 38 + 20 slika, 13 tablica, 219 literaturnih navoda, jezik izvornika: engleski)

Rad je pohranjen u Središnjoj kemijskoj knjižnici Prirodoslovno-matematičkog fakulteta Sveučilišta u Zagrebu, Horvatovac 102a, Zagreb i Repozitoriju Prirodoslovno-matematičkog fakulteta Sveučilišta u Zagrebu

Ključne riječi: imunoprecipitacija, masena spektrometrija, oksitocinski receptor, receptor spregnut sa G-proteinom, validacija antitijela, vazopresinski 1a receptor, western blot

Mentor: izv. prof. dr. Markus Muttenthaler

Neposredni voditelj: dr. Predrag Kalaba

Nastavnik (imenovan od strane Kemijskog odsjeka): doc. dr. sc. Marko Močibob

Ocjenitelji:

1. doc. dr. sc. Marko Močibob

2. izv. prof. dr. sc. Ivan Kodrin

3. prof. dr. sc. Iva Juranović Cindrić

Zamjena: izv. prof. dr. sc. Đani Škalamera

Datum diplomskog ispita: 6. lipnja 2023.





## PROŠIRENI SAŽETAK

Oksitocin (OT) i vazopresin (VP) dva su strukturno veoma bliska ciklička neuropeptida od devet aminokiselina, koji igraju važnu ulogu u mnogim fiziološkim procesima, kao i u regulaciji društvenog i seksualnog ponašanja mnogih vrsta, pa i čovjeka.<sup>I</sup> Spomenuti neuropeptidi djeluju preko četiri, također strukturno slična receptora, koji pripadaju skupini receptora spregnutih sa G-proteinom (GPCR, engl. *G protein-coupled receptor*): OTR (oksitocinski receptor), V1aR (vazopresinski 1a receptor), V1bR (vazopresinski 1b receptor) i V2R (vazopresinski 2 receptor).<sup>II</sup> V1aR djeluje u središnjem živčanom sustavu (CNS, engl. *central nervous system*) i utječe na ponašanja poput agresije ili izbora partnera, ali i na kognitivne funkcije poput memorije. V1aR na periferiji djeluje uglavnom kao vazokonstriktor sistemskih krvnih žila.<sup>III</sup> OTR u CNS-u djeluje na socijalne odnose poput emocionalnog povezivanja ili vezanja majke za dijete. Na periferiji, OTR, igra veoma važnu ulogu u inicijaciji i kontroli kontrakcija tijekom poroda, kao i u sekreciji mlijeka.<sup>IV,V</sup> S obzirom da su izraženi i na periferiji i u CNS-u, gdje igraju važnu ulogu u regulaciji socijalnih ponašanja, OTR i V1aR su dva receptora interesantna za proizvodnju antitijela. Osnovni pristup istraživanju ovog tipa receptora temelji se na upotrebi specifičnih antitijela.<sup>VI</sup> Zbog homologije i velike sličnosti slijeda među spomenuta četiri receptora, proizvodnja specifičnih i za njih selektivnih antitijela nije lak zadatak te takvih antitijela nedostaje. Posljedično, napredak u istraživanju OTR i V1aR je ograničen. Bez antitijela, preciznu lokalizaciju i rasprostranjenost ovih receptora teško je odrediti.<sup>VII</sup>

---

<sup>I</sup> Z. R. Donaldson and L. J. Young, Oxytocin, vasopressin, and the neurogenetics of sociality, *Science* **322** (2008) 900–904.

<sup>II</sup> D. A. Baribeau and E. Anagnostou, Oxytocin and vasopressin: Linking pituitary neuropeptides and their receptors to social neurocircuits, *Front. Neurosci.* **9**, 335 (2015) 1–21.

<sup>III</sup> S. Jard, R. C. Gaillard, G. Guillon, J. Marie, P. Schoenberg, A. F. Muller, M. Manning and W. H. Sawyer, Vasopressin antagonists allow demonstration of a novel type of vasopressin receptor in the rat adenohypophysis, *Mol. Pharmacol.* **30** (1986) 171–177.

<sup>IV</sup> A. Argiolas and G. L. Gessa, Central functions of oxytocin, *Neurosci. Biobehav. Rev.* **15** (1991) 217–231.

<sup>V</sup> H. H. Zingg, Vasopressin and oxytocin receptors, *Baillieres Clin. Endocrinol. Metab.* **10** (1996) 75–96.

<sup>VI</sup> A. Gupta, A. S. Heimann, I. Gomes and L. A. Devi, Antibodies against G-protein coupled receptors: novel uses in screening and drug development, *Comb. Chem. High Throughput Screen.* **11** (2008) 463–467.

<sup>VII</sup> M. Yoshida, Y. Takayanagi, K. Inoue, T. Kimura, L. J. Young, T. Onaka and K. Nishimori, Evidence that oxytocin exerts anxiolytic effects via oxytocin receptor expressed in serotonergic neurons in mice, *J. Neurosci.* **29** (2009) 2259–2271.

Istraživanje veze između strukture receptora i njihove funkcije je također otežano, što dovodi do slabog razumijevanja njihove uloge u fiziološkim procesima i bolestima.<sup>VIII,IX</sup>

Zbog navedenih razloga, postoji veliko zanimanje za razvojem novih monoklonskih antitijela koja bi se mogla koristiti u istraživanju ovih receptora. Shodno tome, cilj je ovog rada bio približiti se validaciji antitijela za OTR i V1aR, slijedeći pritom predložene putove za validaciju antitijela,<sup>X</sup> koristeći pristupe temeljene na proteomici: western blot (WB) te imunoprecipitaciju povezanu s masenom spektrometrijom (IP-MS).

Za validaciju je odabrano deset antitijela za OTR (1A3, 1B2, 1C10, 1E4, 1F1, 1H11, 4E3, 4F3-4, 4F3-5, 5A5) te sedam antitijela za V1aR (1G1, 1H1, 3C1, 3D2, 3F8, 4A7, 4G9). To su zečja monoklonska antitijela u mediju kulture stanica HEK293 proizvedena prema peptidnim fragmentima odgovarajućih receptora karakterističnima za svaki od njih, a koji odgovaraju regijama C- i N- kraja, druge i treće unutarstanične petlje te treće transstanične petlje, tj. regijama s najvećim razlikama među strukturama ovih blisko povezanih receptora.<sup>XI</sup> Navedena antitijela odgovaraju onima koji su na temelju rezultata enzimskog imunotesta na čvrstoj fazi (ELISA, engl. *enzyme-linked immunosorbent assay*) pokazali najbolje rezultate glede reaktivnosti prema odgovarajućim peptidima. Antitijela je proizvela i dostavila tvrtka Origene s partnerima Nacionalnih instituta za zdravlje (NIH, engl. *National Institutes of Health*).

Generalno, antitijela prepoznaju konformacijsku determinantu antigena, linearnu determinantu antigena ili neoantigensku determinantu. Konformacijska determinanta predstavlja značajku trodimenzionalne strukture proteina, tj. oblik proteina koji antitijelo specifično veže. Linearna determinanta definirana je nizom od do otprilike šest susjednih aminokiselina u točno određenoj kombinaciji. Ove determinante mogu se, kao posljedica različitih uvjeta denaturacije proteina, otkriti ili sakriti, a u slučaju linearne determinante može biti dostupna antitijelu i prije i nakon denaturacije. Neoantigeni obično nisu dio antigena, ali su posljedica mutacija, modifikacija i drugih promjena antigena koje rezultiraju prepoznavanjem

---

<sup>VIII</sup> C. J. W. Smith, B. T. DiBenedictis and A. H. Veenema, Comparing vasopressin and oxytocin fiber and receptor density patterns in the social behavior neural network: Implications for cross-system signaling, *Front. Neuroendocrinol.* **53**, 100737 (2019) 1–43.

<sup>IX</sup> M. Meyer, B. Jurek, M. Alfonso-Prieto, R. Ribeiro, V. M. Milenkovic, J. Winter, P. Hoffmann, C. H. Wetzel, A. Giorgetti, P. Carloni and I. D. Neumann, Structure-function relationships of the disease-linked A218T oxytocin receptor variant, *Mol. Psychiatry* **27** (2022) 907–917.

<sup>X</sup> T. Stojanovic, M. Orlova, F. J. Sialana, H. Höger, S. Stuchlik, I. Milenkovic, J. Aradska and G. Lubec, Validation of dopamine receptor DRD1 and DRD2 antibodies using receptor deficient mice, *Amino Acids* **49** (2017) 1101–1109.

<sup>XI</sup> M. Mitre, B. J. Marlin, J. K. Schiavo, E. Morina, S. E. Norden, T. A. Hackett, C. J. Aoki, M. V. Chao and R. C. Froemke, A Distributed Network for Social Cognition Enriched for Oxytocin Receptors, *J. Neurosci.* **36** (2016) 2517–2535.

od strane antitijela.<sup>XII</sup> I linearne i konformacijske determinantne odgovarajućih receptora testirane su metodama WB i IP-MS, koje s obzirom na denaturirajuće/nativne uvjete u kojima su provedene predstavljaju ortogonalne metode koje koriste antitijela.<sup>XIII</sup>

Kao izvor proteina korištenih u eksperimentima poslužile su embrionalne stanice bubrega čovjeka 293 (HEK293, engl. *human embryonic kidney 293*) koje stabilno prekomjerno eksprimiraju OTR-GFP, V1aR-GFP, V1bR-GFP ili V2R-GFP, receptore označene zelenim fluorescentnim proteinom (GFP, engl. *green fluorescent protein*) na C-kraju. Uz četiri navedene, također je korištena i normalna stanična linija HEK293 kao jedan vid kontrole. Stanice su lizirane ultrazvučnom sondom u puferu za homogeniziranje. Ukupna frakcija membranskih proteina nakon lize izolirana je slijedom centrifugiranja, a membranski proteini potom su solubilizirani puferom za solubiliziranje. Taj pufer sadržava neionski deterdžent Triton X-100 kako bi se spriječila denaturacija receptora, što je od iznimnog značaja za eksperimente provedene u nedenaturirajućim uvjetima gdje je važno očuvati nativnu strukturu proteina.<sup>XIV</sup> Za određivanje koncentracije tako dobivene otopine membranskih proteina korištena je metoda bicinhoninske kiseline (BCA, engl. *bicinchoninic acid*), koja omogućuje određivanje koncentracije na mikropločicama s 96 jažica. Detektirana je apsorbancija nastalog kompleksa pri 562 nm i iz linearne regresije apsorbancija standardnih otopina albumina goveđeg seruma (BSA, engl. *bovine serum albumin*) određena je koncentracija proteina.<sup>XV</sup>

## I. WESTERN BLOT

Prilikom izvedbe WB-a korištena je elektroforeza na poliakrilamidnom gelu (PAGE, engl. *polyacrylamide gel electrophoresis*) u denaturirajućim uvjetima, koja je zbog u puferu prisutnog jakog anionskog deterdženta natrijeva dodecilsulfata (SDS, engl. *sodium dodecyl sulfate*) poznatija pod kraticom SDS-PAGE. Dodatnoj denaturaciji proteina doprinose reducirajuće sredstvo  $\beta$ -merkaptetanol te grijanje uzoraka prilikom pripreve.<sup>XVI</sup> Za prijenos

---

<sup>XII</sup> A. K. Abbas, A. H. Lichtman and S. Pillai, *Cellular & Molecular Immunology, 7th Edition*, Saunders, Philadelphia, 2011, pp. 101–103.

<sup>XIII</sup> T. MacNeil, I. A. Vathiotis, S. Martinez-Morilla, V. Yaghoobi, J. Zugazagoitia, Y. Liu and D. L. Rimm, Antibody validation for protein expression on tissue slides: a protocol for immunohistochemistry, *Biotechniques* **69** (2020) 461–468.

<sup>XIV</sup> J. Lebowitz, M. S. Lewis and P. Schuck, Modern analytical ultracentrifugation in protein science: A tutorial review, *Protein Sci.* **11** (2002) 2067–2079.

<sup>XV</sup> J. P. D. Goldring, Protein quantification methods to determine protein concentration prior to electrophoresis, *Methods Mol. Biol.* **869** (2012) 29–35.

<sup>XVI</sup> K. Martínez-Flores, Á. T. Salazar-Anzures, J. Fernández-Torres, C. Pineda, C. A. Aguilar-González and A. López-Reyes, Western blot: a tool in the biomedical field, *Investigación discapac.* **6** (2017) 128–137.

proteina s gela na membranu korišten je polusuhi prijenos (engl. *semi-dry transfer*), a korištena membrana je poliviniliden difluorid (PVDF, engl. *polyvinylidene difluoride*). Membrane su po prijenosu proteina blokirane 5 %-tnom otopinom nemasnog suhog mlijeka (NFDM, engl. *non-fat dried milk*), a potom inkubirane u otopinama antitijela za validiranje. Sekundarna antitijela konjugirana su enzimom peroksidazom hrena (HRP, engl. *horseradish peroxidase*), koja omogućuje detekciju kemiluminiscencijom. Signali su detektirani digitalno, sustavom za snimanje ChemiDoc koji sadrži uređaj sa spregnutim nabojem (CCD, engl. *charge-coupled device*).

Izvedena su dva tipa blotova. Prvi tip gdje je svaki blot sadržavao tri različite mase (10, 20 ili 30  $\mu\text{g}$ ) istog proteina OTR-GFP ili V1aR-GFP, a provjeravala se veza između jačine signala odgovarajućeg antitijela i količine proteina. U drugom tipu svaki je blot sadržavao istu količinu (20  $\mu\text{g}$ ) svakog od četiri receptora i frakcije normalne stanične linije, a provjeravala se specifičnost svakog od validiranih antitijela prema odgovarajućem receptoru u odnosu na ostale.

Od kontrola, izvedena je kontrola korištenog sekundarnog antitijela za oba uzorka OTR-GFP i V1aR-GFP. Također, s obzirom da su svi prekomjerno ekspirirani proteini rekombinantni s GFP oznakom, izveden je blot u kojem je korišteno fluorescentno označeno primarno antitijelo za GFP, gdje su od uzoraka bili nanijeti OTR-GFP, V1aR-GFP i V1bR-GFP. Dodatno, provjerena je specifičnost dva komercijalno dostupna antitijela, jednog za OTR i drugog za V1aR, u odnosu na ostale receptore.

Sve membrane po detekciji obojene su AmidoBlack bojom za proteine kako bi se potvrdila uspješna separacija proteina prilikom elektroforeze te uspješan prijenos proteina na membranu.

### I.I. WB rezultati

Blotovi koji su koristili fluorescentno obilježeno primarno antitijelo za GFP dali su po dvije vrpce u stupcima OTR-GFP i V1aR-GFP. Jedna od vrpce prisutna je na području ulaska u gel, a druga pri oko  $102 \times 10^3$ . Takav rezultat dao bi naslutiti prisutnost agregata, kao i sugerirati specifično prepoznavanje GFP-a od strane antitijela te poziciju receptora u gelu nakon elektroforeze.<sup>XVII</sup>

---

<sup>XVII</sup> E. Selcuk Unal, R. Zhao, A. Qiu and I. D. Goldman, N-linked glycosylation and its impact on the electrophoretic mobility and function of the human proton-coupled folate transporter (HsPCFT), *Biochim. Biophys. Acta Biomembr.* **1778** (2008) 1407–1414.

Komercijalno dostupna antitijela za OTR i V1aR u našim WB eksperimentima nisu se pokazala specifičnima. Ovakav rezultat dovodi u pitanje ispravnost rezultata istraživanja provedenih koristeći ova antitijela.

Od validiranih antitijela za V1aR, samo je antitijelo 1G1 pokazalo specifičnost prema V1aR-GFP u odnosu na ostale receptore. Ovo antitijelo dalo je snažan signal u području membrane koje odgovara ulasku proteina u gel, što je u skladu s pozicijom receptora očekivanom nakon korištenja antitijela za GFP. Ostalih šest antitijela dalo je slabe ili nespecifične signale.

Među OTR antitijelima, snažne, ali nespecifične signale dala su antitijela 5A5, 4E3 i 1H11. Dodatno, vrpce su bile pri različitim molekulskim masama za sva tri antitijela. Ostalih 7 antitijela također je dalo slabe ili nespecifične signale.

Često se u blotovima ponavljala vrpca pri oko  $115 \times 10^3$  za koju je pretpostavljeno da je predstavljala poziciju receptora. Kontrolom je provjereno radi li se možda o nespecifičnom vezanju sekundarnog antitijela. I uistinu, uočeno je pojavljivanje te vrpce nakon otprilike 100 sekundi izloženosti za uzorke V1aR-GFP, što je za mnoga testirana V1aR antitijela odbacilo mogućnost ciljanog prepoznavanja antigena. Za pojavljivanje te vrpce kod kontrole OTR-GFP uzoraka bilo je potrebno više vremena.

Pokazana je pozitivna ovisnost jačine signala o količini nanijetog proteina, a bojenje proteina bojom Amido Black potvrdilo je uspješnost prijenosa proteina na membranu.

## II. IMUNOPRECIPITACIJA

U imunoprecipitaciji su korištene magnetne kuglice obložene proteinom A, koji prepoznaje Fc regiju zečjih antitijela.<sup>XVIII</sup> Kuglice su prvo inkubirane u otopinama validiranih antitijela, a tek potom u otopinama membranskih receptora. Takav redoslijed omogućava bolju kontrolu količine korištenog antitijela, kao i mogućih negativnih utjecaja medija antitijela na receptore od interesa.<sup>XIX</sup> Receptori su prepoznati u svojim nativnim strukturama, a precipitirani kompleksi potom su isprani glicinskim puferom niskog pH. Proteini su istaloženi hladnom otopinom acetona, odvojeni od supernatanta te solubilizirani u puferu ureje. Tako solubilizirani,

---

<sup>XVIII</sup> Affinity of Protein A/G for IgG Types from Different Species | NEB, <https://international.neb.com/tools-and-resources/selection-charts/affinity-of-protein-ag-for-igg-types-from-different-species> (Date accessed: 08/03/2023)

<sup>XIX</sup> J. S. Bonifacio, D. C. Gershlick and E. C. Dell'Angelica, Immunoprecipitation, *Curr. Protoc. Cell Biol.* **71** (2016) 7.2.1-7.2.24.

izloženi su alkiliranju tiolnih skupina jodoacetamidom (IAA, engl. *iodoacetamide*) te pročišćeni na filtrima (engl. *filter units*), gdje su podvrgnuti razgradnji tripsinom. Nastali peptidi su u konačnici analizirani tandemnom masenom spektrometrijom.

Svako od validiranih antitijela inkubirano je u otopini odgovarajućeg receptora. Nakon elucije kompleksa, uzet je alikvot eluata za masenu analizu intaktnih receptora prije razgradnje. Od kontrola, provedene su tri: 1. kontrola nespecifičnim imunoglobulinom G (IgG, engl. *immunoglobulin G*), gdje su umjesto u validiranom antitijelu kuglice inkubirane u otopini normalnog zečjeg IgG; 2. kontrola kuglica, gdje su umjesto u validiranom antitijelu kuglice inkubirane u puferu za solubiliziranje; 3. kontrola receptora, gdje su otopine solubiliziranih receptora bez pročišćavanja magnetnim kuglicama, pri čemu je ostatak protokola proveden normalno, podvrgnute razgradnji tripsinom. Sve kontrole provedene su za oba receptora OTR-GFP i V1aR-GFP.

## II.I. Rezultati imunoprecipitacije

Analiza intaktnih receptora davala je dva signala oko  $73 \times 10^3$  za koje je pretpostavljeno da predstavljaju mali ili veliki lanac antitijela. Također, pokazao se izraženi signal korištenog deterdženta CHAPS-a, što je motiviralo njegovo smanjivanje i u konačnici potpuno uklanjanje u koracima koji su slijedili kako bi se osigurala neometana detekcija peptida nakon razgradnje.

Od sedam V1aR antitijela, najuspješnijim se ponovno pokazalo 1G1, rezultirajući detekcijom čak šest peptida jedinstvenih za V1aR, što odgovara pokrivenosti sekvence od 12 %. Dodatno, 1G1 antitijelo rezultiralo je detekcijom pet peptida koji potječu od GFP. Antitijelo 3D2 dalo je tri jedinstvena peptida koja odgovaraju 7,9 % pokrivenosti sekvence, dok je 1H1 antitijelo rezultiralo samo jednim prepoznatim peptidom sa 6,7 % pokrivenosti sekvence. Ostala četiri antitijela nisu dovela do identifikacije nijednog jedinstvenog peptida za V1aR ili GFP, što daje sugerirati da ne prepoznaju antigene V1aR.

Tri od deset testiranih antitijela za OTR dala su pozitivan rezultat. Antitijelo 1B2, unatoč WB rezultatima koji nisu dali nikakvu informaciju od većeg značaja, najuspješnije je od svih OTR antitijela sa dva prepoznata jedinstvena peptida. Jedan od tih peptida odgovara cijeloj drugoj transmembranskoj uzvojnici, a pokrivenost sekvence ovog antitijela iznosi 14,4 %. Drugo po uspješnosti bilo je antitijelo 5A5 s također dva identificirana jedinstvena peptida i pokrivenosti sekvence od 12,1 %. Antitijelo 4E3 dalo je jedan jedinstveni peptid koji odgovara 5,1 % pokrivenosti sekvence.

Kontrole nespecifičnim imunoglobulinom i kuglicama pokazale su da nema nespecifičnog vezanja V1aR-GFP ili OTR-GFP, odnosno da detektirani peptidi stvarno potječu od usmjerenog prepoznavanja i vezanja receptora odgovarajućim antitijelima. Kontrola receptora za OTR-GFP bila je uspješna i rezultirala je detekcijom jedinstvenih peptida, dok je za V1aR-GFP detekcija izostala.

Ukupno gledano, antitijelo 1G1 za V1aR pokazalo se najuspješnijim od svih testiranih antitijela, i u eksperimentu WB-a i u imunoprecipitaciji, te ima najviše potencijala za daljnja istraživanja. Među OTR antitijelima, najuspješnijim se pokazalo antitijelo 1B2, iako bez značajnijih rezultata WB-a.

Generalno, ovaj rad pružio je vrijedne uvide u efikasnost ovih antitijela prema V1aR i OTR. Međutim, više istraživanja je potrebno provesti kako bi se akumulirao širi spektar korisnih informacija iz kojih bi se sa većom sigurnošću mogao izvesti neki konkretniji zaključak o specifičnosti i selektivnosti testiranih antitijela. Za antitijelo 1G1 koje je pokazalo najveći potencijal valjalo bi provesti WB-ove s izmijenjenim uvjetima kako bi se pokušali izbjeći problemi s agregatima prilikom elektroforeze, kao npr. optimizacijom SDS-a, smanjenjem temperature grijanja, ili korištenjem manje količine proteina. Ili u cilju postizanja boljih rezultata, korištenjem gelova niže gustoće ili otopina antitijela nižih koncentracija. Za detaljnije istraživanje svih antitijela, valjalo bi provjeriti unakrsnu reaktivnost antitijela u eksperimentima imunoprecipitacije prema tri nepripadajuća receptora, svaki zasebno. Također, eksperimente imunoprecipitacije u kojima bi u istoj smjesi bila sva četiri receptora, gdje bi se provjeravala selektivnost antitijela. Budući da su u eksperimentima ovoga rada korišteni rekombinantni receptori označeni GFP-om na C-kraju, potrebno je generirati stanične linije koje bi stabilno ekspimirale nefuzionirane receptore, koji bi vjerodostojnije predstavljali one nativne i koji bi se koristili za provedbu daljnjih eksperimenata.





## § 1. INTRODUCTION

The hypothalamic neuropeptides oxytocin (OT) and vasopressin (VP) are well-studied hormones that play a significant role in many physiological processes. Within the central nervous system (CNS) they are involved in the regulation of social and sexual behavior, such as emotional or maternal bonding, partner selection, territoriality, memory and learning, stress responses, and many more.<sup>1,2</sup> In the periphery, VP regulates renal water absorption and blood pressure, while OT causes uterine contractions and milk secretion.<sup>3,4</sup> OT and VP exert their effects by binding to their respective receptors, the oxytocin receptor (OTR), and the vasopressin 1a receptor (V1aR), both of which are expressed in both the CNS and in the periphery.<sup>5,6</sup> Two more structurally similar receptors exist: vasopressin 1b receptor (V1bR) expressed primarily in the brain, and vasopressin 2 receptor (V2R) expressed only in the periphery.<sup>7</sup>

Antibodies are an essential tool for studying these receptors and their expression at the protein level and are used in a variety of techniques and methods, such as immunofluorescence, immunocytochemistry or immunohistochemistry.<sup>8,9</sup> However, the development of specific antibodies for the OTR and V1aR has been a challenge for scientists, as these receptors, belong to the same class of G protein-coupled receptors (GPCRs)<sup>10</sup> and possess high similarity in their structure.<sup>11</sup> The first extracellular loop and transmembrane helices are the most conserved domains, with the four receptors having a total similarity of 36 to 46% and a transmembrane region-only similarity of 42 to 57%.<sup>12,13</sup> Interestingly, due to their similarity, OTR can also accommodate VP molecule, enabling its binding and making VP promiscuous in that sense.<sup>14</sup> A lack of reliable, specific, and sensitive antibodies for OTR and V1aR stands in the way of progress in this research area.<sup>15</sup> Without antibodies, the precise localization and distribution of these receptors within tissues is difficult to determine.<sup>16</sup> Investigation of the relationship between receptor structures and their function is also hindered, which in turn results in a poor understanding of their role in physiological processes and diseases.<sup>17</sup>

For the reasons mentioned, there is a huge interest in the development of novel monoclonal antibodies that secure lower cross reactivity and are more sensitive than polyclonal antibodies,<sup>18</sup> and which could be used in and facilitate the research of these receptors. The objective of this thesis was to get a step closer to the validation of monoclonal antibodies against OTR and

V1aR, in accordance with established/proposed pathways for antibody validation.<sup>19-21</sup> Ten antibodies against OTR and seven antibodies against V1aR were obtained from partners from National Institutes of Health, USA for validation. Antibodies were anticipated to interact with their respective receptors while displaying specificity, as they were produced against specific and distinctive receptor peptide fragments and selected based on their strength of immune response as determined by ELISA assay. In the validation process, western blot (WB) and immunoprecipitation followed by mass spectrometry (IP-MS) were employed.

## § 2. LITERATURE REVIEW

### 2.1. G protein-coupled receptors

#### 2.1.1. *The overall structure, signaling, and potential of G protein-coupled receptors in drug development*

G protein-coupled receptors (GPCRs) are the largest protein family encoded by the eukaryotic genome.<sup>22</sup> In humans, this family of signaling integral protein receptors includes around 800 different identified GPCRs, which represent around 2% of the human genome.<sup>23,24</sup> A protein should meet two major conditions to be categorized as a GPCR. The first condition is for seven segments of around 25 to 35 successive amino acid residues to have a fairly high predicted hydrophobicity.<sup>25,26</sup> These segments are thought to be seven  $\alpha$ -helices that cross the plasma membrane, establishing a receptor or a recognition unit that allows an external ligand to have a particular impact on the cell.<sup>27</sup> The receptor being able to interact with a G protein is the second most important condition.<sup>25</sup> Since the seven hydrophobic transmembrane stretches constitute a distinguishing structural property of these receptors, and also because signal transduction *via* G proteins is not always observed, these proteins are also known as seven-transmembrane (7TM), heptahelical or serpentine receptors, which may be more technically appropriate, however, GPCR term is more often used.<sup>28–30</sup> Illustration of 7TM GPCR structure is shown in Figure 1.

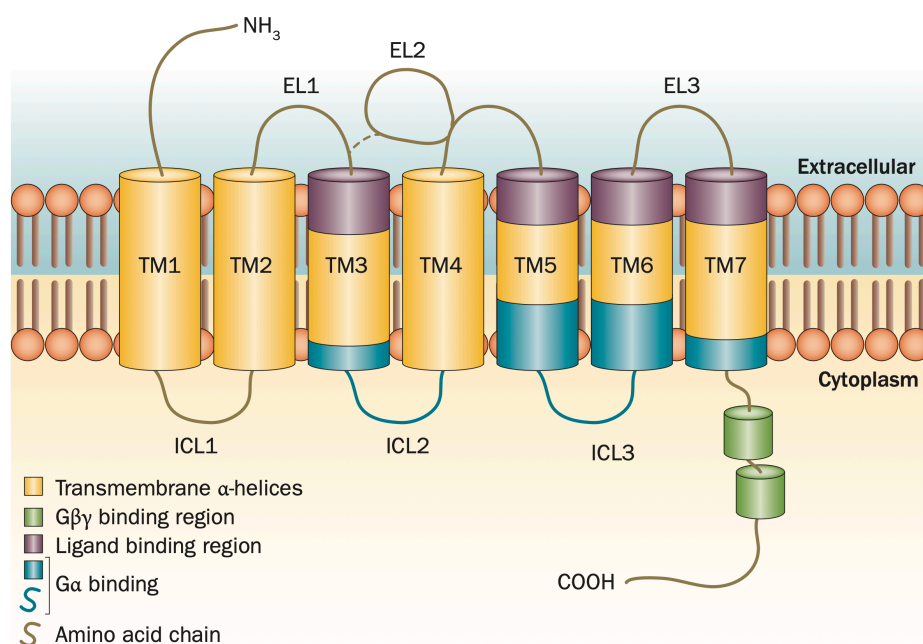


Figure 1. Illustration of 7TM structure of GPCR molecule. The illustration is taken from Neumann *et al.* [31].

The first crystal structure of ground-state bovine rhodopsin was determined in 2000.<sup>32</sup> As GPCRs share a large part of structural properties, solving this crystal structure offered the basis for understanding the transmembrane motif of seven helices connected by three extracellular and three intracellular loops of different and variable lengths, i.e., elements of secondary structure that all receptors have in common, as well as the positions of amino acids conserved in most GPCRs.<sup>33</sup> GPCRs maintain a highly organized structure through numerous interhelical hydrogen bonds and hydrophobic interactions, many of which are enabled by highly conserved amino acid residues of the GPCR primary structure.<sup>34</sup> Disulfide bridges are also present in the extracellular region conserved in most GPCRs, including one between two cysteine residues from extracellular loop EL-2 and the extracellular end of helix TM-3, also from two cysteines in EL-1 and EL-2.<sup>24</sup> Their purpose is to stabilize and restrict the possible number of conformations and preserve the structural integrity of the receptor's heptahelical region.<sup>30</sup>

This protein family has been classified using a variety of classification systems, some of them categorizing receptors based on their ligand way of binding, whereas others consider both physiological and structural factors.<sup>35-38</sup> Extensive phylogenetic analysis showed that there are five major classes of GPCRs family into which vertebrate GPCRs can be classified: glutamate, rhodopsin, adhesion, frizzled/taste2, and secretin, composing a GRAFS classification system,

based on the first letters of the class names.<sup>25,39</sup> All the members of each class have a shared evolutionary origin, but classes demonstrate no sequence similarity.<sup>40</sup> Additional proteins exist that are unable to be classified into formed classes and are referred to separately.<sup>25,41</sup> Among those mentioned, by far the greatest is the rhodopsin class, which consists of four major groups ( $\alpha$ ,  $\beta$ ,  $\gamma$  and  $\delta$ ) with 13 distinct sub-branches.<sup>42</sup> The  $\beta$  group doesn't have any of the main sub-branches, and all the receptors included have peptides as known ligands.<sup>40</sup> Receptors contained in this rhodopsin- $\beta$  group, along with many others, are OTR, V1aR, V1bR and V2R.<sup>10,43</sup> Most rhodopsin receptor ligands bind inside a pocket between the transmembrane regions, apart from ligands binding the N-terminus.<sup>44</sup> Except for the rhodopsin class, all the classes have a long N-terminus. Just a few receptors in the rhodopsin class also have it long.<sup>25</sup>

GPCRs communicate messages through the cell membrane in response to the recognition of diverse extracellular ligands, such as ions (e.g.,  $\text{Ca}^{2+}$ ), organic odorants, amines, and small molecules such as amino acid residues, nucleotides, nucleosides, lipids, peptides, proteins, but also photons in case of rhodopsin.<sup>24,30,40</sup> Signals are enhanced and transduced to downstream effectors within cells mainly through interactions with G proteins. When activated, receptors initiate complex cascades of events that control fundamental cellular and physiological functions.<sup>45</sup> Discovery and characterization of cyclic adenosine monophosphate (cAMP) as the first secondary messenger of glucagon and epinephrine activity in the metabolic pathways of glucose, as well as the discovery of adenylyl cyclase responsible for its biosynthesis, was the first stepping stone in clarification of the signaling cascades connecting ligands with intracellular effector proteins *via* membrane receptors.<sup>46</sup> The most extensively researched of a variety of cAMP effectors is protein kinase A (PKA), with a large number of targets and downstream signaling pathways.<sup>47</sup> Also, a lot of other molecules were identified and characterized as secondary messengers in GPCR signaling pathways, such as cyclic guanosine monophosphate (cGMP), diacylglycerol, inositol (1,4,5)-trisphosphate, phosphatidyl inositol (3,4,5)-trisphosphate, arachidonic acid, phosphatidic acid, and free intracellular calcium.<sup>48</sup> Downstream effector systems in the GPCR signaling pathways include adenylyl and guanylyl cyclases, phosphodiesterases, phospholipases, and kinases, with the purpose of promoting or inhibiting the synthesis of corresponding secondary messengers. Additionally, ion channels play an important role in ion and small molecules flux.<sup>49</sup>

G proteins are in fact heterotrimeric ( $\alpha$ ,  $\beta$  and  $\gamma$  subunits) guanosine triphosphate (GTP) binding proteins, consisting of four major classes:  $G_s$  (activates adenylyl cyclase),  $G_{i/o}$  (inhibits

adenylyl cyclase),  $G_{q/qq}$  (activates phospholipase C) and  $G_{12,13}$  (unknown function) and/or  $\beta$ -arrestin (scaffolding protein).<sup>28</sup> In the guanosine diphosphate (GDP) bound, heterotrimeric form, G proteins are inactive and must be activated by guanine nucleotide exchange catalyzed by the receptor, that is GTP binding to the  $\alpha$ -subunit.<sup>50</sup> GTP binding causes  $G_{\alpha}$ -GTP to separate from  $G_{\beta\gamma}$  subunits and activate downstream effectors through both separated  $G_{\alpha}$ -GTP and  $G_{\beta\gamma}$  subunits.<sup>51,52</sup> Known GPCR structure offers some insight into the molecular mechanisms of GPCR ligand recognition and receptor activation processes. Experiments show that the transition from inactive to active form due to ligand binding is accompanied by a shift in the relative orientation of TM-3 and TM-6 (twist of TM-6 and its distancing from TM-3), affecting the conformation of the intracellular loops, pulling ICL-3 inside the cell, where G protein is recognized and activated.<sup>40</sup> One receptor may activate many G proteins, but various receptors can also converge on one G protein, resulting in different combinations of transduced signals.<sup>24,30,53</sup>

Approximately 40% of all approved and marketed drugs are used to target GPCRs.<sup>54</sup> Around 17% of human GPCRs and GPCR-related genes/proteins (those upstream or downstream from GPCRs in the signaling pathway) are targets for approved drugs, with GPCRs alone accounting for approx. 12% of drug targets, making them the most frequently therapeutically targeted gene/protein family.<sup>28</sup> Drugs targeting these receptors and related proteins are mostly peptides and other small molecules.<sup>55</sup> The prospective for new drug development in this area is huge since created drugs target only a limited subset of GPCRs.<sup>56</sup>

### 2.1.2. Oxytocin receptor and vasopressin 1a receptor

In mammals, the OTR, V1aR, V1bR, and V2R are four closely related GPCRs that neuropeptides OT and VP bind to and activate to regulate their biological function.<sup>13,57,58</sup> The transmembrane helices, alongside the first extracellular loop, are the most conserved domains among these receptors, suggesting a strong relationship between these receptors, with the total similarity of the four receptors to each other in humans ranging from approximately 36 to 46%, and from 42 to 57% in the transmembrane region alone.<sup>12,13</sup> A number of conserved residues found in EL-1 and EL-2 are present only in the vasopressin/oxytocin group of the GPCR family and so may be components of the recognition sites for the structurally closely related ligands OT and VP.<sup>4</sup> Recently, the structure of active human OTR with bound OT has been solved by cryo-electron microscopy (cryo-EM), confirming the importance of extracellular loops and

transmembrane helices' hydrophobic pocket in binding.<sup>14</sup> Determined structure model of the active OTR complex is given (Figure 2). N and C terminus, along with intracellular loops, are less conserved areas.<sup>1</sup> However, all VP and OT receptors have two consecutive Cys residues at their C-terminus areas, which is a characteristic highly conserved across the whole GPCR family. At these residues, the C-terminus of the protein is attached to the inside of the cell membrane by prenylation.<sup>4</sup> Significant differences in ICL-3 may be responsible for diverse interactions with G proteins.<sup>59</sup>

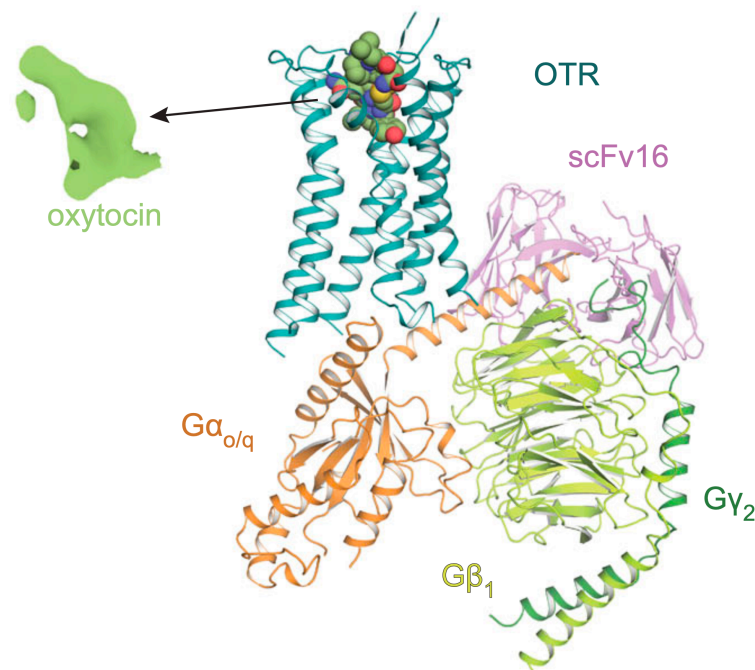


Figure 2. Cryo-EM molecular model of OTR complex with OT and mini-G protein, stabilized by scFv16. The model is taken from Waltenspühl *et al.* [14].

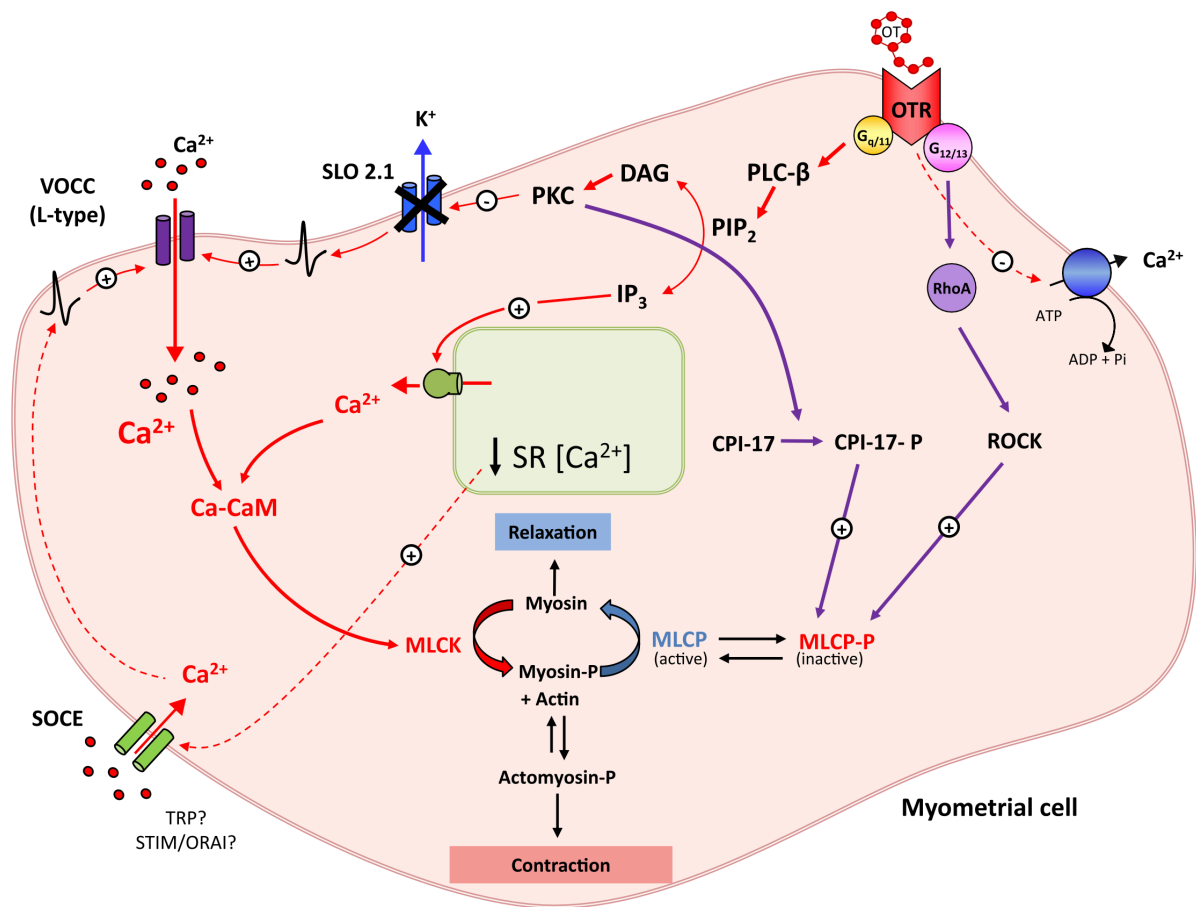
OT has only one known receptor, while VP has three. These receptors mediate a wide range of activities in both the central nervous system (CNS) and periphery, which are separated by the blood-brain barrier,<sup>60</sup> and have different roles depending on the localization.<sup>61</sup> VP operates in the CNS on its two receptor subtypes, V1a and V1b, and is responsible for behavioral functions, such as aggressiveness, partner selection, sexual behaviour or cognitive functions like memory and face recognition,<sup>62</sup> but is also responsible for central endocrine roles, and central cardiovascular activity regulation.<sup>5</sup> Of the two, V1aR is the more important in vasopressinergic regulation of social behavior, so the majority of studies looking at VP's function in controlling social behavior focuses on the V1aR.<sup>2</sup> While V1bR is expressed mainly in the brain,<sup>7</sup> V1aR is also found in liver, uterus, smooth muscle cells, and acts as a vasoconstrictor of systemic



vessels.<sup>5,63</sup> On the other hand, V2R is located only in the periphery with the primary location in the kidney, where it mediates renal water absorption and so acts on fluid homeostasis and blood pressure regulation.<sup>4</sup> OTR is in the brain expressed in large amounts and mediates the effects of OT on social behaviors, such as emotional bonding, sexual behavior or maternal bonding.<sup>17,64</sup> The most well-known function of the OTR system in the periphery is the initiation of myometrial contractions within the uterus and their regulation during labor.<sup>4,6</sup> It is also expressed in the mammary glands where it causes secretion of milk.<sup>3</sup>

The requirement of these receptors to accept cyclic peptides, whose structures will be shown later, may be indicated by the enlarged binding pocket located in the upper part of the transmembrane region to the extracellular area.<sup>57</sup> This characteristic is shared by all four members of this strongly related OT and VP receptor family.<sup>12</sup> Additionally, it has been demonstrated that conserved extracellular residues play a part in ligand binding and activation of the receptor.<sup>65</sup> Ligand binding induces reorientation of the transmembrane region, and consequently the arrangement of the intracellular region, enabling the opening of docking sites for interacting with different G proteins.<sup>12,66</sup> All four receptors are coupled to various G proteins, or even other signaling molecules (e.g.,  $\beta$ -arrestins),<sup>67</sup> making them promiscuous in that matter, triggering a variety of signaling pathways, and controlling a variety of cellular functions.<sup>6,12,68,69</sup> Upon activation, the V2R stimulates adenylyl cyclase and increases the synthesis of intracellular cAMP. On the other hand, the OTR, V1aR, and V1bR largely signal through the activation of different phospholipases, namely C, D, or A2.<sup>4,70-72</sup>

Upon phospholipase C activation, phosphatidylinositol-4,5-bisphosphate (PIP<sub>2</sub>) is hydrolyzed to produce inositol-1,4,5-trisphosphate (IP<sub>3</sub>) and diacylglycerol (DAG), which in turn stimulate the release of Ca<sup>2+</sup> from the sarcoplasmic reticulum and the activation of protein kinase C (PKC), respectively.<sup>6,73</sup> An increase in the level of intracellular Ca<sup>2+</sup> is additionally a result of extracellular Ca<sup>2+</sup> influx, which is connected to a long-lasting phospholipase D activation, or voltage-gated calcium channels downstream from PKC.<sup>4,74</sup> Elevated Ca<sup>2+</sup> concentration finally stimulates calmodulin that activates myosin light chain kinase (MLCK), which then phosphorylates light chains of myosin at Ser-19, enabling its interaction with actin, which causes cell contractions. These are particularly important in myometrium during labor.<sup>6,73</sup> Scheme of the signaling pathway described is illustrated in Figure 3 for the OTR.



Current Opinion in Physiology

Figure 3. OTR in the myometrium after activation leads to contraction. Phospholipase C activation after OTR activation causes phosphatidylinositol-4,5-bisphosphate (PIP<sub>2</sub>) hydrolysis to inositol-1,4,5-trisphosphate (IP<sub>3</sub>) and diacylglycerol (DAG), which stimulate the release of Ca<sup>2+</sup> from the sarcoplasmic reticulum and the activation of protein kinase C (PKC), respectively. An increased intracellular Ca<sup>2+</sup> is also due to extracellular Ca<sup>2+</sup> influx through voltage-operated Ca<sup>2+</sup> channels (VOCC) downstream from PKC. Elevated Ca<sup>2+</sup> stimulates calmodulin that activates myosin light chain kinase (MLCK), which then phosphorylates light chains of myosin, enabling its interaction with actin, and causing cell contractions. The image is taken from Arrowsmith [6].

Mammal cell plasma membranes contain a significant amount of cholesterol, which has been found to have a crucial role in membrane protein regulation. Several GPCRs, including the OTR, have been reported to have their function modified by cholesterol.<sup>75,76</sup> This can be accomplished by either modifying the lipid bilayer's physical properties (e.g., membrane fluidity) or directly through interactions with proteins.<sup>57,77</sup> GPCRs are allosteric molecules by

nature, and the monovalent cation  $\text{Na}^+$  negatively regulates many of them. Divalent cations like  $\text{Mg}^{2+}$  (but also  $\text{Ni}^{2+}$ ,  $\text{Zn}^{2+}$ ,  $\text{Mn}^{2+}$ , and  $\text{Co}^{2+}$ ) have on the other hand been demonstrated to act as positive allosteric modulators of the OTR.<sup>78,79</sup> In order to restrict prolonged stimulation upon agonist binding and receptor activation, desensitization follows in many GPCRs. Phosphorylation and concurrent sequestration/internalization have been linked to ligand-occupied receptor desensitization. Receptor phosphorylation may be caused by a variety of protein kinases. GPCR kinases (GRKs) are those that phosphorylate the agonist-occupied receptor. Other kinases, including the cAMP-dependent and  $\text{Ca}^{2+}$ -dependent (e.g., PKC) protein kinases, can also phosphorylate receptors. Since these are activated by a rise in secondary messengers, they may help attenuate receptor activity, as indicated for a V1aR that has a number of PKC phosphorylation sites.<sup>70,80</sup>

## 2.2. Oxytocin and vasopressin

### 2.2.1. Oxytocin and vasopressin – two structurally similar neuropeptides with significant tasks

OT and VP homologs have been found in a variety of organisms, including worms, molluscs, insects, vertebrates, and hydra, and date all the way back to at least 700 million years ago.<sup>2,4</sup> A local duplication led to the evolution of OT and VP from a single ancestor gene in a gnathostome.<sup>81</sup> Mammalian OT and VP are nonapeptides differentiated by only two amino acids in positions 3 and 8. While OT contains Ile in position 3 VP contains Phe, and in position 8 OT has Leu and VP Arg.<sup>2</sup> Structures are presented in Figure 4. An ancestral molecule, present in other, non-mammalian, vertebrates is vasotocin, containing Ile in position 3 and Arg in position 8.<sup>82</sup> These peptides are structurally specific for their cyclized structure realized through cysteines at positions 1 and 6, forming a disulfide bridge.<sup>83</sup>

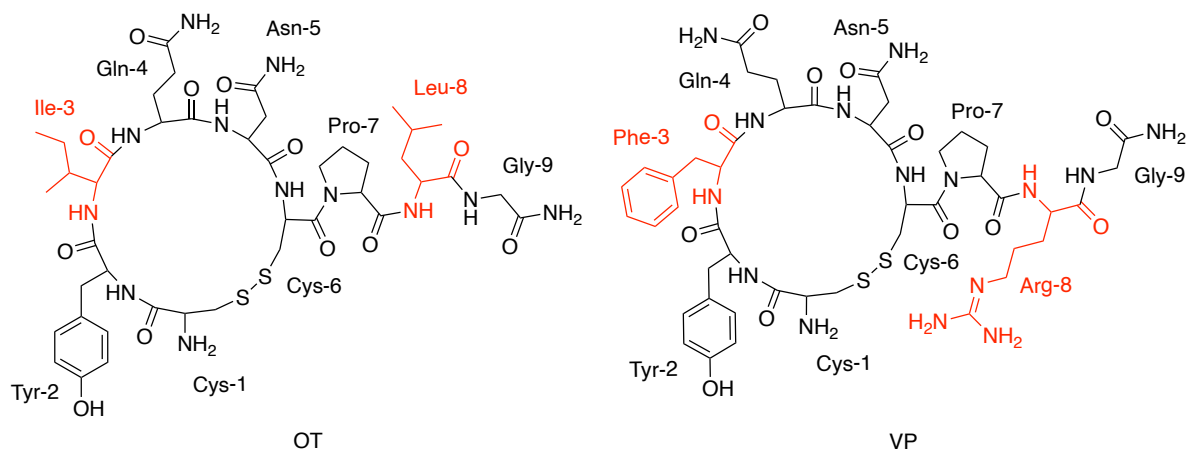


Figure 4. Structures of cyclized nonapeptides OT and VP, with distinct amino acid residues highlighted in red.

In contrast to VP, which is more promiscuous, binding to both VP and OT receptors with high affinity, OT is a rather selective ligand for the OTR.<sup>14</sup> This is supported by the  $K_i$  values stated in Table 1.

Table 1. Selectivity of the human OTR and human V1aR, V1b, and V2R for OT and VP. Values represent binding affinity defined as  $K_i / \text{nmol dm}^{-3}$ . Following a selectivity criterion stating that for the receptor to be selective the receptor/ligand  $K_i$  is required to be two orders of magnitude lower than for other receptors and that ligand. Only hOTR is defined as selective for OT. Adapted from Manning *et al.* [<sup>84</sup>]

Ligand	$K_i / \text{nmol dm}^{-3}$			
	hOTR	hV1aR	hV1bR	hV2R
OT	0.8	120	>1000	3500
VP	1.7	1.1	0.7	1.2

In mammals, the hypothalamic brain areas are the primary sites of OT and VP production.<sup>2</sup> These peptides are next sent to the pituitary for peripheral secretion or directed to other regions of the brain.<sup>85,86</sup>

Both OT and VP influence behavior in males and females,<sup>2</sup> and frequently exhibit sexually dimorphic expression and behavioral impacts on animals.<sup>87</sup> In mammals, OT has taken on quite diverse roles in female sociosexual responses crucial for mammalian reproduction, including sexual behavior, uterine contractions during parturition,<sup>88</sup> lactation,<sup>89</sup> maternal attachment, and

pair bonding.<sup>2,4</sup> OT also modulates social and emotional responses, including social bonding, trust, aggressiveness, anxiety, fear, and many more.<sup>17,90</sup> VP, on the other hand, typically affects male sociosexual behavior, so it's related to erection and ejaculation and moreover influences aggression and territoriality, but also affects pair bonding in different species.<sup>2,91</sup> In general, the particular social behaviors these peptides have an impact on demonstrate wide variations among species, but also between the individuals within the same species.<sup>92,93</sup> Instead of peptide differences, these behavioral effects are more likely to be mediated by variability in the genetic regulation of their receptors and variance in brain receptor patterns.<sup>94</sup>

The physiological functions of VP and OT are distinct. VP causes vasoconstriction and regulates blood pressure and osmolarity by stimulating the reabsorption of water by the kidneys.<sup>4</sup> Apart from that, VP is comparable to OT as it's also a strong stimulant of uterine contractions.<sup>95</sup> OT on the other hand in addition to uterine and mammary cells' contractions can affect proliferation in developing mammary glands, but also differentiation in breast cancer cells.<sup>3</sup>

### 2.2.2. *Oxytocin and vasopressin analogs as medications*

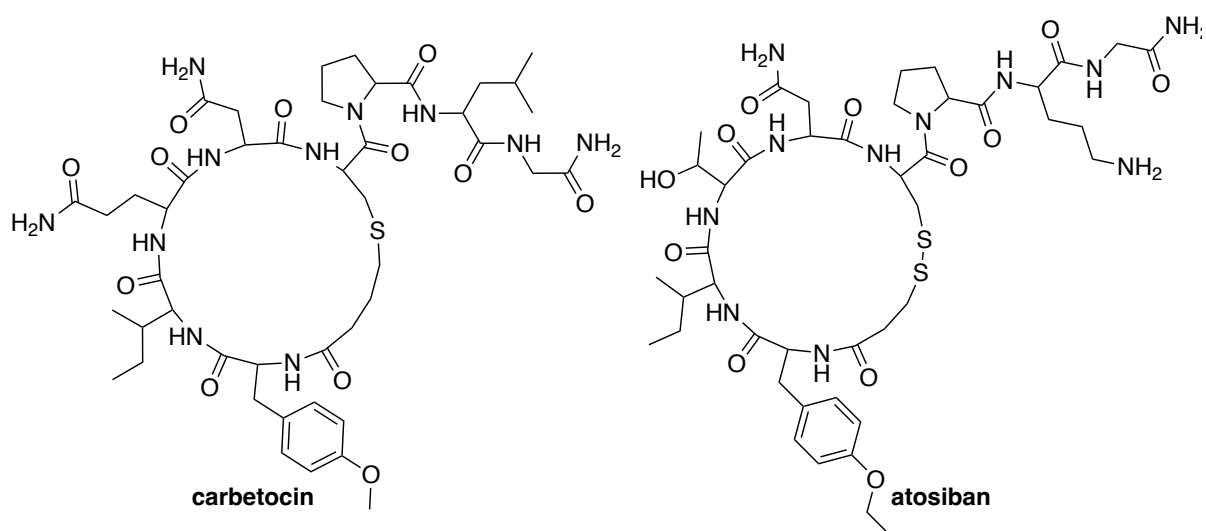
OT as a OTR agonist is clinically used as a medication, predominantly infused intravenously or less frequently intramuscularly to stimulate uterine contractions and initiate labor.<sup>96,97</sup> It is suggested by WHO to be given in order to control or stop heavy postpartum bleeding, one of the main causes of maternal deaths in developing countries.<sup>98</sup> Sometimes OT can be administered intranasally to improve lactation.<sup>99</sup> It has also been investigated for a treatment of autism and related intellectual conditions, and in general has a great clinical potential for treating mental health disorders.<sup>100</sup>

Thousands different peptidic and non-peptidic OT/VP analogs have been developed over the years, and while mainly used in research, they have also been synthesized and employed for therapeutic purposes.<sup>84</sup> Carbetocin (Figure 5) is a peptidic OT/VP analog effectively used to prevent postpartum hemorrhage in vaginal deliveries.<sup>101</sup> In contrast to OT employed for this use, carbetocin has a prolonged time of action, and can also remain active for a longer period of time in warm and humid conditions, making it quality-wise a better choice for utilization in less developed countries.<sup>102</sup> It acts as an OTR agonist and has been used to investigate the OTR/Gq coupling function in the brain.<sup>103</sup> Interestingly, while activating the OTR, it acts as an antagonist towards V1aR and V1bR.<sup>104</sup>

Atosiban, a peptidic OT derivative (Figure 5), is an effective OTR antagonist, a potent molecule in preventing preterm labor by suppressing uterine contractions.<sup>4,105</sup> At the same time, it acts as a competitive antagonist on OTR-G $\alpha_q$  and as an agonist of OTR-G $\alpha_i$  coupling, thereby becoming the first coupling-selective/biased antagonist of OTR.<sup>12,106</sup> The only medications used expressly to treat preterm labor are OTR antagonists, with atosiban being the only OTR antagonist approved for this use at the moment,<sup>6,107</sup> but not in the USA owing to the potential link to the preterm newborn deaths.<sup>108</sup> Despite all of this, atosiban is an unusual drug in which it has a reduced affinity for the OTR and acts mainly as a V1aR antagonist, so it has been unclear on which receptor it acts antagonistically and potential side effects of its use have been considered.<sup>6,109</sup>

Another potential tocolytic, peptidic OT analog barusiban (Figure 5), is being developed.<sup>55,110</sup> It is also OTR antagonist, somewhat smaller than atosiban, but unlike atosiban demonstrates a roughly 300-fold greater affinity for OTR than for V1aR.<sup>111</sup> However, it did not manifest efficacy in preventing premature labor other than placebo effect.<sup>6</sup>

Retosiban is another really effective, though non-peptidic (Figure 5), OTR antagonist with over 1400-fold selectivity for OTR over the three VP receptors.<sup>57,112</sup> In vitro studies on human myometrial explants were promising.<sup>113</sup> In a phase 2 proof-of-concept research, retosiban demonstrated good performance and safety profiles for the prevention of spontaneous premature labor.<sup>114</sup>



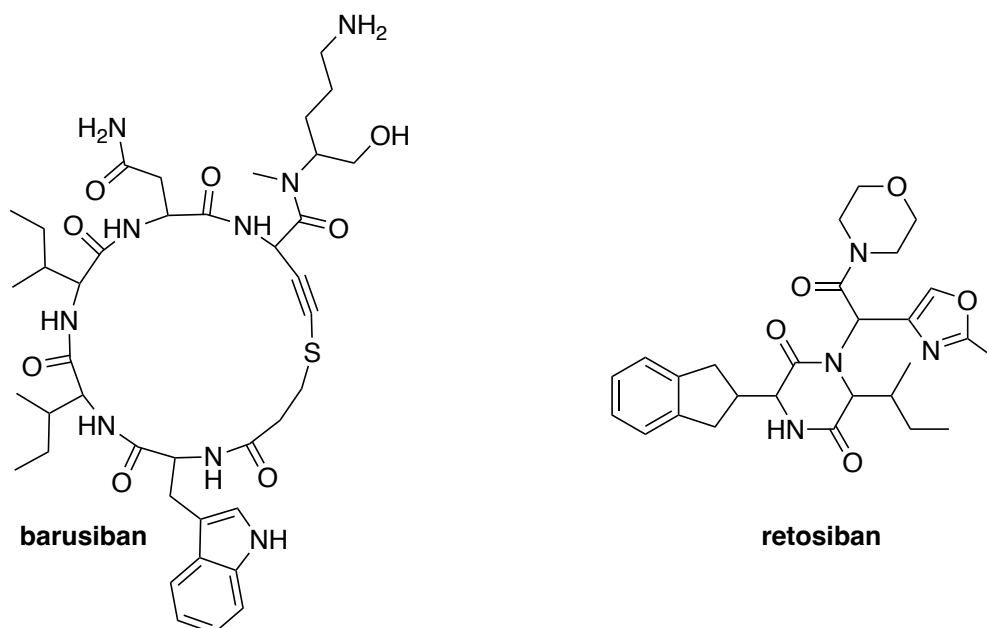


Figure 5. Molecular structures of peptidic OTR agonist carbetocin and OTR antagonists; peptidic atosiban and barusiban, and non-peptidic retosiban.

### 2.3. Methods used for validation of antibodies

For an antibody to be validated, it has to be shown selective, specific, and reproducible in the settings of the intended way of use.<sup>19</sup> Specific antibody is the one that recognizes a single epitope and discriminates the similar epitopes displayed by off-target proteins. Selective antibody is the one binding to the unique target protein epitope that is not present across different off-target proteins.<sup>115</sup> A set of guidelines to adhere to in the process of antibody validation has been proposed,<sup>21</sup> and was followed in the study of dopamine receptors 1 and 2.<sup>20</sup> In that study, validated antibodies were tested by western blots (WBs) and immunohistochemistry, and further by immunoprecipitation coupled with mass spectrometry (IP-MS). Conducted work covered by this thesis on the antibodies against OTR and V1aR includes experiments with WBs and IP-MS, therefore a shorter review of these methods will be given in the following pages. For these methods to be employed and performed successfully, isolation and quantification of receptor proteins of interest had to be completed and will also be covered accordingly in the following sections.

Generally, antibodies can be either polyclonal, targeting various antigen regions, or monoclonal, targeting only a particular region of antigen.<sup>18,116</sup> Regarding antigen recognition, antibodies can recognize either conformational antigen determinant, linear antigen determinant,

or neoantigenic determinant (Figure 6).<sup>117</sup> Conformational determinants are the parts of an antigen that are in contact with an antibody, and they usually involve the shape of the antigen, i.e., the feature of the 3D structure is a recognition element.<sup>118</sup> This determinant in protein is lost due to denaturation since the native structure disappears.<sup>119</sup> Linear determinants are the parts of an antigen formed by around six neighboring amino acid residues.<sup>120</sup> This determinant in a protein is a feature of the primary structure, and it can be hidden (inaccessible to the antibody) within the protein 3D structure until the denaturation reveals it. It can also be accessible in both the native and denatured form, if it's on the surface of the native structure, and remains accessible after denaturation.<sup>121</sup> Neoantigens are molecules or their parts that are not normally present on the surface of the antigen but can be recognized by antibodies. These can be derived from mutations, post-translational modifications, or other changes to the antigen, such as proteolytic cleavage.<sup>122</sup> Hence, the denaturing conditions of SDS-PAGE can cause the loss of, but also the appearance of new recognition patterns. Later will be discussed that the goal of IP-MS on the other hand is to preserve the native protein conformation. Here lies the reasoning for the combination of various antibody validation approaches, as different conditions affect recognition sites in different manners, changing and shifting the antibody efficacy. Approaching the problem with two distinctive, orthogonal methods in sense of determinant denaturation represents one of the key points of antibody validation.<sup>123</sup>



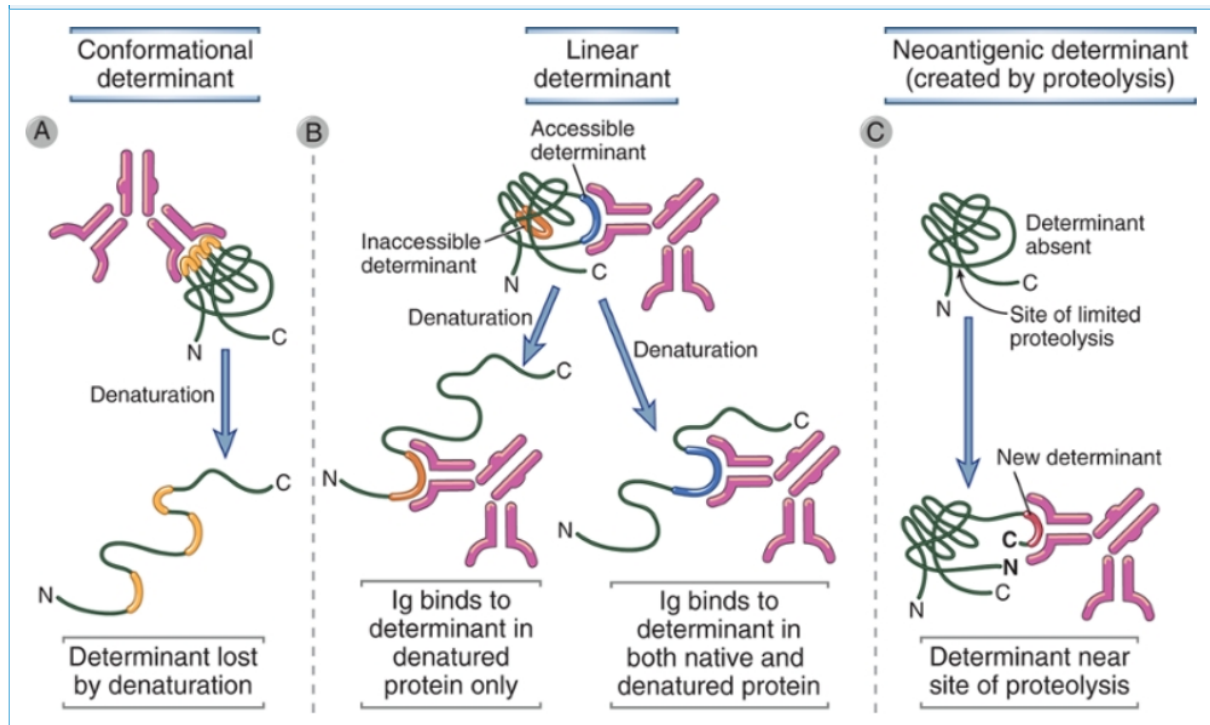


Figure 6. Antigenic determinants and their properties. Antigenic determinants marked in sequence thickening depend on both the tertiary and primary structure. A – Certain determinants are available in native proteins and are lost with denaturation; B – others become accessible only after protein unfolding; C – post-translational modifications stand behind the antigenic determinants. The image is taken from *Cellular & Molecular Immunology* [117].

### 2.3.1. Western blot

#### 2.3.1.1. Membrane protein isolation

Proteins used in WB experiments can be extracted from a variety of sources, including cells and tissues. For their extraction, especially from tissue samples reflecting a higher structural degree, mechanical and chemical methods are employed.<sup>124</sup> The most popular mechanical methods include homogenization, sonication, and disintegration with metallic or glass beads. In chemical methods, lysis buffers are used. The presence of ionic detergents like sodium dodecyl sulfate (SDS) in some buffers enables the solubilization of proteins. Other detergents, such as non-ionic or zwitterionic, are also an option, and the choice is based on the necessary lysis speed and extraction efficacy of the protein of interest. While, for example, SDS may quickly lyse cells, it also denatures proteins. Triton X-100 on the other hand, as a non-ionic detergent, may lyse cells gently while preventing protein denaturation, which is important if the protein structure needs to be preserved for further experiments.<sup>125</sup>

To prevent protein denaturation and its degradation by proteases and phosphatases, samples of cells and tissues after incubation and prior to protein isolation should be frozen, and the whole procedure of protein extraction should be performed on ice. It's important to keep in mind that repeated freezing and thawing will result in lower sample quality. Hence, if not frozen, samples should be lysed as soon as possible after incubation.<sup>126–128</sup> Release of proteases and phosphatases during lysis calls for the addition of their inhibitors to the lysis buffer to maximize the amount of protein obtained with a maintained structure that would be recognizable by the appropriate antibodies.<sup>116</sup>

Following the sample lysis procedure, cellular fractions can further be separated using differential centrifugation. First centrifugation is performed to remove unlysed cells and larger bits of debris contained in the pellet from the supernatant containing both membrane and cytosolic proteins. The second one, ultracentrifugation employing higher speeds, enables the separation of soluble cytosolic proteins contained in the supernatant from the fraction containing total membrane proteins in a form of a pellet.<sup>129</sup> Membrane proteins from the pellet are further solubilized in a solution containing non-ionic detergent aiming to preserve their functional conformation outside the lipid bilayer environment in a process implicating the emergence of protein:detergent micelles.<sup>130,131</sup>

### 2.3.1.2. Protein quantification methods

Before preparing the samples for loading into the wells for gel electrophoresis, the concentration of the isolated proteins needs to be determined.<sup>132</sup> Loaded protein amounts need to be uniform between different wells and consistent throughout many gels so that the results obtained can be comparable.<sup>133</sup> Numerous different methods enabling protein quantification are available,<sup>134</sup> and in the text following the more popular of them will be briefly explained. The bicinchoninic acid assay, the method used for determining protein concentration in our laboratory, will be explained in more detail.

The simplest of all the methods is by determining protein absorbance at 280 nm since aromatic amino acid residues absorb ultraviolet radiation at that wavelength. The absorbance at this wavelength is mostly contributed to by the amino acids tryptophan and tyrosine, with their relatively high molar extinction coefficients, but also somewhat by phenylalanine with a notably smaller extinction coefficient. The method complies with the Beer-Lambert law, so the protein concentration is proportional to the determined absorbance.<sup>135</sup>

Another important method, based on the well-known biuret reaction, is the Lowry method. What differentiates this method from the biuret reaction is improved detection sensitivity, accomplished by adding a mixture of phosphomolybdic and phosphotungstic acid.<sup>136</sup> In the biuret reaction, four nitrogen atoms from the peptide bonds combine with copper creating a cuprous complex. By adding the acids mixture and their interaction with cuprous ions and the tyrosine, tryptophan, and cysteine residues, a blue-green coloration detectable between 650 and 750 nm is produced.<sup>135</sup>

Bradford protein assay is another method for protein quantification and is based on Coomassie Brilliant Blue G-250 dye binding to protein. This dye principally interacts with arginine, but slightly also with another basic (lysine, histidine), and aromatic (tyrosine, tryptophan, and phenylalanine) residues under acidic conditions.<sup>135,137</sup> Free dye is brown-red with an absorption maximum of 465 nm. Binding to protein shifts the maximum to 595 nm, causing a blue coloration, and is almost complete in only around 2 minutes, staying stable for about 1 hour. Because of the relatively high dye-protein complex extinction coefficient, the method is highly sensitive. The presence of detergents causes interferences, so this method is not suitable for determining membrane protein concentrations, where some of the most often used detergents enabling protein solubilization, like Triton X-100, cause high background.<sup>138,139</sup>

Among all the mentioned methods, the Bicinchoninic Acid (BCA) assay was developed last.<sup>140</sup> It is similar to the Lowry method in that it uses a biuret reaction to transform  $\text{Cu}^{2+}$  ions under alkaline conditions into cuprous  $\text{Cu}^+$  ions, which then further react with the sodium salt of bicinchoninic acid, forming a complex with the absorbance maximum at 562 nm, causing a purple coloration.<sup>135</sup> As the BCA reagent is stable under alkaline conditions, the method has the benefit over the Lowry method in that it can be performed in one step, while the Lowry method requires two steps, making it less complicated to carry out.<sup>141</sup>

Two reagents composing the BCA assay, reagents A and B, can be purchased as part of a kit from different suppliers. Reagent A is a solution containing bicinchoninic acid, sodium carbonate, sodium tartrate, and sodium bicarbonate at a final pH of 11.25 adjusted with NaOH or  $\text{NaHCO}_3$ . Reagent B is a copper(II) sulfate pentahydrate ( $40 \text{ g dm}^{-3}$ ) solution.<sup>142</sup> Kept at room temperature (RT) of approximately  $25 \text{ }^\circ\text{C}$ , they stay stable and are fine to use after a long time of non-use. As the amino acid content influences the BCA assay outcome, absolute protein concentration cannot be measured. For that reason, relative concentration is determined in comparison to the calibration curve formed by measuring the set of standard samples of, most

commonly, bovine serum albumin (BSA), whose concentrations are known.<sup>141</sup> This assay can be conducted both at RT and at higher temperatures up to 60 °C to improve the sensitivity.<sup>135</sup> An additional benefit of the BCA assay is its compatibility with the chemicals interfering with the Lowry assay. It is unaffected by a variety of detergents (up to 5%)<sup>135</sup> and denaturing chemicals.<sup>141</sup> This assay can also be performed in a 96-well plate, reducing the amount of necessary reagents, and adding to all the aforementioned benefits. Concern to have in mind is that, since the assay employs the  $\text{Cu}^{2+}$  reagent, chelating agents such as EDTA greatly interfere with the measuring outcome. Also, reducing agents and reducing sugars that reduce  $\text{Cu}^{2+}$  to  $\text{Cu}^+$ , interfere with this assay.<sup>135,141</sup>

### 2.3.1.3. Sodium dodecyl sulfate polyacrylamide gel electrophoresis

After knowing the protein concentration, samples can be prepared for separation on a gel electrophoresis system. Gel electrophoresis comes in a variety of forms, but the most common is the one that for protein separation employs polyacrylamide gels.<sup>127</sup> This polyacrylamide gel electrophoresis (PAGE) can be run under either non-denaturing/naive or under denaturing conditions. The former uses non-denaturing and non-reductive loading buffers, such as Tris-glycine in a pH range of 8.3 to 9.5, to preserve the structure of the protein. Under these conditions, separation depends on the protein's electric charge, size, and form.<sup>125</sup> On the other side, denaturing polyacrylamide gel electrophoresis, also known as SDS-PAGE, uses a buffer that contains strong anionic detergent sodium dodecyl sulfate (SDS) and reducing agent  $\beta$ -mercaptoethanol, and employs the effect of heat. SDS disrupts the hydrophobic interactions and denatures the protein covering proteins in a negative charge,<sup>128</sup> while  $\beta$ -mercaptoethanol aided with heating the samples breaks the disulfide bonds, additionally assisting in denaturation by structure dissociation. The binding of SDS ensures that all the proteins have the same negative charge, enabling their separation by molecular weight only.<sup>125–127</sup>

The most frequently used type of electrophoresis is exactly the SDS-PAGE.<sup>127</sup> Protein samples for electrophoresis are prepared in a loading buffer, colored due to bromophenol blue present to enable visibility and tracking of separation progress, and dense because of glycerol to enable sample loading into the gel's well. In the preparation, the samples are heated at temperatures of 70 to 95 °C to aid the denaturation of orderly protein structures.<sup>125</sup> Prepared samples are loaded onto the gel along with a molecular weight marker, and since being covered in the negative electric charger, they travel through the gel towards the positive electrode after

applying the voltage.<sup>124</sup> The most commonly employed polyacrylamide gel consists of two gels (discontinuous system); an upper ‘stacking’ gel with a lower percentage of acrylamide and, and a lower ‘resolving’ gel. Two of the gels have different pH values and ionic strengths because of the different buffers used in their preparation, with the stacking gel being weakly acidic at pH 6.8, and the resolving gel being basic at pH 8.8.<sup>124,143</sup> Gels can be either purchased precast or made in the lab to regulate acrylamide and bisacrylamide percentages, which in turn determines the pore sizes in the gel. Proteins move through the gel at varying rates, with smaller proteins traveling faster, causing their separation into distinct bands within every lane.<sup>126,127</sup>

#### 2.3.1.4. Protein transfer methods

After the proteins have been separated using the SDS-PAGE system, they’re transferred from the gel onto the solid phase. The most employed solid phases are microporous materials and membranes such as cellulose, cellulose acetate, polyethersulfone, nylon, nitrocellulose (NC), and polyvinylidene difluoride (PVDF). These materials have a high capacity for protein binding as they have a high volume-to-surface ratio. They can store the immobilized proteins for short or long times, as well as permit the interaction of the immobilized protein with the solubilized reagents. They allow for greatly reproducible results due to the low number of interferences during detection procedures. Microporous materials are used as sheets or membranes, and their interaction with the proteins is of a non-covalent type, with the details of the interaction not entirely known.<sup>144,145</sup>

The membrane used in this work was PVDF, which structurally is a linear polymer composed of repeating  $-(CF_2-CH_2)-$  groups, and it achieves protein binding through both dipole and hydrophobic interactions. What gives it an advantage over some other membranes is its strong mechanical properties and compatibility with numerous organic solvents and chemicals in use.<sup>145,146</sup> They can also be stripped and reprobed after the blot has already been probed, something the NC membrane doesn’t allow.<sup>124</sup>

Proteins from the gel after SDS-PAGE can be transferred to the PVDF membrane in different ways, such as simple diffusion blotting, vacuum blotting, and electroblotting methods.<sup>147</sup> The most used of the methods is electroblotting for its rapid and efficient transfer, and it comes in different variations, such as a semi-dry or wet transfer. Both of these require the preparation of a ‘transfer sandwich’, where it’s of crucial importance that the gel and the membrane stay together in direct contact, with the filter paper surrounding it from both sides.<sup>126</sup>

And while the wet transfer is more suitable for the transfer of larger proteins,<sup>143</sup> it demands a larger amount of transfer buffer and takes more time to perform, on top of the need for the cooling system due to excessive heat generation (2–12 h at 4 °C), in comparison to the semi-dry transfer (7–30 min at RT).<sup>125</sup> The more trustworthy of the two is considered to be the wet transfer since it more effectively keeps both the gel and the membrane from drying out, but at the expense of time, resources, and effort put in. For these reasons, it is frequently substituted with a semi-dry transfer, which is the type used for the purposes of this thesis.

Since the PVDF is hydrophobic, the membrane must be wet/activated in methanol or ethanol before packing into the sandwich, to be able to interact with the aqueous buffer used.<sup>145</sup> Buffers in use are based on the one from Towbin, containing Tris (25 mmol dm<sup>-3</sup>), glycine (192 mmol dm<sup>-3</sup>), methanol ( $\phi = 20\%$ ), and none to 0.1 g dm<sup>-3</sup> SDS.<sup>145,148</sup> Buffers are usually preferred without SDS when the membrane used is PVDF, since the proteins tend not to bind properly if SDS is used,<sup>149</sup> except for the cases when the proteins are prone to aggregation, then the use of SDS is advised.<sup>145</sup> Also, the complete removal of methanol from the transfer buffer is possible and advised when trying to preserve conformational sites of transferred proteins, as well as to prevent the changes in the size of the used polyacrylamide gel that could otherwise shrink,<sup>145</sup> and so restrict the transfer of proteins.<sup>150</sup> The prepared sandwich must be placed in a way so that the membrane stands in between the gel and the positive electrode, since the principle of protein transfer is almost the same as in the SDS-PAGE, with the negatively charged proteins moving towards the positive electrode, with the membrane on their way to catch them.<sup>124</sup> Sandwich is placed in between two plate electrodes that provide a homogenous electric field. The smaller proteins migrate faster from the gel and blot more efficiently on the membrane. Also, the thinner the gel used or the lower the percentage of acrylamide in the gel, the faster the protein transfer.<sup>145</sup>

Once transferred from the gel, the proteins maintain their original distribution in the membrane. Becoming easier to manipulate on the membrane, proteins can be used in immunodetection to interact with specific antibodies.

#### *2.3.1.5. Washing, blocking, and primary/secondary antibody incubation*

Blocking the membrane, after protein transfer, reduces the background by preventing the nonspecific binding of primary antibody against the target protein to the membrane.<sup>124</sup> The most used blocking solution is 5% bovine serum albumin (BSA) or 5% non-fat dried milk (NFDM)

in phosphate-buffered saline (PBS) or in Tris-buffered saline (TBS) often with moderate addition of Tween 20.<sup>126</sup> Membrane is soaked into the prepared blocking solution and slowly agitated, occupying the membrane protein-binding sites with inert protein.<sup>125</sup> Since it is relatively cheap and easy to procure, using the NFDm is often the way to go. But it must be considered that the milk protein casein is actually a phosphoprotein, so it is unsuitable as a blocking agent if the primary antibody reacts against phosphoproteins as it could cause false positives and high background.<sup>124,143</sup>

After blocking, the primary antibody solution against the specific protein on the membrane is added to the membrane and incubated overnight at 4 °C or for an hour or two at RT. The primary antibody is diluted in a blocking solution to the optimal concentration, since the signal could stay absent or become too strong with a higher background.<sup>124,126</sup> This concentration needs to be determined by testing different concentrations in a process known as primary antibody titration.<sup>151</sup>

After incubation, the membrane is washed from the excess primary antibody by multiple rinses with a buffer previously used for the preparation of blocking solution, for example, TBS-T. After washing, a secondary antibody solution is added to the membrane and incubated typically for around an hour at RT. The prepared secondary antibody solution also needs to be of the appropriate concentration and determined experimentally.<sup>126</sup> It targets the species-specific region of the primary antibody, which is usually the Fc region with its' constant heavy chains,<sup>152</sup> and carries a label that allows for direct or indirect detection, with horseradish peroxidase (HRP) or alkaline phosphatase (ALP) being two important examples.<sup>126,143</sup>

#### 2.3.1.6. Membrane visualization

If the secondary antibody with a radiolabel was used, protein detection is direct and uses autoradiographic film to capture the signal. More widely used chromogenic or fluorogenic labels require an extra substrate and allow for indirect protein detection. Secondary antibodies may also be fluorescently labeled and require no additional reagents for detection. As mentioned above, two examples of chemiluminescent labels are HRP and ALP. These labels employ the chemiluminescence substrate, cleave it and the reaction product emits luminescence. The resulting light is then detected either on photographic film or digitally using a charge-coupled device (CCD) camera, providing better resolution and sensitivity.<sup>125–127</sup>

One of the more popular methods, enhanced chemiluminescence (ECL), uses the ECL mix. ECL mix is a combination of two substrates: luminol/enhance reagent and peroxide reagent. When luminol in the presence of peroxide is oxidized by HRP, it goes over a peroxy intermediate to form a 3-aminophthalate dianion in the excited state and consequently results in light emission.<sup>153</sup> Described mechanism is presented in Figure 7. It requires only the short membrane incubation of a few minutes and ensures high sensitivity.<sup>116</sup>

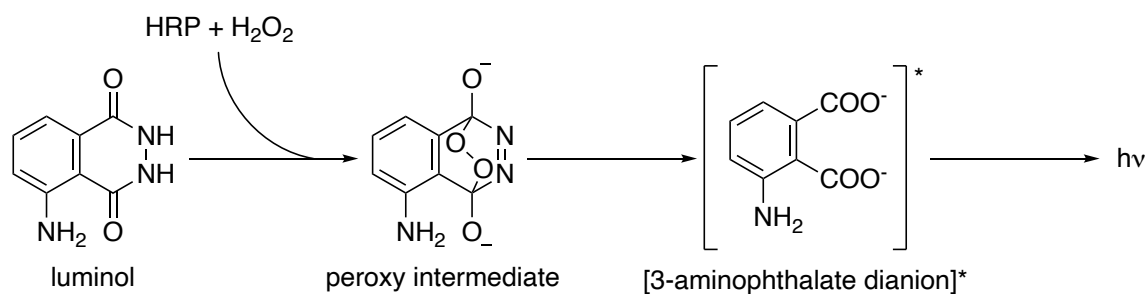


Figure 7. Chemiluminescence by ECL substrate and HRP. In the presence of H<sub>2</sub>O<sub>2</sub> luminol is oxidized by HRP and over the peroxy intermediate leads to the formation of 3-aminophthalate dianion in the excited state and consequently to the emission of light. Mechanism is adapted from Bio-Rad ECL instruction manual [<sup>153</sup>].

Captured images are further analyzed. Multiple software have been developed and are available for this purpose, enabling automatic or manual analysis, or a combination of the two, with many analysis and editing options included. CCD cameras often come with their own data capture, processing, and analysis software.<sup>127</sup>

### 2.3.2. Immunoprecipitation coupled with mass spectrometry

An immunoprecipitation (IP) method combined with a mass spectrometry (MS) technique is a typical approach for studying, discovering, and validating protein interactions.<sup>154,155</sup> The IP step in IP-MS is responsible for the isolation of the protein of interest from a complex protein mixture, usually a cell lysate.<sup>156</sup> This is generally performed by employing a specific antibody that binds to protein A- or G-coated agarose or magnetic beads, along with the protein of interest (antigen), called a 'bait protein'.<sup>154,157</sup> Either monoclonal or polyclonal antibodies could be utilized, and they may identify the protein of interest, a specific posttranslational modification (PTM), or in the case of an overexpressed protein an epitope tag. Their Fc regions, depending on the species of origin (Table 2), are recognized by the immobilized protein A or G, where protein A is the less expensive of the two, but protein G binds a broader range of classes of



antibodies. In the Table 2 is visible that Protein A has a somewhat stronger affinity to rabbit antibodies.<sup>156,158</sup> These two proteins are originally bacterial receptors that bind Fc regions of the broad variety of immunoglobulins. Protein A comes from *Staphylococcus aureus* and has 5 binding sites for IgG, while protein G with 2 IgG binding sites comes from strains G and C streptococci.<sup>155,159,160</sup> The use of a non-denaturing lysis buffer that contains a non-ionic detergent such as Triton X-100 or CHAPS leads to the release of membrane (except for a smaller fraction) proteins, enabling the IP that employs antibodies targeting native protein epitopes. In case antibodies cannot reach to recognize these epitopes, or the non-ionic detergent is unable to isolate the antigen from the cell, denaturing conditions should be used.<sup>155</sup>

The order of steps, regarding the adding of the antibody to the protein mixture or binding it to the beads first, can vary among the different protocols. Traditionally, an antibody is added directly to the protein sample (lysate) and the formed complex is then captured onto the protein A- or G-coated beads. The alternative way is to bind the antibody to the suitably coated beads before being exposed to the protein mixture.<sup>156</sup> The arguments for the latter sequence are strong, since prebinding antibody to the beads enables unbound antibody to be removed, hence allowing for better control over the amount of antibody employed and consequently for a more effective recovery of immunoprecipitated protein. Furthermore, potential interactions of the other proteins other than desired antibody (e.g., serum proteins) from the antibody sample with the target protein in the protein mixture are eliminated due to not coming in touch with the lysate, avoiding any potential negative effect of these proteins on target protein isolation.<sup>155</sup>

After incubation of the antibody with the beads coated with the corresponding protein A or G, the antibody is bound to the bead in a non-covalent manner.<sup>155</sup> The cell lysate (protein mixture) is then incubated with the resulting antibody-bead complex for a certain period, allowing the antibody to bind to the target proteins, forming a protein-antibody-bead complex. This complex is separated from the sample by centrifugation (in the case of agarose beads), or by using the magnetic rack to pull the complex to the walls of the tube (in the case of magnetic beads). Magnetic beads have an advantage in that they allow for complete buffer removal without unintentional bead loss and without the buffer carry over, but they also allow for quicker washing due to a lower porosity.<sup>155</sup> The pellet is then subjected to denaturing or low-pH conditions to break down and elute the complex.<sup>156</sup> The most often used elution buffer is 0.1 M glycine in HCl, pH 2.5-3.0, effectively breaking antibody-antigen and protein-protein

interactions without altering protein structures.<sup>161</sup> Released proteins can further be analyzed using enzyme-linked immunosorbent assay (ELISA), immunoblotting, or MS.<sup>162</sup>

Table 2. Antibody-binding to Protein A and Protein G affinities, where the number of plusses represents the binding strength and minus represents no binding. The table is adapted from New England Biolabs [<sup>158</sup>].

Species	Immunoglobulin	Binding to Protein A	Binding to Protein G
Human	IgG (normal)	++++	++++
	IgG1	++++	++++
	IgG2	++++	++++
	IgG3	-	++++
	IgG4	++++	++++
	IgM	-	-
	IgA	-	-
	IgE	-	-
Mouse	IgG1	+	++++
	IgG2a	++++	++++
	IgG2b	+++	+++
	IgG3	++	+++
Rat	IgG1	-	+
	IgG2a	-	++++
	IgG2b	-	++
	IgG2c	+	++
Goat	IgG	+/-	++
Rabbit	IgG	++++	+++
Sheep	IgG	+/-	++

In the IP-MS, eluted proteins are then digested using one or sometimes a combination of proteolytic enzymes.<sup>154,163</sup> Owing to its high efficiency and specificity, along with its availability at a relatively low cost, trypsin is the most commonly used protease in proteomics analyses. It breaks the proteins down into smaller peptides with an average size of  $1.8 \times 10^3$  hydrolyzing the peptide bonds after two basic and frequently occurring amino acids: arginine and lysine.<sup>164</sup> Membrane proteins with their large transmembrane regions naturally consist of a greater amount of hydrophobic amino acids, and the number of trypsin recognition sites is reduced. For that reason, chymotrypsin with an affinity for hydrophobic Phe, Trp, and Tyr,<sup>165</sup> or some other proteases, can be used along the trypsin in the analysis of transmembrane

proteins, providing a piece of extra information about the protein sequence.<sup>164</sup> These peptides are further analyzed employing a powerful and sensitive technique; MS, allowing for the identification and quantification of the proteins.<sup>166</sup>

## § 3. EXPERIMENTAL SECTION

### 3.1. Materials

#### 3.1.1. Validated antibodies

For conducting WB and IP experiments, rabbit monoclonal antibodies in a HEK293 (human embryonic kidney 293) cell culture media without antibiotics ( $\gamma \approx 5-7 \mu\text{g/mL}$ ) produced against specific OTR or V1aR peptide fragments and selected based on ELISA assay results were obtained from the NIH and Origene company. Ten antibodies against OTR (1A3, 1B2, 1C10, 1E4, 1F1, 1H11, 4E3, 4F3-4, 4F3-5, 5A5), and seven antibodies against V1aR (1G1, 1H1, 3C1, 3D2, 3F8, 4A7, 4G9) were obtained, as indicated in Table 3 and Table 4 with the ELISA results displaying reactivity towards the plate-coupled peptides, respectively. Peptides of interest correspond to either C- or N-terminus, intracellular loops 2 or 3, or transcellular loop 3. The amounts of antibodies obtained were limited and in total received in two rounds: 3 mL in the first round, and 5 mL in the second round (only 1B2 was produced in 10 mL culture and concentrated by ultrafiltration to ca. 3 mL).

Table 3. Ten antibodies against OTR with the ELISA results displaying activity towards the peptides/epitopes corresponding to the C-terminal, TCL-3, and ICL-2 regions of OTR. Stronger interactions are marked in more intense color; antibodies are ordered according to the interactions from the most to the least active, and the epitope regions as well.

OTR antibody	OD for different peptides		
	C-TERM	TCL-3	ICL-2
4F3-5	2.90	0.12	0.09
1B2	2.54	1.35	0.21
1A3	2.53	1.32	0.21
4F3-4	2.19	0.27	0.10
1F1	2.11	1.53	0.23
4E3	0.08	0.09	1.85
1E4	0.09	1.50	0.09
5A5	0.09	0.10	1.48
1H11	1.38	0.21	0.27
1C10	0.09	0.90	0.09
1B2 batch 2	3.26	1.80	0.41
1B2 batch 3	3.10	2.14	0.36

Table 4. Seven antibodies against V1aR with the ELISA results displaying activity towards the peptides/epitopes corresponding to the C-terminal, N-terminal, and ICL-3 regions of V1aR. Stronger interactions are marked in more intense color; antibodies are ordered according to the interactions from the most (green) to the least (white) active, and the epitope regions as well.

V1aR antibody	OD for different peptides		
	C-TERM	N-TERM	ICL-3
1H1	2.54	0.10	0.10
3C1	2.47	0.09	0.09
3F8	2.43	0.09	0.08
3D2	0.09	1.67	0.09
4A7	1.60	0.09	0.09
4G9	0.08	0.09	1.00
1G1	0.28	0.68	0.08

### 3.1.2. Protein isolation and quantification

The following chemicals and solvents were used in protein isolation: ROTISOLV® HPLC gradient grade water (Carl Roth), Dulbecco's phosphate-buffered saline (modified, without calcium chloride and magnesium chloride, 10×, liquid, sterile-filtered, suitable for cell culture; Sigma-Aldrich), HEPES (Sigma-Aldrich), CaCl<sub>2</sub> (Sigma-Aldrich), D(+)-saccharose (Carl Roth), sodium chloride (Sigma Aldrich), glycerol (Sigma-Aldrich), sodium hydroxide (pellets; Merck), sodium phosphate monobasic, anhydrous (Sigma-Aldrich), sodium phosphate dibasic dihydrate (Sigma-Aldrich), Triton X-100 (Sigma-Aldrich), cOmplete protease inhibitor cocktail tablets (Roche), PhosSTOP phosphatase inhibitor cocktail tablets (Roche).

For determining the solubilized protein concentration, the following solutions and kits were used: pre-diluted protein assay standards: bovine serum albumin (BSA) set (Thermo Scientific), Pierce™ BCA protein assay kit (Thermo Scientific).

### 3.1.3. Western blot and protein staining

For preparing the gels for the electrophoresis, the following reagents were used: acrylamide (2× cryst.; Carl Roth), *N,N'*-methylenebisacrylamide (Carl Roth), hydrochloric acid fuming 37% (Carl Roth), Trizma® base (Sigma-Aldrich), ammonium persulfate (APS; Bio-Rad), sodium dodecyl sulfate (SDS, ultra-pure; AppliChem), 2-propanol (Sigma-Aldrich), glycine (Sigma-Aldrich), TEMED (Carl Roth).

For preparing the samples and running the electrophoresis, transferring and detecting the proteins, the following solvents, agents, and compounds were used: Milli-Q (from ELGA lab water purification system, Veolia Water), Laemmli sample buffer (4×; Bio-Rad), 2-mercaptoethanol (Bio-Rad), PageRuler™ plus prestained protein ladder (Thermo Scientific), methanol (LiChrosolv®, gradient grade for chromatography; Merck Millipore), Tween® 20 (Carl Roth), skim milk powder (Sigma-Aldrich), FITC goat polyclonal anti-GFP (ab6662, GR3286332-13, Abcam), peroxidase-AffiniPure donkey anti-goat IgG (H+L) (260310, Jackson ImmunoResearch), rabbit monoclonal [EPR5642] to AVPR1A/V1aR (ab124907; Abcam), rabbit monoclonal [EPR24409-146] to oxytocin receptor (ab300443; Abcam), peroxidase-AffiniPure donkey anti-rabbit IgG (H+L) (711-035-153; Jackson ImmunoResearch), Clarity™ western ECL substrate – peroxide solution and luminol/enhancer solution (Bio-Rad), Clarity Max™ western ECL substrate – peroxide solution and luminol/enhancer solution (Bio-Rad)

For staining purposes, the following was used: acetic acid (99–100%; Carl Roth), Coomassie® Brilliant Blue G 250 (Fluka), Ponceau S solution (Sigma-Aldrich), naphthol blue black (Sigma-Aldrich).

#### 3.1.4. Immunoprecipitation

For performing IP, the following reagents were used: SureBeads™ protein A magnetic beads (Bio-Rad), phosphate-buffered saline (PBS, 10×; Bio-Rad), acetone (LiChrosolv®, Merck Millipore), urea (Sigma-Aldrich), triethylammonium bicarbonate buffer (1.0 M, pH 8.5 ± 0.1; Sigma Aldrich), CHAPS (Carl Roth), DTT (Carl Roth), IAA (Carl Roth), trypsin (sequencing grade modified, porcine; Promega), trypsin resuspension buffer (Promega), formic acid (Thermo Fisher Scientific), universal indicator (MColorpHast™ pH-indicator strips, 1.09535.0001; Krackeler Scientific)

#### 3.1.5. Instruments

For the practical work, following tools and equipment were used: precision balance BCE62021-1S (Sartorius, Göttingen, Germany), vortex-genie 2 (Scientific Industries, New York, USA), lab pH meter pH 7110 (inoLab, Kladno, Czech Republic), WTW pH electrode SenTix® 41 (Xylem Analytics, Weilheim, Germany), see-saw rocker SSL4 (Stuart Equipment, Stone, UK), PURELAB® pulse, ELGA LabWater (Veolia Water, Paris, France), centrifuge 5702 R (Eppendorf, Hamburg, Germany), centrifuge 5804 (Eppendorf, Hamburg, Germany), Sonopuls

HD 2200 (Bandelin electronic, Berlin, Germany), Sonopuls UW 2200 (Bandelin electronic, Berlin, Germany), Sonopuls LS 5 (Bandelin electronic, Berlin, Germany), centrifuge 5427 R (Eppendorf, Hamburg, Germany), Optima MAX-XP ultracentrifuge (Beckman Coulter, Brea, USA), GloMax<sup>®</sup>-multi+ detection system (Promega, Madison, USA), thermomixer compact (Eppendorf, Hamburg, Germany), PowerPac<sup>™</sup> basic (BioRad, Hercules, USA), vertical midi-format electrophoresis Criterion<sup>™</sup> cell, 18-well (Bio-Rad, Hercules, USA), Trans-Blot<sup>®</sup> SD semi-dry transfer cell (Bio-Rad, Hercules, USA), ChemiDoc<sup>™</sup> MP imaging system (Bio-Rad, Hercules, USA), rotator SB3 (Stuart Equipment, Stone, UK), concentrator 5301 (Eppendorf, Hamburg, Germany).

### 3.1.6. Software

Instinct<sup>®</sup> Software (Promega, Madison, USA) was used to read and export data from the microplate reader for determining protein concentration. Image Lab software (Version 6.1.0.07; Bio-Rad, Hercules, USA) was used for the analysis of gel and blot images. Xcalibur (Version 4.5; Thermo Fisher Scientific, Waltham, USA) was used for processing raw data from a Thermo Fisher Scientific Mass Spectrometer. MaxQuant (Max Planck Institute, München, Germany) and Protein Prospector (Version 6.4.5; University of California, San Francisco, USA) were used for MS data analysis and database search. ChemDraw (Version 21.0.0.28; PerkinElmer, Waltham, USA) was used for drawing molecule structures and chemical reactions. Protter (Version 1.0; Wollscheid Lab, ETH Zürich, Germany; “<https://wlab.ethz.ch/protter/start/>”) was used to predict tryptic cleavage sites based on protein sequences and visualize identified peptides following the IP.

## 3.2. Methods

### 3.2.1. Western blot and protein staining

#### 3.2.1.1. Membrane protein isolation

For homogenization and solubilization buffers to be prepared, following solutions were prepared: 10 mL of HEPES (1 mol dm<sup>-3</sup>) by dissolving 2.38 g of HEPES (M = 238.30 g/mol) in HPLC-grade water, referred to as ultra-pure water (UPW); 10 mL of CaCl<sub>2</sub> (0.1 mol dm<sup>-3</sup>) by dissolving 0.111 g of CaCl<sub>2</sub> (M = 110.98 g/mol) in UPW; 10 mL of sucrose (2 mol dm<sup>-3</sup>) by dissolving 6.85 g of sucrose in UPW; 10 mL of NaCl (2 mol dm<sup>-3</sup>) by dissolving 1.17 g of NaCl (M = 58.44 g/mol) in UPW; 10 mL of glycerol ( $\varphi = 50\%$ ) by mixing 5 mL of glycerol ( $\varphi$

= 100%) with 5 mL of UPW; 100 mL of NaOH (5 mol dm<sup>-3</sup>) by dissolving 20.0 g of NaOH (M = 40 g/mol) in UPW; 0.5 L of phosphate buffer (1 mol dm<sup>-3</sup>, pH = 7.4) by dissolving 23.52 g of NaH<sub>2</sub>PO<sub>4</sub> (M = 119.98 g/mol) and 54.109 g of Na<sub>2</sub>HPO<sub>4</sub> × 2H<sub>2</sub>O (M = 177.99 g/mol) in around 400 mL of UPW and further titrating with prepared NaOH (5 mol dm<sup>-3</sup>) up to pH of 7.4 (measured with the pH-meter) and then filling up to 0.5 L; 0.5 L of phosphate buffer (0.1 mol dm<sup>-3</sup>, pH = 7.4) by diluting 50 mL of prepared phosphate buffer (1 mol dm<sup>-3</sup>, pH = 7.4) with 450 mL of UPW; 10 mL of Triton X-100 ( $\varphi$  = 10%) by dissolving 1 mL of Triton X-100 in UPW.

For the preparation of 10 mL of homogenization buffer, mixed was 100  $\mu$ L of HEPES (1 mol dm<sup>-3</sup>), 10  $\mu$ L of CaCl<sub>2</sub> (0.1 mol dm<sup>-3</sup>), 1.6 mL of sucrose (2 mol dm<sup>-3</sup>), 1 tablet of cOmplete, and 1 tablet of PhosSTOP and adjusted to 10 mL with UPW. Homogenization buffer composition: HEPES (10 mmol dm<sup>-3</sup>), CaCl<sub>2</sub> (0.1 mmol dm<sup>-3</sup>), sucrose (320 mmol dm<sup>-3</sup>), 1× cOmplete, 1× PhosSTOP.

For the preparation of 10 mL of solubilization buffer, mixed was 1 mL of Triton X-100 ( $\varphi$  = 10%), 750  $\mu$ L of NaCl (2 mol dm<sup>-3</sup>), 1 mL of glycerol ( $\varphi$  = 50%), 1 mL of phosphate buffer (0.1 mol dm<sup>-3</sup>, pH = 7.4), 1 tablet of cOmplete, and 1 tablet of PhosSTOP and adjusted to 10 mL with UPW. Solubilization buffer composition: Triton X-100 ( $\varphi$  = 1%), NaCl (150 mmol dm<sup>-3</sup>), glycerol ( $\varphi$  = 5%), phosphate buffer (10 mmol dm<sup>-3</sup>), 1× cOmplete, 1× PhosSTOP.

To obtain the proteins to work with, C-terminally GFP-tagged hOTR, hV1aR, hV1bR, and hV2R overexpressing cells (HEK293) from stably transfected cell lines were grown, together with native HEK293 cell line. Cell lines were prepared within the Institute of Biological Chemistry, Vienna, and available for use. All steps upon obtaining frozen or fresh cell pellets were performed on ice to prevent protein complex degradation and all the reagents and equipment used were pre-cooled prior to the start of isolation. For the easier following, a simplified scheme of the workflow that will be described in this paragraph is depicted in Figure 8. After being brought in a medium, cells were first spun down for 5 min at 1200 g. The pellets was resuspended in 5 mL of 1× PBS, then centrifugated for 3 min at 1000 g. The supernatant was discarded and to the pellet was added 700  $\mu$ L of ice-cold homogenization buffer and then transferred to a 2 mL Eppendorf tube. The residue was collected by adding 300  $\mu$ L more of homogenization buffer and transferring it to the same tube. Homogenization using an ultrasonic bath in parallel with an ultrasonic needle (sonicator) was tried, and the needle was around



doubly effective, so the content of the tube was homogenized with an ultrasonic needle – 10 s on 50% (5 shots of 10%), and then centrifugated for 15 min at 1000 g at 4 °C. Supernatant was collected in a new ice-cold ultracentrifugation tube, and the pellet was resuspended in 400 µL of homogenization buffer and once again centrifugated for 15 min at 1000 g at 4 °C. Second supernatant was added to the ultracentrifugation tube with the first supernatant. Supernatants were ultracentrifugated for 1 h 10 min at 110,000 g at 4 °C. Supernatants (containing cytosolic fraction) were discarded, and the pellets (containing total membrane fraction) were further solubilized by adding 400 µL of ice-cold solubilization buffer and gently resuspending without creating bubbles. Samples were solubilized on ice for 1 h by vortexing every 5 min for 30 s, after which they were centrifugated for 1 h 5 min at 14,000 g at 4 °C. Supernatants (containing only solubilized membrane proteins, GPCRs included) were collected in new microtubes and stored at –20 °C, and pellets (containing insoluble proteins) were discarded.

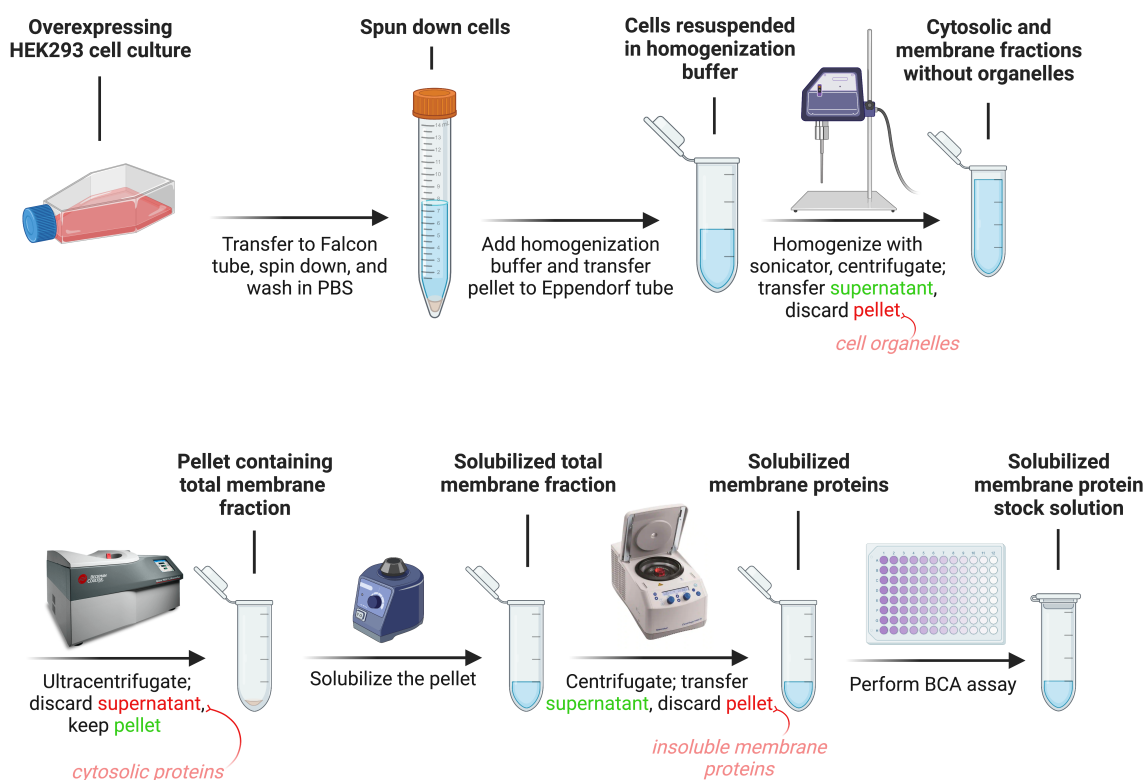


Figure 8. Workflow for membrane protein extraction from overexpressing and native cell lines. Created with BioRender.com [167].

### 3.2.1.2. Protein quantification

To each well of a 96-well microplate was pipetted 10  $\mu\text{L}$  of each dilution from the set of BSA standard dilutions (125, 250, 500, 750, 1000, 1500, and 2000  $\mu\text{g}/\text{mL}$ ) in triplicates. To each well of the microplate, 10  $\mu\text{L}$  of solubilized protein stock samples was further pipetted. This was also performed in triplicates. If the samples were too concentrated and out of the range, they were diluted with solubilization buffer before being loaded onto the microplate. A Blank solution was prepared by mixing 10  $\mu\text{L}$  of solubilization buffer with 40  $\mu\text{L}$  of HPLC-grade water (1:5 ratio) and 10  $\mu\text{L}$  was pipetted to each well of the microplate in triplicate. To each well was further added 200  $\mu\text{L}$  of freshly prepared BCA working reagent, mixed according to the manufacturer instructions (50:1, Reagent A:B).<sup>168</sup> The prepared microtiter plate was covered and shaken on a plate shaker for 1 min at 450 rpm and then incubated for 30 min at 37 °C. After cooling to RT, absorbance was measured at  $\lambda = 560$  nm on microplate reader. The Blank solution's average absorbance measurement was subtracted from all other individual standard and solubilized protein sample replicates. Blank-corrected measurements for each standard dilution were plotted against their known concentration to form a standard curve. The concentrations of solubilized protein stock samples were determined from the standard curve, with the dilution factor prior to loading considered at calculating stock concentrations.

### 3.2.1.3. Sodium dodecyl sulfate polyacrylamide gel electrophoresis

For carrying out the SDS-PAGE, following solutions were prepared: 200 mL of acrylamide mix (300  $\text{g dm}^{-3}$ ) by dissolving 58.4 g of acrylamide ( $M = 71.08$  g/mol) and 1.6 g of *N,N'*-methylenebisacrylamide ( $M = 154.17$  g/mol) in UPW on a magnetic mixer overnight at 450 rpm; 40 ml of HCl (aq, 1:1) by mixing 20 ml of fuming hydrochloric acid with 20 mL of UPW; 200 mL of stacking buffer Tris (0.50  $\text{mol dm}^{-3}$ , pH = 6.8) by dissolving 12.13 g of Trizma base ( $M = 121.14$  g/mol) in around 150 mL of UPW water and further titrating with prepared HCl (aq, 1:1) down to pH of 6.8 (measured with the pH-meter) and then filling up to 200 mL; 400 mL of separation buffer – Tris (1.50  $\text{mol dm}^{-3}$ , pH = 8.8) by dissolving 72.63 g of Trizma base ( $M = 121.14$  g/mol) in around 350 mL of UPW and further titrating with prepared HCl (aq, 1:1) down to pH of 8.8 (measured with the pH-meter) and then filling up to 400 mL; 30 mL of APS (100  $\text{g dm}^{-3}$ ) by dissolving 3 g of ammonium persulfate ( $M = 228.20$  g/mol) in UPW, after which the volume was separated into 30 microtubes (1 ml to each) and stored at  $-20$  °C to prevent freezing and thawing; 50 mL of SDS (100  $\text{g dm}^{-3}$ ) by dissolving 5 g of sodium dodecyl sulfate ( $M = 288.38$  g/mol) in UPW on a magnetic mixer at 20 °C; 50 mL

of isopropanol ( $\varphi = 50\%$ ) by mixing 25 mL of UPW with 25 mL of 2-propanol; 5 L of 10× Laemmli SDS-Running Buffer by dissolving 151.4 g of Trizma base, 750.7 g of glycine and 50 g of SDS in Milli-Q water (MQW), making the composition of the buffer: Tris ( $250 \text{ mmol dm}^{-3}$ ), glycine ( $2 \text{ mol dm}^{-3}$ ), SDS ( $10 \text{ g dm}^{-3}$ ); 1 L of 1× Laemmli SDS-Running Buffer by mixing 100 mL of prepared 10× Laemmli SDS-Running Buffer with MQW and filling up to 1 L.

1 L of 10× transfer buffer by dissolving 58.11 g of Trizma base ( $M = 121.14 \text{ g/mol}$ ), 29.3 g of glycine ( $M = 75.07 \text{ g/mol}$ ), and 3.75 g of SDS ( $M = 288.38 \text{ g/mol}$ ) in MQW; 1 L of 1× transfer buffer by mixing 100 mL of prepared 10× transfer buffer with MQW and filling up to 1 L; 1 L of 10× TBS by dissolving 15.76 g of Trizma base ( $M = 121.14 \text{ g/mol}$ ) and 90.00 g of NaCl ( $M = 58.44 \text{ g/mol}$ ) in around 900 mL of MQW and further titrating with prepared HCl (aq, 1:1) down to pH of 7.5 (measured with the pH-meter) and then filling up to 1 L; 1 L of 1× TBS-T by mixing 100 mL of prepared 10× TBS with MQW, dissolving 1 mL of Tween 20 and filling up to 1 L; 0.5 L of 1× TBS by mixing 50 mL of prepared 10× TBS with MQW and filling up to 500 mL; 50 mL of NFDM ( $50 \text{ g dm}^{-3}$ , blocking solution) by dissolving 2.5 g of skim milk powder in prepared 1× TBS-T.

To cast a gel, 10 mL of 10% or 8% resolving/separation gel solution was prepared by mixing the volumes of prepared reagents as stated in Table 5. First, all the reagents except for APS ( $100 \text{ g dm}^{-3}$ ) and TEMED were mixed, and the solution was vortexed. Worth noting here is that SDS ( $100 \text{ g dm}^{-3}$ ) needed to be heated to 40–50 °C every time before use since it crystallized at RT. Right before loading the gel solution into the gel casting cassette, APS ( $100 \text{ g dm}^{-3}$ ) was added, the solution was vortexed, and then the TEMED was added, and the solution was vortexed again. The volume of 8.5 mL of so prepared solution was quickly loaded into the gel casting cassette by pipetting and on top was evenly added 1 mL of isopropanol ( $\varphi = 50\%$ ), so the gel wouldn't dry out while polymerizing. After the gel polymerized, which was noticeable by the smile effect (slightly downwards directed edges), isopropanol was poured out from the top of the gel and the gel was rinsed with water, followed by drying the cassette with a paper towel. After it was dried of any water, 4 mL of stacking gel solution was prepared the same way but following the volumes of prepared reagents as stated in Table 6 and quickly loaded into the gel casting cassette on top of the polymerized resolving gel, after which the well-creating comb was inserted in a way that no bubbles were trapped under it. The gel was left to polymerize for at least an hour, then wrapped in a wet paper towel and additionally

wrapped in a plastic foil, and stored at 4 °C for a day or two to prevent unpolymerized acrylamide from cross-linking with proteins,<sup>169</sup> when it was to be loaded with samples for running on the SDS-PAGE.

Table 5. Amounts of reagents required for the preparation of 10 mL of 10% resolving gel.

Reagent	10 mL – 10%	10 mL – 8%
HPLC-grade H <sub>2</sub> O	4.05 mL	4.63 mL
300 g dm <sup>-3</sup> acrylamide mix	3.30 mL	2.66 mL
1.50 mol dm <sup>-3</sup> Tris, pH 8.8	2.50 mL	2.50 mL
100 g dm <sup>-3</sup> SDS	100 µL	100 µL
100 g dm <sup>-3</sup> APS	100 µL	100 µL
TEMED	10 µL	10 µL

Table 6. Amounts of reagents required for the preparation of 4 mL of 4% stacking gel.

Reagent	4 mL – 4%
HPLC-grade H <sub>2</sub> O	2.22 mL
300 g dm <sup>-3</sup> acrylamide mix	680 µL
0.50 mol dm <sup>-3</sup> Tris, pH 6.8	1 mL
100 g dm <sup>-3</sup> SDS	40 µL
100 g dm <sup>-3</sup> APS	40 µL
TEMED	4 µL

First, 10% gels were loaded to check for the chemiluminescent signal-to-protein amount ratio for each of the validated antibodies and their corresponding receptor proteins; 10, 20, and 30 µg/well of solubilized membrane proteins containing recombinantly expressed OTR-GFP or V1aR-GFP was loaded onto the gel, in a way presented in Table 7. Samples were prepared and diluted with Laemmli running buffer based on protein stock concentration, ensuring uniform loading volumes for different amounts. The protein aliquot diluted with the solubilization buffer was mixed with the 4× Laemmli Sample Buffer (4× LSB) mix in a 3:1 ratio. The 4× LSB mix was prepared by mixing 4× LSB with β-mercaptoethanol in a 9:1 ratio. Mixed samples were heated for 10 min at 70 °C shaking at 450 rpm, then left to cool to RT and loaded onto the gel, together with 4 µL of PageRuler Plus Prestained Protein Ladder. Electrophoresis was run with the following program: 1. 30 min at 50 V, 2. 30 min at 100 V, 3. 40 min at 150 V.

Table 7. Gel (10%) arrangement for SDS-PAGE to compare how different amounts of the same receptor protein (either OTR-GFP or V1aR-GFP) loaded per well result in different chemiluminescent signal strength after developing the WB with the corresponding antibody to be validated, where: L – 4  $\mu$ L of PageRuler Plus Ladder.

		OTR-GFP						OTR-GFP						OTR-GFP			
		∇						∇						∇			
		V1aR-GFP						V1aR-GFP						V1aR-GFP			
1	2	3	4	5	6	7	8	9	10	11	12	13	14	15	16	17	18
	L	10	20	30		L	10	20	30		L	10	20	30			
		$\mu$ g	$\mu$ g	$\mu$ g			$\mu$ g	$\mu$ g	$\mu$ g			$\mu$ g	$\mu$ g	$\mu$ g			

Then, 8% gels were loaded to check for the specificity of the validated antibodies for the corresponding receptor among the other receptor proteins; 20  $\mu$ g/well of OTR-GFP, V1aR-GFP, V1bR-GFP, V2R-GFP, and HEK293 solubilized membrane proteins were loaded onto the gel, in a way presented in Table 8. Samples were prepared the same way, loaded onto the gel, and the electrophoresis was run with the same program: 1. 30 min at 50 V, 2. 30 min at 100 V, 3. 40 min at 150 V.

Table 8. Gel (8%) arrangement for SDS-PAGE to test the specificity of validated antibodies for the corresponding receptor among the same amount of other receptor proteins, where: L – 4  $\mu$ L of PageRuler Plus Ladder.

						OTR-GFP		V1aR-GFP		V1bR-GFP		V2R-GFP		HEK293			
1	2	3	4	5	6	7	8	9	10	11	12	13	14	15	16	17	18
				L		20		20		20		20		20			
						$\mu$ g		$\mu$ g		$\mu$ g		$\mu$ g		$\mu$ g			

Two 10% gels were loaded in the same arrangement as the 8% gels would normally be loaded for testing the specificity. These two gels would be used as a control checking the specificity of two commercially available antibodies against OTR and V1aR.

Gels (10%) that had some spare lanes were additionally loaded with 20  $\mu$ g of OTR-GFP or 20  $\mu$ g of V1aR-GFP with 4  $\mu$ L of PageRuler Plus Ladder in the first lane to the left of it. These were to be cut and used as a secondary antibody control.

Another 10% gel was loaded as presented in Table 9 with samples of 5  $\mu$ g of OTR-GFP, V1aR-GFP, and V1bR-GFP diluted so that the loading volume was 30  $\mu$ L and prepared the

same way as before to carry out the WB employing a primary FITC-labeled antibody against GFP, as all the receptors used were GFP-tagged.

Table 9. Gel (10%) arrangement for SDS-PAGE to test a FITC-labeled antibody against GFP after developing the WB, where: L – 4  $\mu$ L of PageRuler Plus Ladder.

		OTR-GFP	V1aR-GFP	V1bR-GFP													
1	2	3	4	5	6	7	8	9	10	11	12	13	14	15	16	17	18
	L		5 $\mu$ g														

#### 3.2.1.4. Transfer and detection

Two pieces of Whatman filter paper and one piece of PVDF membrane were cut to size 7,5 cm  $\times$  14 cm. Whatman papers were soaked in 1 $\times$  transfer buffer for around 15 min. The membrane was activated by soaking in methanol for 1 min, then washed 3 $\times$  with 1 $\times$  transfer buffer and soaked in 1 $\times$  transfer buffer for another 10 min. The gel casting cassette after electrophoresis was disassembled, stacking gel was cut off, and the resolving gel was washed with MQW, then 3 $\times$  with 1 $\times$  transfer buffer and soaked in 1 $\times$  transfer buffer for 5 min. A sheet of Whatman paper was placed on a semi-dry transfer device, a PVDF membrane was placed on top of it, then the gel was laid down, and on top came the other sheet of Whatman paper. The prepared sandwich was rolled over with a roller to remove any trapped air bubbles. The sandwich was covered with semi-dry device lids, and the current was set to run as follows: for 10% gels at 210 mA for 45 min; for 8% gel at 210 mA for 40 min. After the transfer had finished, the membrane was rinsed 3 $\times$  with MQW, washed 3 $\times$  with 1 $\times$  TBS-T for 10 min on a see-saw shaker, and then soaked in 50 mL of prepared blocking solution for 2.5 h on a see-saw shaker. Membranes coming from 10% gels were then cut into three pieces with equal lane disposition, while the ones from 8% were kept in one piece. Primary antibody solutions were prepared by mixing 1 mL of validated antibody ( $\gamma \approx 5\text{--}7 \mu\text{g/mL}$ ) in a cell medium with 4 mL of blocking solution (around 1:1000) and cut membrane pieces were then incubated in so prepared antibody solutions overnight at 4  $^{\circ}\text{C}$ , with the containers wrapped in plastic foil. Prepared primary antibody solutions were reused to incubate membranes from 8% gels for the specificity check. After incubation, the membranes were washed 3 $\times$  with 1 $\times$  TBS-T for 5 min on a see-saw shaker at RT, then incubated for 1 h at RT in a secondary antibody solution prepared by mixing 6  $\mu$ L

of HRP-conjugated donkey anti-rabbit antibody (DoxRb-HRP, 711-035-153, 1:2 in glycerol) with 30 mL of blocking solution (around 1:10,000). After incubation, the secondary antibody solution was poured out and the membrane was washed 3× with 1× TBS-T for 10 min on a see-saw shaker at RT, and then washed once again with 1× TBS only, since Tween 20 could later interfere with ECL and disturb the chemiluminescent signal during detection causing high background.<sup>170</sup> The solution excess from the membrane was collected with a piece of paper, the membrane was laid on a plastic folder and properly covered in detection substrate ECL max freshly prepared in a brown Falcon tube according to the manufacturer instructions (1:1, luminol/enhancer solution:peroxide solution), depending on the size of the membrane but no more than 6 mL per membrane. After incubation for 5 min, the plastic folder was closed, and the remaining liquid was squeezed out. The covered membrane was then laid into the ChemiDoc imaging system and chemiluminescence was detected. The exposure settings used were either rapid autoexposure or manual exposure, adjusted to avoid overexposed images to the time limit where the image started to appear or disappear. The ladder was also detected without moving the membrane using the colorimetric program.

Western blotting workflow is depicted in a simplified form in Figure 9 to be easier to visualize and understand the important steps.

Control blots employing two commercially available antibodies against OTR and V1aR were carried out, testing their specificity among four different receptors and normal membrane protein fraction. Primary ab124907 rabbit to V1aR and ab300443 rabbit to OTR antibody solutions (1:500) were used, and secondary DoxRb-HRP antibody solution (1:10,000) was used.

Secondary antibody control WBs were performed on the membranes obtained from gels loaded with 20 µg of OTR-GFP or 20 µg of V1aR-GFP. Instead of incubating in the primary antibody solutions, membranes were incubated in the blocking solution under the same conditions. After the incubation in the secondary antibody (DoxRb-HRP; 1:10,000) solution and the ECL reagent, chemiluminescence was detected after both the rapid autoexposure and manual exposure time of 100 s, so that the exposure time and blots obtained are comparable with those from validated antibodies.

Primary FITC-labeled goat polyclonal anti-GFP antibody (ab6662) 1:1000 solution was prepared and the membrane after the transfer was then incubated in it overnight at 4 °C. Since the FITC tag has an excitation maximum of 493 nm and an emission maximum of 528 nm, the

signal after the primary antibody incubation was acquired on the Alexa 488 program. A secondary antibody (DoxGoat-HRP, 260310) 1:2000 solution was used to finish the blot, and the chemiluminescence was detected together with the colorimetric blot.

In some of the first experiments performed while optimizing conditions for conducting WBs, gels after SDS-PAGE or after transfer were stained to visualize separated protein bands or transfer success, respectively. These images will not be included as they served only to determine conditions under which all the other blots would later be performed, and do not provide any significant information for the purpose of this study. To conduct such an experiment, the following solutions were prepared: 1 L of fixation solution by mixing 500 mL of methanol with 100 mL of acetic acid and filling up with MQW to 1 L; 150 mL of staining solution by dissolving 0.15 g of Coomassie Brilliant Blue dye in 150 mL of prepared fixation solution; 1 L of acetic acid ( $\varphi = 7.5\%$ , destaining solution) by mixing 75 mL of acetic acid with MQW.

Proteins in the gel after SDS-PAGE or after transfer for some of the experiments leading to the optimization of conditions were fixed by incubating in prepared fixation solution for 10 min on a see-saw shaker for 10 min. After fixation, the gel was stained with the prepared staining solution until it appeared blue and then soaked in acetic acid ( $\varphi = 7.5\%$ ) solution to remove excess coloring. Results will also not be included for the reasons discussed.

Another type of staining was tried in the initial experiments to showcase the success of the semi-dry transfer, but instead of staining the gel, the membrane was stained. After the transfer finished, the membrane was taken out of the semi-dry device and rinsed 3× with Milli-Q water, and then soaked in Ponceau S solution for around 5 min on a see-saw shaker at RT. Ponceau S is a reversible dye,<sup>171</sup> and was successfully washed off in water, which enabled the protein bands to be distinguishable if present at all. Results will also not be included for the reasons discussed.

Yet another way of staining the membrane was employed, this time after chemiluminescence detection to prove the success of transfer and visualize the presence of separated protein bands on the membrane. These images will be included to support blot images provided. To conduct such an experiment, the following solutions were prepared: 100 mL of amido black staining solution by mixing 25 mL of propan-2-ol with 10 mL of acetic acid, dissolving 100 mg of naphthol blue black and filling up with UPW, making the composition of



the solution: naphthol blue black ( $1 \text{ g dm}^{-3}$ ), propan-2-ol ( $\varphi = 25\%$ ), acetic acid ( $\varphi = 10\%$ ); 500 mL of acetic acid ( $\varphi = 5\%$ , destaining solution) by mixing 25 mL of acetic acid with MQW.

Membranes after chemiluminescence detection were washed in water on a see-saw shaker overnight at RT and then stained with amido black staining solution for 1 min. Then, destained with acetic acid ( $\varphi = 5\%$ ) by washing twice for 1 min. Membranes were then washed in water twice for 10 min, and after washing left to air-dry. When dried, membranes were laid into the ChemiDoc imaging system and an amido black signal was detected. One could assume that due to the presence of the blocking reagent BSA on the membrane, no bands would be distinguishable. But, the cationic residues of basic amino acids bind the anionic groups of the dye, resulting in different proteins being able to bind the dye with varying affinities, allowing for the distinction of the proteins on the membrane.<sup>172</sup>

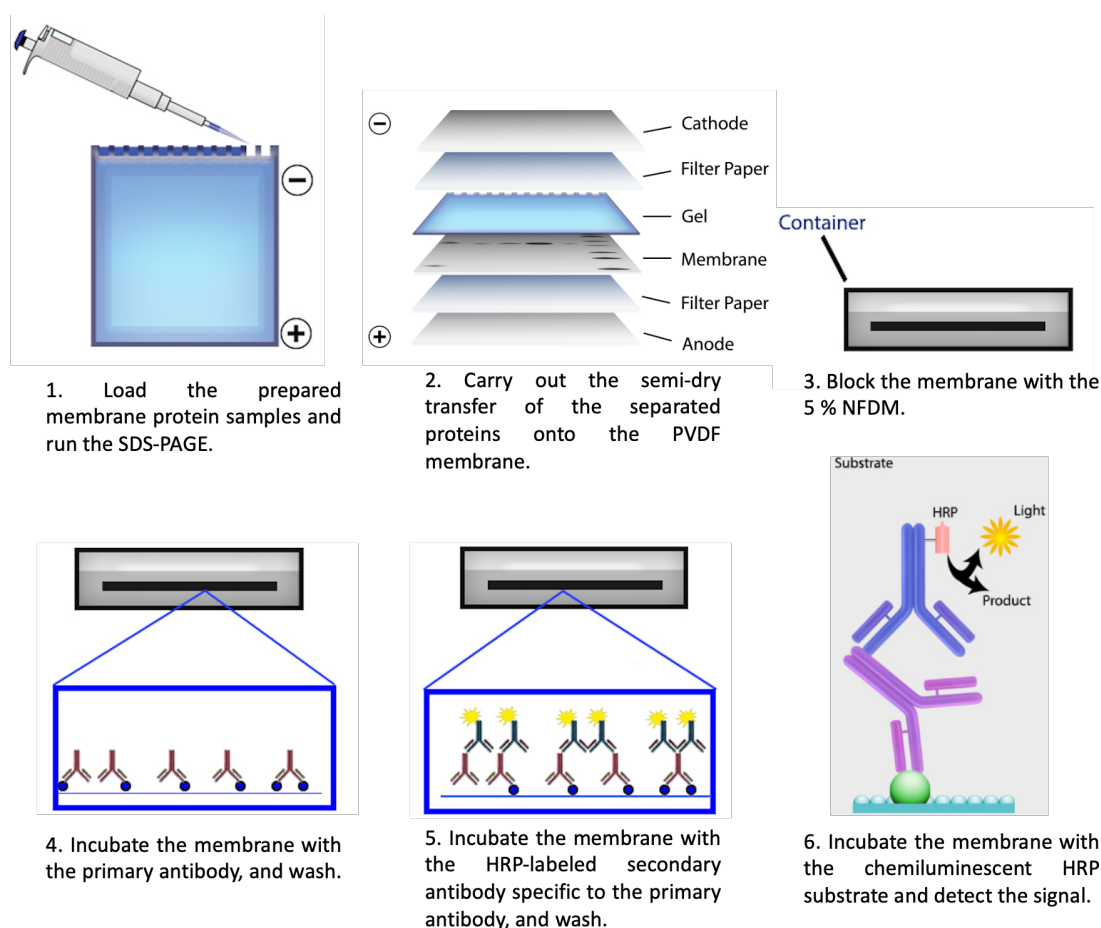


Figure 9. Workflow for the western blotting procedure. Taken and adapted from BioLegend.com [<sup>173</sup>].

### 3.2.2. Immunoprecipitation

To conduct the IP, the following solutions were prepared: 400 mL of 1× PBS-T (1× PBS + Tween 20,  $\varphi = 0.1\%$ ) by dissolving 400  $\mu\text{L}$  of Tween 20 in PBS and filling up to 400 mL; 100 mL of glycine (200  $\text{mmol dm}^{-3}$ , pH 2.0) by dissolving 1.50 g of glycine ( $M = 75.07 \text{ g/mol}$ ) in around 90 mL of UPW and further titrating with prepared HCl (aq, 1:1) down to pH of 2.0 (measured with the pH-meter) and then filling up to 100 mL; 100 mL of urea buffer without EDTA by mixing 48.05 g of urea ( $M = 60.06 \text{ g/mol}$ ), 5 mL of TEAB (1.0  $\text{mol dm}^{-3}$ , pH  $8.5 \pm 0.1$ ), 4 g of CHAPS ( $M = 614.9 \text{ g/mol}$ ) and 1.54 g of DTT ( $M = 154.25 \text{ g/mol}$ ), dissolving in UPW and filling up to 100 mL, making the composition of the buffer: urea (8  $\text{mol dm}^{-3}$ ), TEAB (50  $\text{mmol dm}^{-3}$ ), CHAPS (40  $\text{g dm}^{-3}$ ), DTT (100  $\text{mmol dm}^{-3}$ ); 100 mL of urea (8  $\text{mol dm}^{-3}$ ) in TEAB (50  $\text{mmol dm}^{-3}$ ) by mixing 48.05 g of urea ( $M = 60.06 \text{ g/mol}$ ) and 5 mL of TEAB (1.0  $\text{mol dm}^{-3}$ , pH  $8.5 \pm 0.1$ ), dissolving in UPW and filling up to 100 mL; 100 mL of TEAB (50  $\text{mmol dm}^{-3}$ ) by mixing 5 mL of TEAB (1.0  $\text{mol dm}^{-3}$ , pH  $8.5 \pm 0.1$ ) with UPW and filling up to 100 mL; IAA (0.5  $\text{mol dm}^{-3}$ ) by dissolving IAA ( $M = 184.96 \text{ g/mol}$ ) in MQW after which the volume was separated into microtubes containing 1 ml of so prepared solution and stored in dark at  $-20 \text{ }^\circ\text{C}$ .

Since all validated antibodies were of rabbit origin, protein A-coated magnetic beads were used.<sup>158</sup> SureBeads Protein A were thoroughly resuspended in their solution and 100  $\mu\text{L}$ , i.e., 1 mg of SureBeads ( $\gamma = 10 \text{ mg/mL}$ ) was transferred to 1.5 mL low-binding tubes labeled accordingly. Beads were magnetized on the magnetic rack and the supernatant was discarded. Beads were then washed 4× with 1 mL of PBS-T, with each wash step including short vortexing, spin-down, magnetizing, and discarding the supernatant. To the washed SureBeads was added 1 mL of validated antibody ( $\gamma \approx 5\text{--}7 \text{ } \mu\text{g/mL}$ ) in a cell medium and the tubes were rotated for 1.5 h at the speed of 18 rpm at RT. Antibody-bound beads were magnetized, supernatants were stored (to reuse in case no antibody would bind) and the beads were washed 4× with 1 mL of PBS-T. Depending on the concentration of the solubilized OTR-GFP and V1aR-GFP stock solutions, the appropriate volume (from approx. 200 to 400  $\mu\text{L}$ ) that corresponded to around 200  $\mu\text{g}$  of receptor protein on average was added to corresponding antibody-bound beads and the volume was adjusted to 500  $\mu\text{L}$  in each tube with the solubilization buffer. Tubes were rotated for 2 h at the speed of 18 rpm at RT. Beads were magnetized, supernatants were collected as an FT (flow-through) fraction and the beads were washed 4× with 1 mL of PBS-T, all washings collected in the same falcon tube as a W

(washing). Beads were then eluted by adding 25  $\mu\text{L}$  of glycine (200  $\text{mmol dm}^{-3}$ , pH 2.0) and incubating for 5 min on a shaker at 600 rpm at RT. Beads were magnetized and the eluate was transferred to a new tube labeled with E (eluate fraction). Elution was repeated with another 25  $\mu\text{L}$  of glycine, and the eluate was then combined with the already collected fraction. Beads were, after adding 1 mL of PBS-T, stored at 4 °C. Since the concentration of target protein in the eluate fraction was supposed to be high (before further dilutions) and no detergent to interfere with signals on MS spectra should have been present, from each eluate was taken 10  $\mu\text{L}$  for MS-analysis to search for the intact/undigested receptors. To the remaining 40  $\mu\text{L}$  of each eluate was added 200  $\mu\text{L}$  of ice-cold acetone (1:5, eluate:acetone) and was left overnight at -20 °C to precipitate. Precipitated samples were centrifugated for 30 min at 14,000 g at 4 °C. Supernatants were transferred to other tubes and protein precipitates were left out on air for several minutes to dry. After, proteins were solubilized by adding 90  $\mu\text{L}$  of urea buffer without EDTA and vortexing several times, then leaving on a shaker for 3 h at RT. To each sample was added 10  $\mu\text{L}$  of IAA (0.5  $\text{mol dm}^{-3}$ ), samples were vortexed and then left to incubate for 30 min in the dark. VIVACON 500 filter units (cut-off  $30 \times 10^3$ ) were washed by adding 200  $\mu\text{L}$  of urea (8  $\text{mol dm}^{-3}$ ) in TEAB (50  $\text{mmol dm}^{-3}$ ) and centrifugated for 15 min at 12,000 g at 21 °C. Flow-through was discarded from the collection tube. To each sample after incubation in the dark was added 100  $\mu\text{L}$  of urea (8  $\text{mol dm}^{-3}$ ) in TEAB (50  $\text{mmol dm}^{-3}$ ), samples were vortexed, and all 200  $\mu\text{L}$  of samples were transferred to the filter units and then centrifugated for 15 min at 12,000 g at 21 °C. Filter units were transferred to new collection tubes, washed 3 $\times$  by adding 200  $\mu\text{L}$  of urea (8  $\text{mol dm}^{-3}$ ) in TEAB (50  $\text{mmol dm}^{-3}$ ) and centrifugating for 15 min at 12,000 g at 21 °C to eliminate the CHAPS from the samples. Together with CHAPS, DTT could have been eliminated because once it reduced all disulfide bridges, all the produced thiol groups were alkylated with IAA into a form that cannot be reoxidized back into disulfide bridges.<sup>174</sup> Filter units were additionally washed 3 $\times$  by adding 100  $\mu\text{L}$  of TEAB (50  $\text{mmol dm}^{-3}$ ) and centrifugating for 10 min at 12,000 g at 21 °C. Collecting tubes with the flow-through were discarded and filter units were transferred to new collecting tubes. To filter units was then added 40  $\mu\text{L}$  of TEAB (50  $\text{mmol dm}^{-3}$ ) to avoid them from drying while preparing trypsin for digestion. To a vial of trypsin was added 200  $\mu\text{L}$  of trypsin resuspension buffer, and to each filter unit was then added 40  $\mu\text{L}$  of prepared trypsin solution. Filter units were closed and wrapped in parafilm, shaken for 1 h at 37 °C, and left to incubate overnight at 37 °C without shaking. After an overnight (around 16 h) digestion, filter units were centrifugated for 20 min

at 12,000 g at 21 °C into the clean collection tubes, into which was collected every solution onward. Filter units after adding 100 µL of TEAB (50 mmol dm<sup>-3</sup>) were centrifugated for 10 min at 12,000 g at 21 °C, and this step was repeated once. To stop digestion, 10 µL of pure formic acid was then added directly into the collection tube and vortexed, pH was checked with a universal indicator to be around 2. Samples were taken to a Speed-Vac (45 °C) to evaporate for a couple of hours and then brought to MS-centre for analysis. See Figure 10 for the visual representation of the IP protocol.

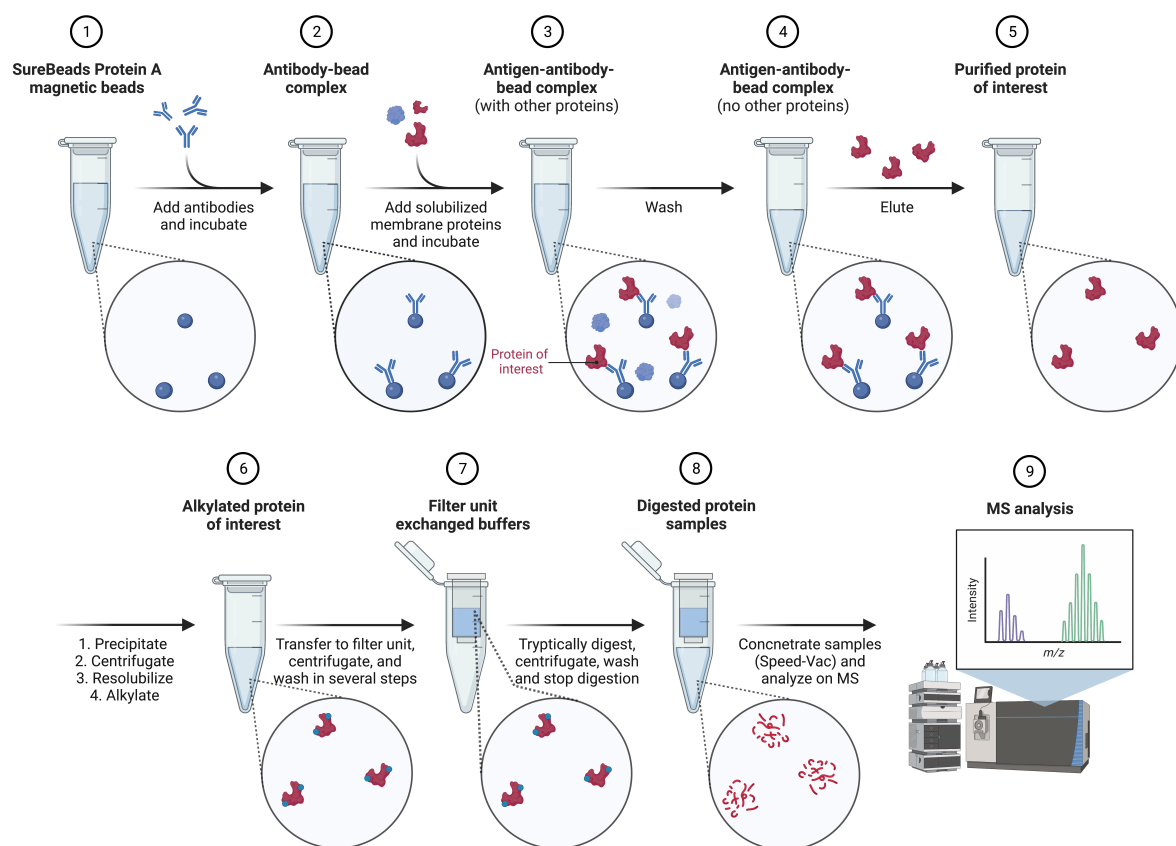


Figure 10. IP workflow. Created with BioRender.com [167].

Controls that were carried out for the IP include the following: non-specific IgG control, where 5 µL = 5 µg of Normal Rabbit IgG was added to 200 µL of solubilization buffer and added to beads instead of validated antibodies; Beads control, where 200 µL of solubilization buffer was added to beads instead of validated antibodies. The IP procedure was followed for both controls as described above for both the OTR-GFP and V1aR-GFP samples.

Another control was performed: Receptor control, where the samples of solubilized receptors for both OTR-GFP and V1aR-GFP were tryptically digested, without prior purification with magnetic beads. To 90  $\mu\text{L}$  of solubilized OTR-GFP (1062.9  $\mu\text{g}/\text{mL}$ ) and to 90  $\mu\text{L}$  of solubilized V1aR-GFP (867.4  $\mu\text{g}/\text{mL}$ ) was added 10  $\mu\text{L}$  of IAA, left in the dark for 30 min, and after dark incubation added 100  $\mu\text{L}$  of urea (8  $\text{mol dm}^{-3}$ ) in TEAB (50  $\text{mmol dm}^{-3}$ ) and transferred to filter units. The rest of the procedure leading to digestion and peptide detection on MS stayed the same as described.

To check that the protein concentration after the binding was reduced, the BCA protein assay as described before was conducted for FT fractions, considering the decrease of concentration caused by adjusting the volume to 500  $\mu\text{L}$  in each tube in the calculation. BCA assay was also conducted for pure W fractions, to check if any protein was washed off from the beads during the washing steps. Results will not be included as they don't provide any meaningful information for this research but will be briefly discussed here. The concentrations determined for FT fractions after the binding decreased, indicating that the beads bound with antibody had pulled down some protein from the protein mixture. Ideally, the pulled down protein should be the corresponding receptor. Concentrations determined for W fractions were negative values, suggesting that during the washing steps, no undesired washout had occurred.

### 3.2.3. Mass spectrometry

#### 3.2.3.1. Nano liquid chromatography tandem mass spectrometry Velos method - digested protein

Mass spectra were obtained using LTQ Orbitrap Velos mass spectrometer (Thermo Fisher Scientific, Bremen, Germany) equipped with a nanospray ion source, coupled to the nano HPLC-system (UltiMate 3000, Dionex). 5  $\mu\text{L}$  of the sample was first loaded on a pre-column (trap column) Acclaim PepMap100 (Thermo Scientific, 100  $\mu\text{m} \times 2 \text{ cm}$ , nanoViper C18, 5  $\mu\text{m}$ , 100  $\text{\AA}$ ) using ( $\varphi(\text{ACN}) = 2\%$ ,  $\varphi(\text{H}_2\text{O}) = 98\%$ ,  $\varphi(\text{FA}) = 0.1\%$ ) at a flow rate of 10  $\mu\text{L}/\text{min}$ . Separation was carried out on a C18 analytical column Acclaim PepMap RSLC (Thermo Scientific, 75  $\mu\text{m} \times 50 \text{ cm}$ , nanoViper C18, 2  $\mu\text{m}$ , 100  $\text{\AA}$ ) at a flow rate of 300  $\text{nL}/\text{min}$ .

- Column Oven Temperature = 40.0  $^{\circ}\text{C}$
- Mobile phase A: ( $\varphi(\text{ACN}) = 2\%$ ,  $\varphi(\text{H}_2\text{O}) = 98\%$ ,  $\varphi(\text{FA}) = 0.1\%$ )
- Mobile phase B: ( $\varphi(\text{ACN}) = 80\%$ ,  $\varphi(\text{H}_2\text{O}) = 20\%$ ,  $\varphi(\text{FA}) = 0.1\%$ )
- Gradient: see Table 10

Table 10. Flow gradient for peptide separation on a C18 analytical column.

Retention / min	Flow / $\mu\text{L min}^{-1}$	$\varphi(\text{B}) / \%$	$\varphi(\text{A}) / \%$	Curve
0.000	0.300	2.0	98.0	-
0.000	0.300	2.0	98.0	5
10.000	0.300	5.0	95.0	5
105.000	0.300	60.0	40.0	5
110.000	0.300	100.0	0.0	5
115.000	0.300	100.0	0.0	5
118.000	0.300	2.0	98.0	5
135.000	0.300	2.0	98.0	5

MS1 scans were acquired in positive ion mode at 350–1500 m/z range at a resolution of 60,000 (FWHM at 400 m/z). Using a data-dependent acquisition mode, the 6 most intense precursor ions of all precursor ions with +2 to +4 and up charge were selected for fragmentation at 35% normalized collision energy and analyzed in the orbitrap at a resolution 15,000 (at m/z = 400) (digested\_HR) and the second acquisition were analyzed in the ion trap (digested\_LR). The dynamic exclusion for the selected ions was 30 s. The electrospray voltage was 2.1 kV and the ion transfer capillary temperature was 300 °C.

### 3.2.3.2. Nano liquid chromatography tandem mass spectrometry Velos method - intact protein

Mass spectra were obtained using LTQ Orbitrap Velos mass spectrometer (Thermo Fisher Scientific, Bremen, Germany) equipped with a nanospray ion source, coupled to the nano HPLC-system (UltiMate 3000, Dionex). 5  $\mu\text{L}$  of the sample was first loaded on a  $\mu$ -precolumn (trap column) PepMap300 (Thermo Scientific, 300  $\mu\text{m}$  i.d.  $\times$  5 mm, C4, 5  $\mu\text{m}$ , 300  $\text{\AA}$ ) using ( $\varphi(\text{ACN}) = 2\%$ ,  $\varphi(\text{H}_2\text{O}) = 98\%$ ,  $\varphi(\text{FA}) = 0.1\%$ ) at a flow rate of 10  $\mu\text{L}/\text{min}$ . Separation was carried out on a C4 analytical column Accucore (Thermo Scientific, 75  $\mu\text{m}$   $\times$  50 cm, nanoViper C4, 2.6  $\mu\text{m}$ , 150  $\text{\AA}$ ) at a flow rate of 300 nL/min.

- Column Oven Temperature = 40.0 °C
- Mobile phase A: ( $\varphi(\text{ACN}) = 2\%$ ,  $\varphi(\text{H}_2\text{O}) = 98\%$ ,  $\varphi(\text{FA}) = 0.1\%$ )
- Mobile phase B: ( $\varphi(\text{ACN}) = 80\%$ ,  $\varphi(\text{H}_2\text{O}) = 20\%$ ,  $\varphi(\text{FA}) = 0.1\%$ )
- Gradient: see Table 11

Table 11. Flow gradient for protein separation on a C4 analytical column.

Retention / min	Flow / $\mu\text{L min}^{-1}$	$\varphi(\text{B}) / \%$	$\varphi(\text{A}) / \%$	Curve
0.000	0.300	2.0	98.0	-
0.000	0.300	2.0	98.0	5
10.000	0.300	10.0	90.0	5
25.000	0.300	60.0	40.0	5
26.000	0.300	100.0	0.0	5
30.000	0.300	100.0	0.0	5
31.000	0.300	2.0	98.0	5
35.000	0.300	2.0	98.0	5

MS1 scans were acquired in positive ion mode at 400–2500 m/z range at a resolution of 7500 (FWHM at 400 m/z) (second acquisition at a resolution of 60000). The electrospray voltage was 2.1 kV and the ion transfer capillary temperature was 300 °C.

## § 4. RESULTS

### 4.1. Western blot

Seven rabbit monoclonal antibodies against V1aR and ten rabbit monoclonal antibodies against OTR obtained from Origene company were tested by WBs using solubilized membrane protein fractions of C-terminally GFP-tagged hOTR, hV1aR, hV1bR and hV2R stably overexpressing cells (HEK293) and native HEK293 cells. Two types of blots were conducted: one type exhibiting different signal strengths due to different amounts of the receptor for the appropriate antibody tested; and the second type testing the specificity of the tested antibody among four different receptors and normal membrane protein fraction.

The specificity of two commercially available antibodies was also tested by WB among four different receptors OTR-GFP, V1aR-GFP, V1bR-GFP, V2R-GFP and native HEK293 membrane protein fraction.

Since no native receptors, but rather the GFP-tagged receptors were used for the experiments, a WB employing primary FITC-labeled antibody against GFP was performed, and the signal was acquired on Alexa 488 program. As visible in Figure 11A, weak bands are present at  $\sim 102 \times 10^3$  for OTR-GFP and  $\sim 85 \times 10^3$  for V1bR-GFP, together with some weak bands accumulated at the entry to the gel. A secondary DoxGoat-HRP antibody was employed to finish the blot, and the result is displayed in Figure 11B. Strong bands are visible at  $\sim 102 \times 10^3$  and at the entry for OTR-GFP, medium strong bands at  $\sim 85 \times 10^3$  and at the entry for V1bR, and weak bands at  $\sim 102 \times 10^3$  and at the entry for V1aR-GFP. The same localization of the primary and secondary antibody signals suggests that the secondary antibody only bound to, and thus amplified the signal of the primary antibody. Furthermore, the presence of only two bands per lane suggests that the lower one denotes the position of the migrated receptor, while the upper one possibly indicates receptor aggregates that did not enter the gel.<sup>22</sup>



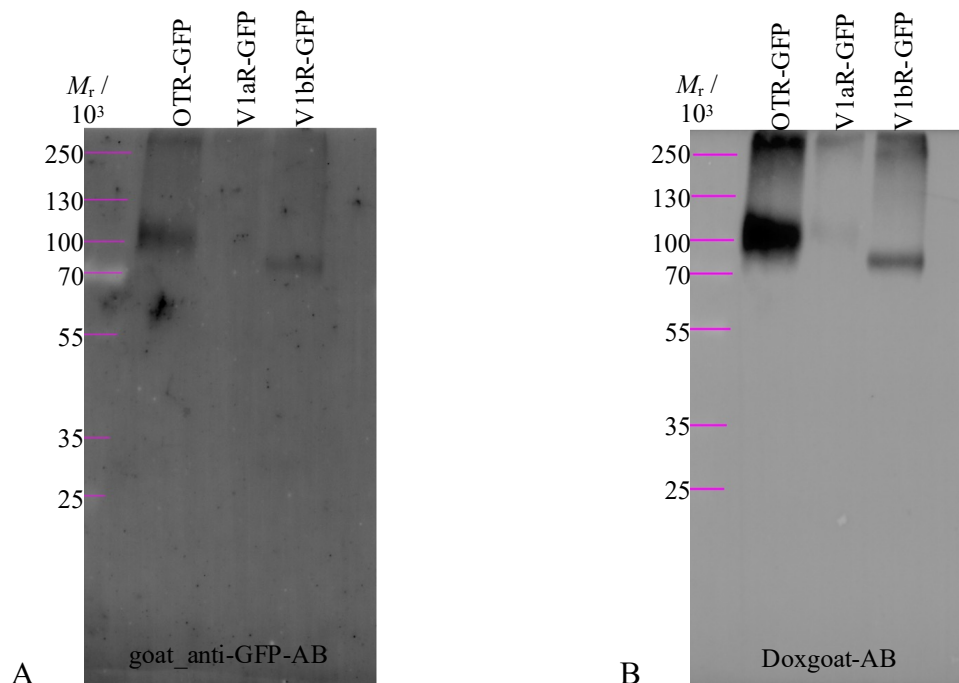


Figure 11. A – Alexa 488 acquired signal after incubation in primary FITC goat anti-GFP antibody, ab6662 (1:1000), 2 s manual exposure; B – Chemiluminescence acquired signal after incubation in secondary DoxGoat-HRP antibody (1:2000) and Clarity, 9.412 s rapid autoexposure; Each lane contains 5  $\mu\text{g}$  of the marked receptor.

WBs employing two commercially available antibodies against OTR and V1aR have also been carried out to test for their specificity. Primary ab124907 rabbit to V1aR and ab300443 rabbit to OTR antibody solutions (1:500) were used, and secondary DoxRb-HRP antibody solution (1:10,000) was used. Figure 12A displays the result of the V1aR antibody blot, with multiple bands visible, and two prominent bands at  $\sim 115 \times 10^3$  and  $\sim 130 \times 10^3$  across all the lanes. The manufacturer-reported WB results indicate the presence of a single band at  $\sim 47 \times 10^3$ , which corresponds to the size of native human V1aR. Since our samples contain C-terminally GFP-tagged receptors, the presence of multiple bands at higher molecular weights for all the lanes, including HEK2393 control that does not have the receptor expressed, implies that the tested antibody lacks specificity. The lower of the two more prominent bands (highlighted in red) was assumed to be due to PTMs related to the previously observed band in the blot experiment employing an anti-GFP antibody.<sup>175</sup> The V1aR-GFP band position expected from the anti-GFP antibody blot is also indicated under the observed band. Alternatively, the signals may be non-specific since the tag-altered receptors may not be recognized by the antibody. However, the

10 s exposure time that was used to acquire the image likely means that the signal is coming from the secondary antibody bound strictly to the primary, as it often takes longer to obtain a signal, as later will be seen. Figure 12B presents an amido black staining of the membrane after the chemiluminescence detection, confirming the success of the transfer.

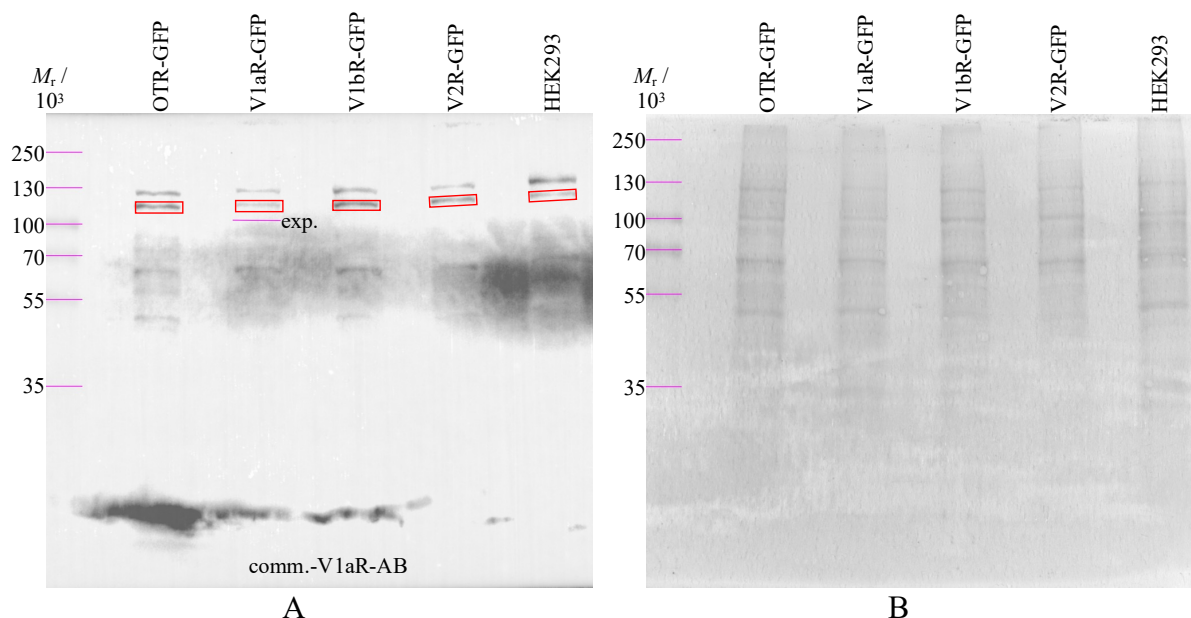


Figure 12. A – Specificity of commercial primary rabbit to V1aR antibody, ab124907 (1:500) after incubation in secondary DoxRb-HRP antibody (1:10,000) and Clarity Max, 10 s manual exposure, in red  $\sim 115 \times 10^3$ ; B – Amido black staining after chemiluminescence detection.

The outcome of the commercial OTR antibody blot is presented in Figure 13A, with two stronger bands repeating across all the lanes, one at  $\sim 53 \times 10^3$  and the other at  $\sim 115 \times 10^3$ . A single lane observed by the manufacturer for the native human OTR is at  $\sim 55 \times 10^3$ , which differs from the sequence predicted band position at  $\sim 43 \times 10^3$ , likely due to PTMs, such as glycosylation for which OTR has three N-glycosylation sites,<sup>176</sup> or phosphorylation which was observed to happen before.<sup>177</sup> Such modifications are known to commonly reduce binding of SDS to transmembrane proteins, which in turn decreases the protein migration rate and shifts the band to higher molecular weights.<sup>178,179</sup> If not for PTM, shift could be due to recognition of another protein. The presence of multiple bands in our receptor samples and in the HEK293 control without the receptor expression suggests that the tested antibody also lacks specificity. The higher of the two more prominent bands (highlighted in red) could be related to the already observed band in the blot experiment using an anti-GFP antibody, and to the band observed while testing the other commercial antibody against V1aR. The OTR-GFP band position

expected from the anti-GFP antibody blot is also indicated under the observed band. The lower band found at around the same position as the one observed by the manufacturer suggests that it may represent the same protein, which in that case would not be OTR, but something else. Signal acquisition lasted for 50 s, and the longer exposure time is comparable to the manufacturer's WB, which took 3 min for the OTR antibody, and up to 1 min for the V1aR antibody. Figure 13B demonstrates the success of the transfer with an amido black stain.

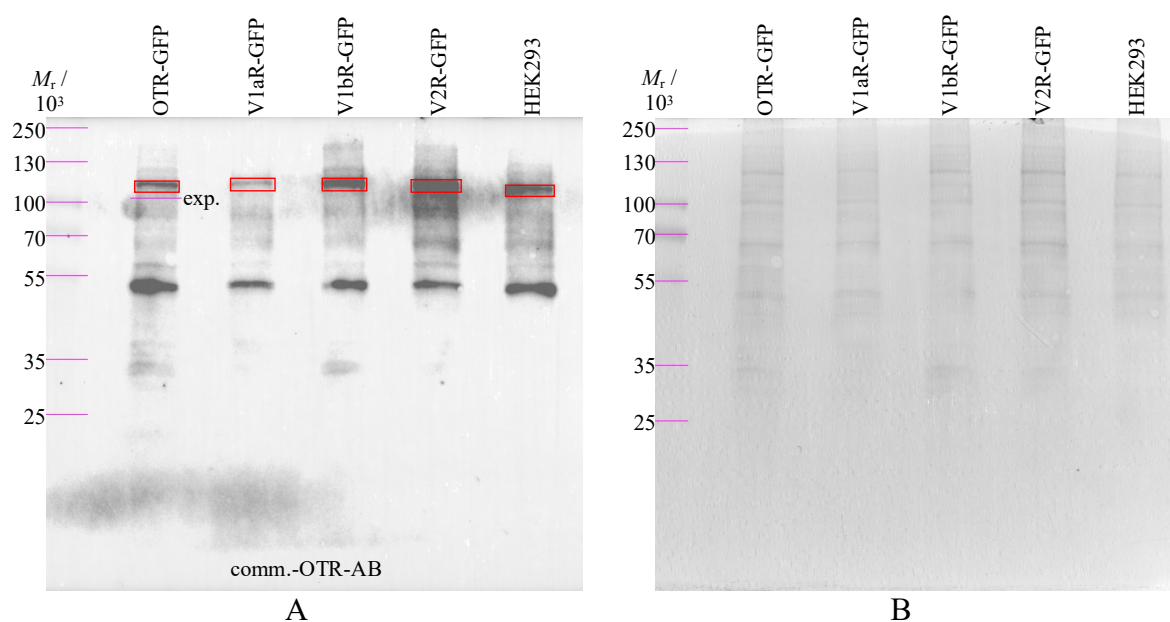


Figure 13. A – Specificity of commercial primary rabbit to OTR antibody, ab300443 (1:500) after incubation in secondary DoxRb-HRP antibody (1:10,000) and Clarity Max, 50 s manual exposure, in red  $\sim 115 \times 10^3$ ; B – Amido black staining after chemiluminescence detection.

#### 4.1.1. Antibodies against vasopressin 1a receptor

One of the most promising WB results comes from the 1G1 primary antibody against V1aR. The blot demonstrating the chemiluminescent signal's reliance on receptor protein load is presented in Figure 14A, with the confirmation of successful transfer in Figure 14B. Strong bands are located on top of the membrane, at the position corresponding to that of the entry to the gel, suggesting the presence of the aggregates being recognized and strongly bound by the 1G1 antibody. Really weak bands are barely visible at  $\sim 115 \times 10^3$  (highlighted in red), possibly due to only a smaller part of the receptor protein entering the gel, hence causing a faint signal. The V1aR-GFP band position expected from the anti-GFP antibody blot is also indicated under the observed band. A more interesting result is displayed in Figure 15A, with the signal present

in only one lane – the one corresponding to the V1aR-GFP sample. Given that the tested 1G1 is indeed an antibody raised against V1aR peptide, demonstrating the highest reactivity towards its N-terminus epitope, and that such a strong signal was observed after only 15 s of exposure, this strongly suggests that the antibody selectively recognized V1aR-GFP and that it is specific for V1aR-GFP. The faint band is also present at  $\sim 115 \times 10^3$ , which as mentioned earlier could be the smaller proportion of the receptor entering the gel. However, if this explanation was correct, then receptor protein aggregates should be visible at the entry to the gel for all the antibodies' blots that have this band at  $115 \times 10^3$ . Such aggregate bands were observed in the blot employing the anti-GFP antibody, along with equally strong bands something lower, at  $\sim 102 \times 10^3$ . Yet, no aggregate bands were observed for the commercial antibodies, which raises doubts about the source of the recurrent bands at  $\sim 115 \times 10^3$ . To confirm the identity of this protein band, in-gel or on-membrane digestion could be performed and generated peptides sent to MALDI-MS or LC-MS/MS for analysis and protein characterization.<sup>169,180,181</sup>

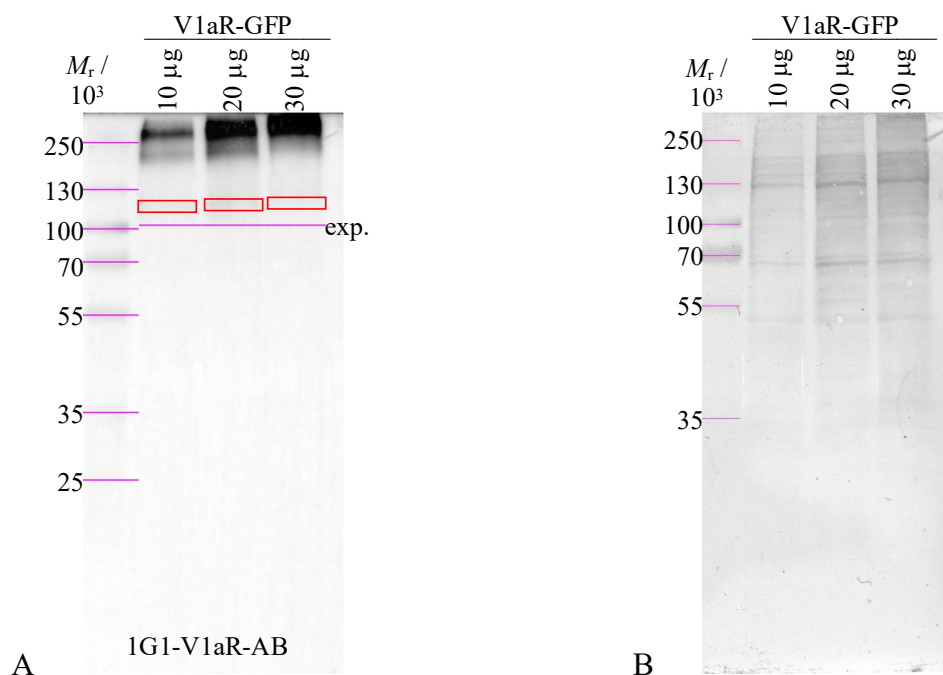


Figure 14. A – 1G1 antibody ( $\sim 1:1000$ ) signal dependence on V1aR-GFP load after incubation in secondary DoxRb-HRP antibody (1:10,000) and Clarity Max, 8.260 s rapid autoexposure, in red  $\sim 115 \times 10^3$ ; B – Amido black staining after chemiluminescence detection.

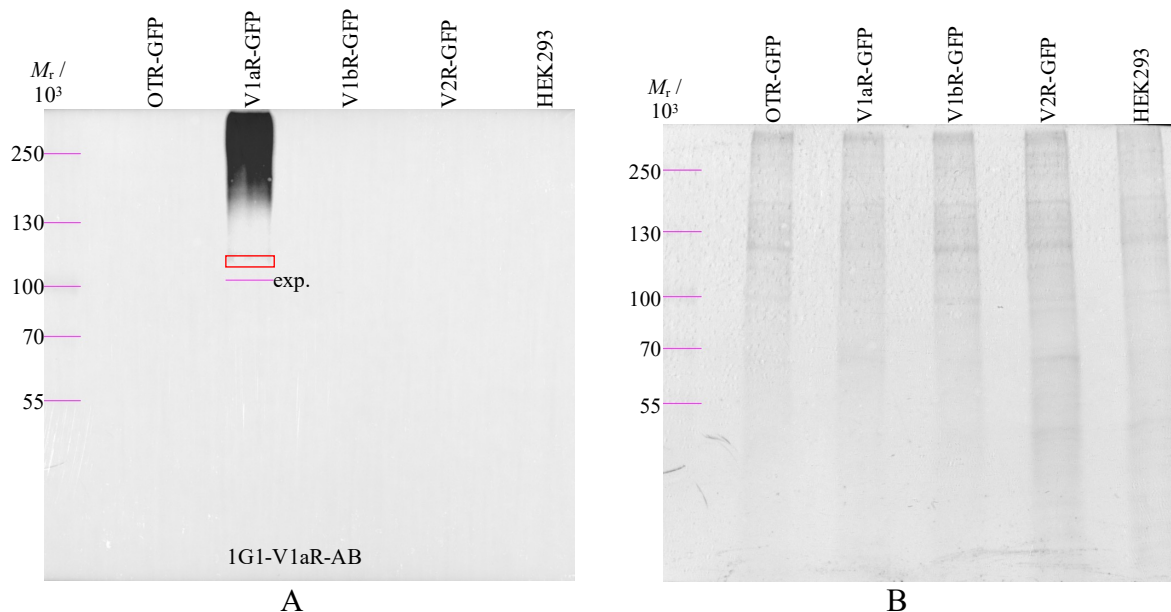


Figure 15. A – Specificity of primary 1G1 antibody ( $\sim 1:1000$ ) after incubation in secondary DoxRb-HRP antibody (1:10,000) and Clarity Max, 15 s manual exposure, in red  $\sim 115 \times 10^3$ ; B – Amido black staining after chemiluminescence detection.

An interesting case happened with the 4G9 antibody against V1aR (Figure 16A). The antibody strongly recognized some protein at the lower part of the membrane (highlighted in green), out of range to accurately determine the molecular weight based on the visible ladder bands. Figure 16B demonstrates the transfer success. The molecular weight of the recognized protein was determined to be  $\sim 30 \times 10^3$  from the specificity blot in Figure 17A, where the more visible ladder allowed for it. The same band is present for all four receptor samples, but also for the HEK293 control, proving its' non-specificity for the target protein.

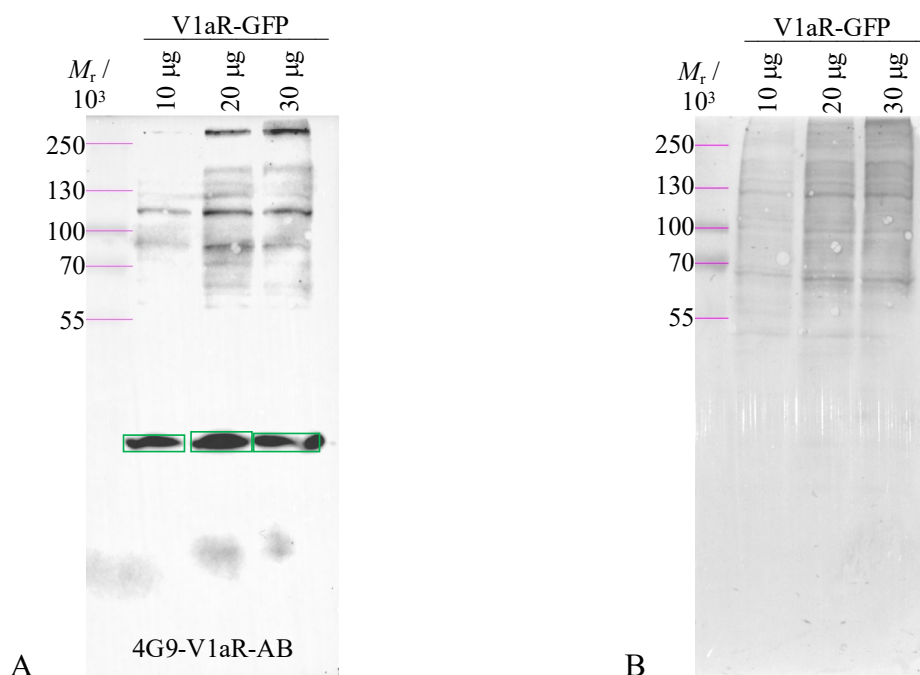


Figure 16. A – 4G9 antibody (~1:1000) signal dependence on V1aR-GFP load after incubation in secondary DoxRb-HRP antibody (1:10,000) and Clarity Max, 66.839 s rapid autoexposure, in green  $\sim 30 \times 10^3$ ; B – Amido black staining after chemiluminescence detection.

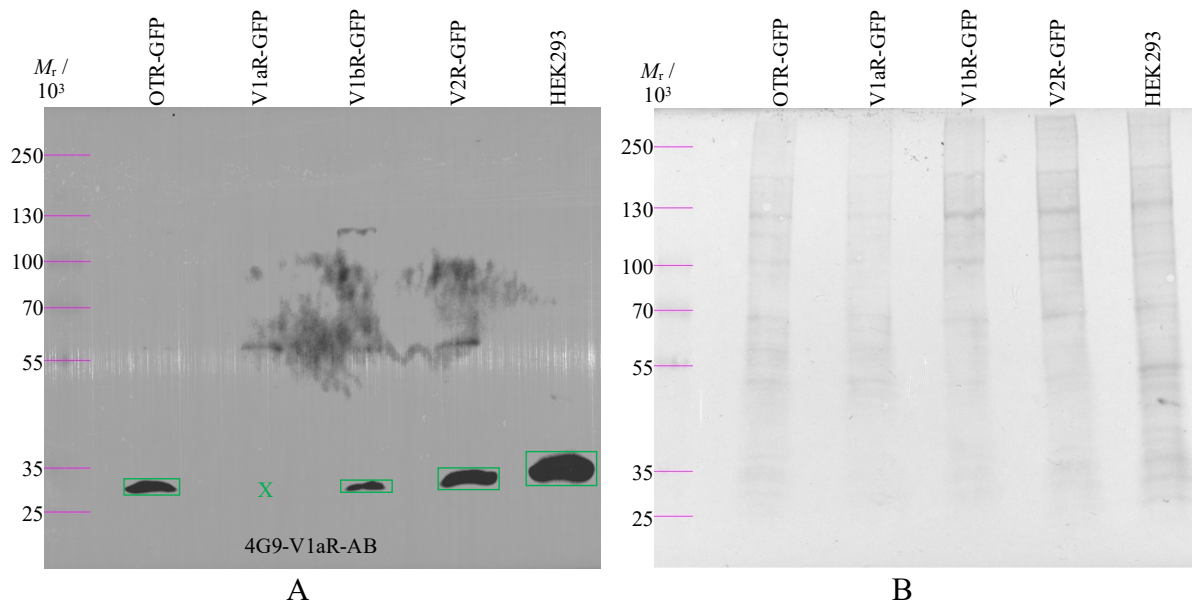


Figure 17. A – Specificity of primary 4G9 antibody (~1:1000) after incubation in secondary DoxRb-HRP antibody (1:10,000) and Clarity Max, 30 s manual exposure, in green  $\sim 30 \times 10^3$ ; B – Amido black staining after chemiluminescence detection.



Although not representable, two additional V1aR antibodies' blots will be discussed as these antibodies successfully bound V1aR-GFP in IP experiments, as will be demonstrated later.

The first of the two antibodies, 3D2, exhibited no bands after a rapid autoexposure of  $\sim 127$  s, as can be seen in Figure 18A. The transfer was not a problem as it was shown successful (Figure 18B). On the specificity test at 100 s manual exposure, many non-specific bands appeared, as displayed in Figure 19A. Some of the faint bands are also present at  $\sim 115 \times 10^3$ , but not in the V1aR-GFP lane. This raises the question of whether these bands originate from the non-specific binding of the secondary antibody, and thus the secondary antibody control blot needed to be performed. The transfer was successful (Figure 19B), revealing that the V1aR-GFP protein lane appeared somewhat fainter, which could explain the missing band. SDS-PAGE, and thus WB, linearizes proteins and the recognition determinant can be lost, contrary to IP where the antibody has the ability to recognize conformational epitopes of native 3D protein structures. This is why IP may still result in a positive outcome, even when WB fails to demonstrate any results.

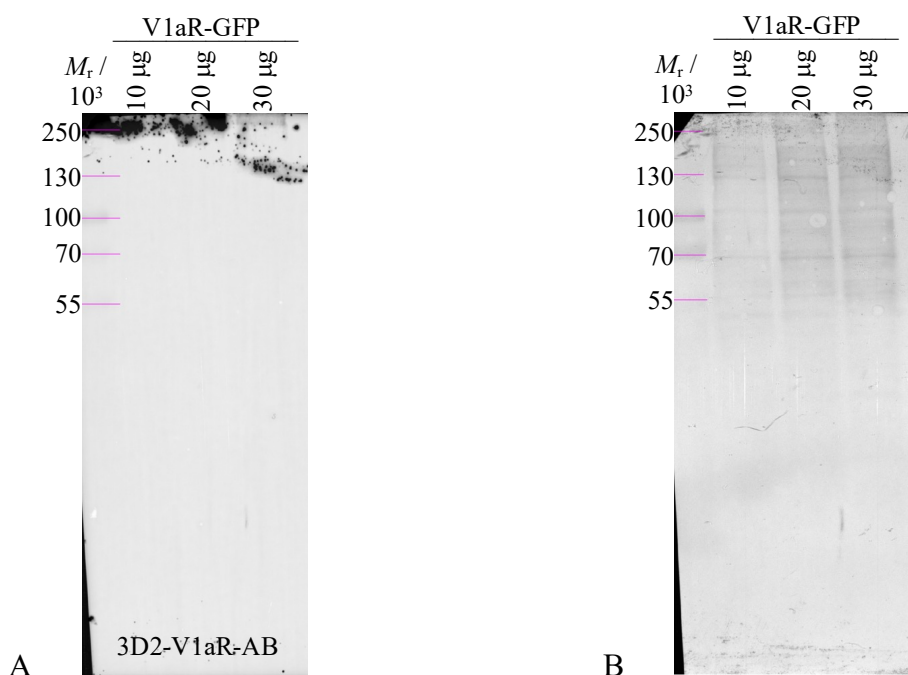


Figure 18. 3D2 antibody ( $\sim 1:1000$ ) signal dependence on V1aR-GFP load after incubation in secondary DoxRb-HRP antibody (1:10,000) and Clarity Max, 126.951 s rapid autoexposure; B – Amido black staining after chemiluminescence detection.

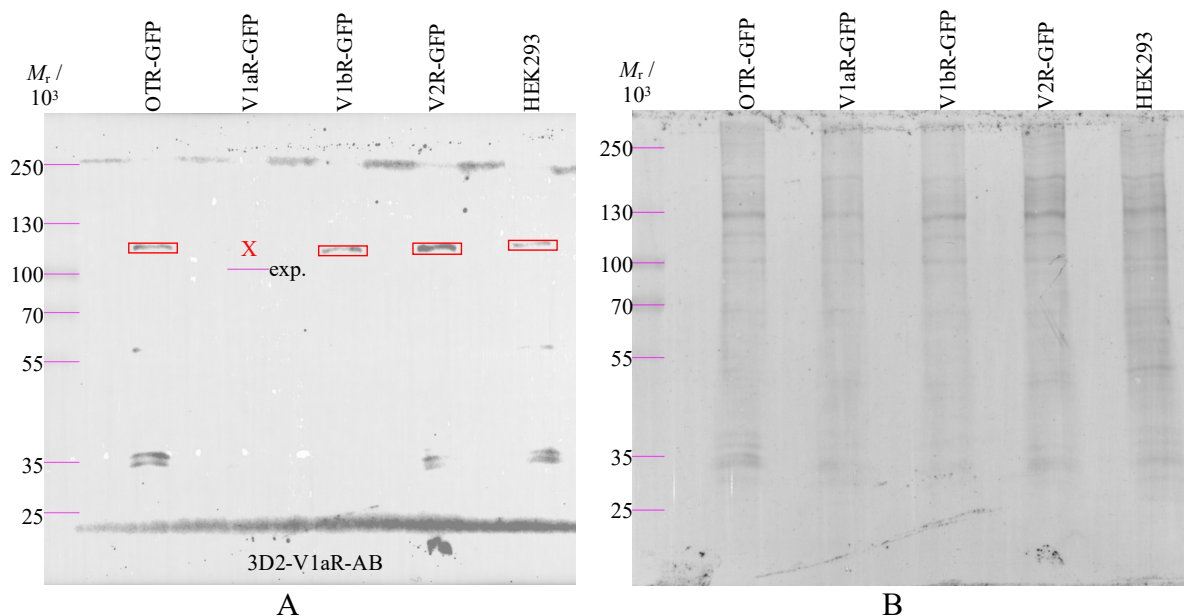


Figure 19. Specificity of primary 3D2 antibody ( $\sim 1:1000$ ) after incubation in secondary DoxRb-HRP antibody (1:10,000) and Clarity Max, 100 s manual exposure, in red  $\sim 115 \times 10^3$ ; B – Amido black staining after chemiluminescence detection.

The second of the two antibodies, 1H1, also displayed no bands after autoexposure of  $\sim 88$  s (Figure 20A). The transfer was successful (Figure 20B). On the specificity test at 180 s manual exposure, many non-specific bands appeared (Figure 21A), with the strongest bands at  $\sim 115 \times 10^3$  present in all five lanes. Here, it took almost double the exposure time to result in band signals, which raises serious suspicions about the non-specific secondary antibody binding. Looking at the receptor regions targeted by the antibodies displaying this band, nothing could be concluded about their connections. The successful transfer is presented (Figure 21B).



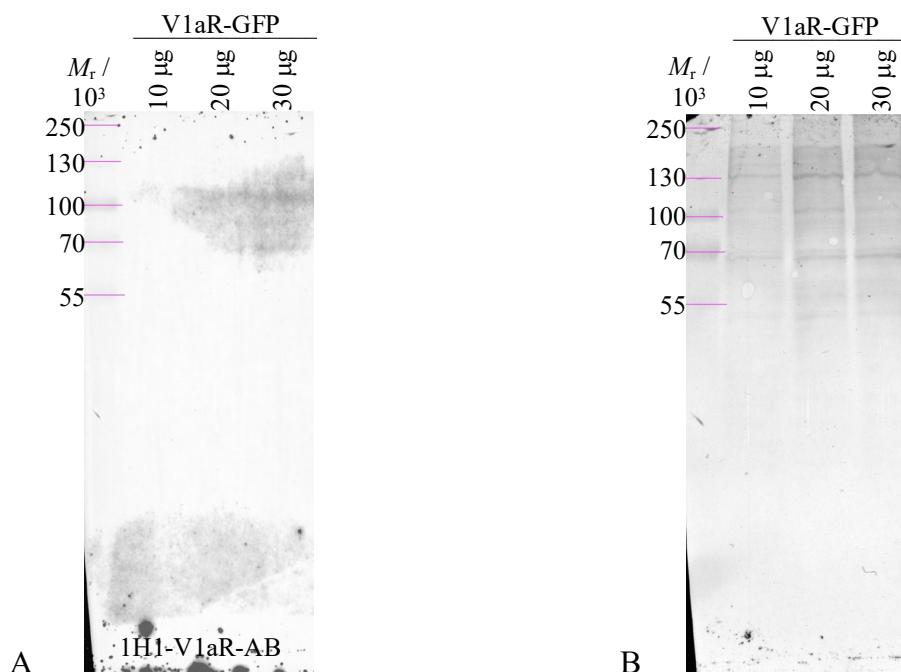


Figure 20. 1H1 antibody (~1:1000) signal dependence on V1aR-GFP load after incubation in secondary DoxRb-HRP antibody (1:10,000) and Clarity Max, 88.164 s rapid autoexposure; B – Amido black staining after chemiluminescence detection.

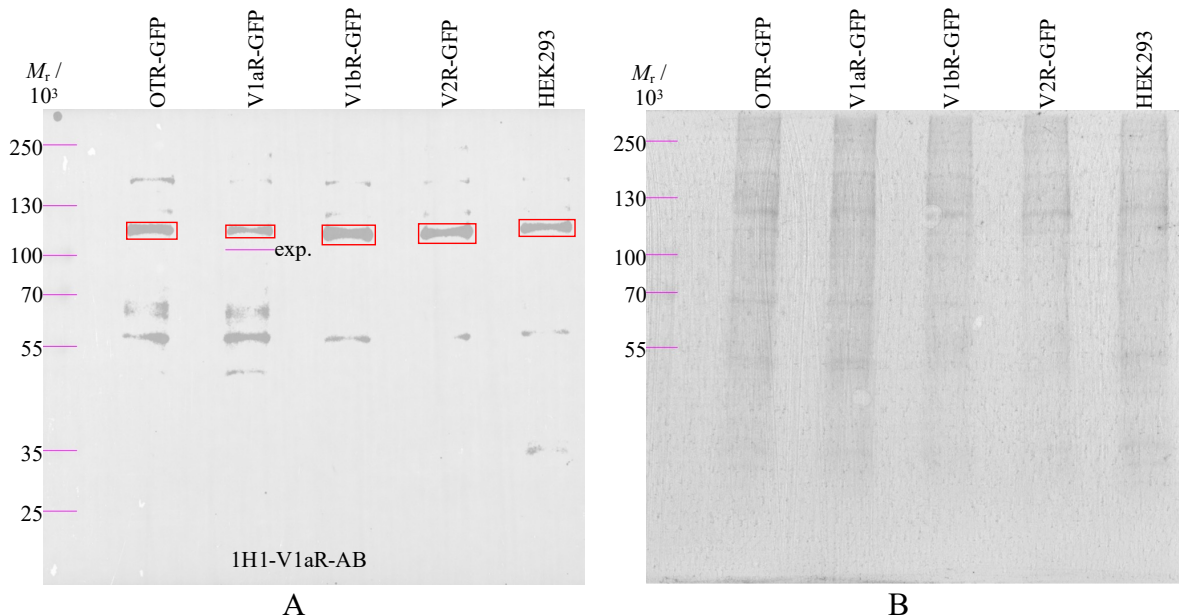


Figure 21. Specificity of primary 1H1 antibody (~1:1000) after incubation in secondary DoxRb-HRP antibody (1:10,000) and Clarity Max, 180 s manual exposure, in red ~115 × 10<sup>3</sup>; B – Amido black staining after chemiluminescence detection.

As mentioned, a secondary antibody control was needed to assess the exposure time needed for the non-specific signals to appear and compare it to the exposure times of the blots carried out with the primary antibodies being validated. Figure 22A exhibits many non-specific bands, the one at  $\sim 115 \times 10^3$  included and being the strongest, after  $\sim 8$  min of rapid autoexposure. To make the exposure times comparable with other signal acquisitions, chemiluminescence was also detected after 100 s manual exposure (Figure 22C). Faint bands are visible to start appearing, with the one at  $\sim 115 \times 10^3$  being the strongest, thus indicating that for such long exposure times for V1aR-GFP samples the band signals originate from the secondary antibody non-specific binding. This leads to the conclusion that for 3D2 and 1H1 antibodies with manual exposure times greater than 100 s blots do not accurately reflect their recognition of the receptor, but rather non-specific signals from the secondary antibody.

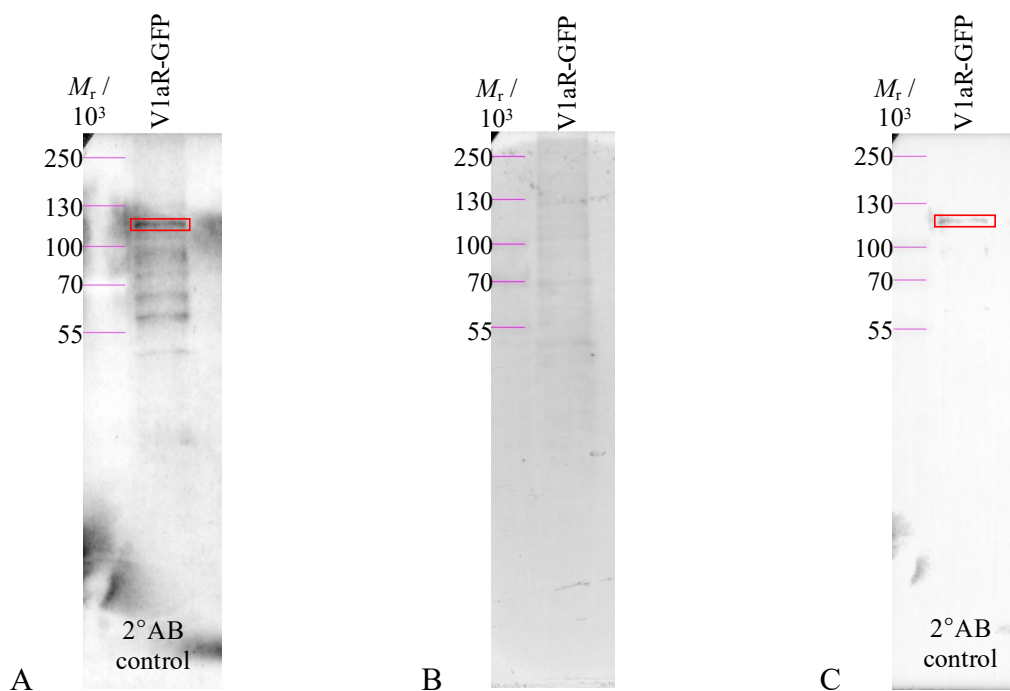


Figure 22. A – secondary antibody (DoxRb-HRP; 1:10,000) control with Clarity Max to 20  $\mu\text{g}$  V1aR-GFP, 487.242 s rapid autoexposure, in red  $\sim 115 \times 10^3$ ; B - Amido black staining after chemiluminescence detection; C – secondary antibody control, 100 s manual exposure, in red  $\sim 115 \times 10^3$ .

The rest of the images of the WB for the antibodies validated against V1aR is given in the appendix.

#### 4.1.2. Antibodies against oxytocin receptor

Secondary antibody control was also performed for the OTR-GFP samples. Figure 23A presents the bands resulting from the non-specific secondary antibody binding after  $\sim 13.5$  min, with the band at  $\sim 115 \times 10^3$  appearing the most prominent. After 100 s manual exposure (Figure 23C), a time comparable to other signal acquisitions, no signal was detected. This leads to the conclusion that for the OTR-GFP samples, secondary antibody generally requires more time to cause non-specific bands than for the V1aR-GFP samples. This could be due to differences in the amount of protein in the loaded samples, or slight variations in concentrations of the antibody solutions, as all these preparations are prone to smaller inconsistencies.

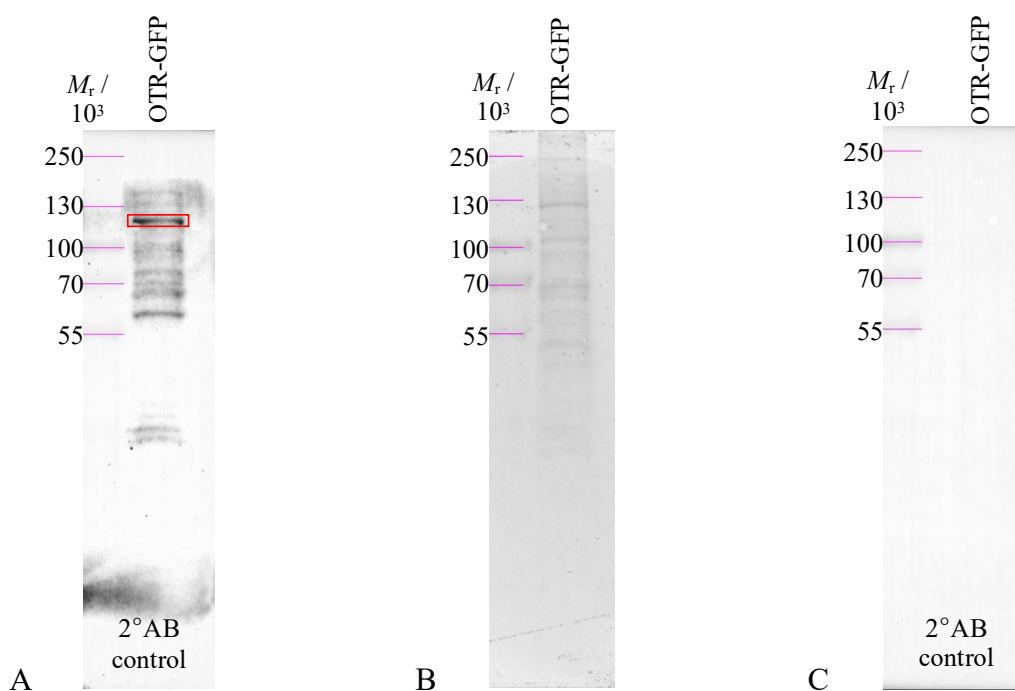


Figure 23. A – secondary antibody (DoxRb-HRP; 1:10,000) control with Clarity Max to 20  $\mu\text{g}$  OTR-GFP, 800.695 s rapid autoexposure, in red  $\sim 115 \times 10^3$ ; B - Amido black staining after chemiluminescence detection; C – secondary antibody control, 100 s manual exposure.

One of the OTR antibodies, 5A5, produced extraordinarily strong bands at  $\sim 115 \times 10^3$  after  $\sim 109$  s rapid autoexposure (Figure 24A) and 50 s manual exposure (Figure 25A) for all the loaded samples. Blots, however, contain some more non-specific bands. To conclude is that despite the primary antibody aiding strong signal production at the band pointed out, the

antibody did not demonstrate any particular specificity towards the receptor of interest compared to the other receptors and proteins present in the loaded samples. It is worth mentioning that the faint bands are visible at the gel entry positions and for the OTR-GFP lanes only, which goes well with the earlier given explanation of possible aggregates formation. Figure 24B and Figure 25B depict successful protein transfers.

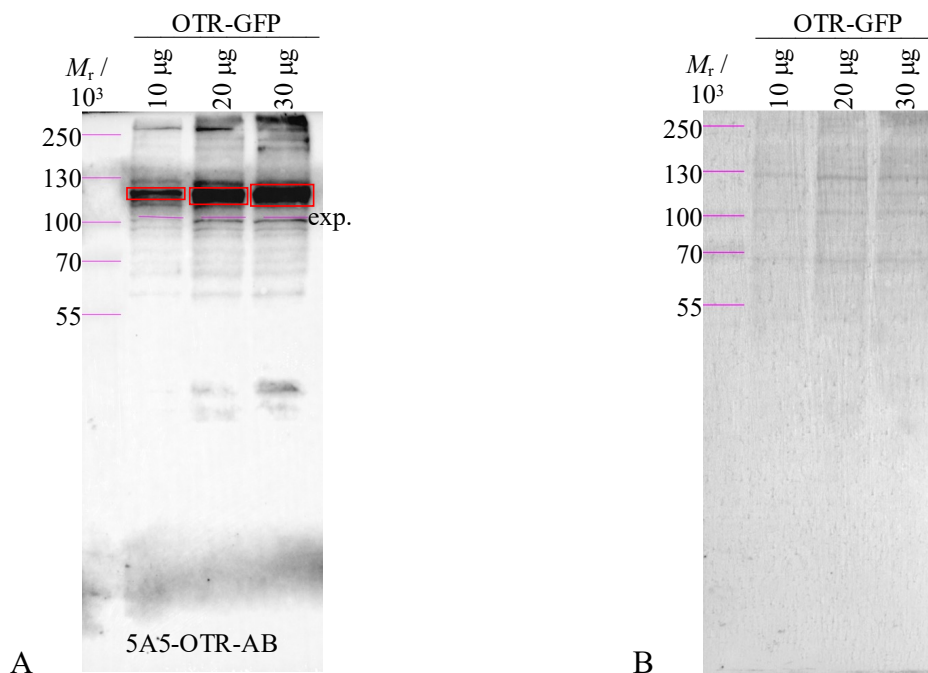


Figure 24. 5A5 antibody ( $\sim 1:1000$ ) signal dependence on OTR-GFP load after incubation in secondary DoxRb-HRP antibody (1:10,000) and Clarity Max, 108.817 s rapid autoexposure, in red  $\sim 115 \times 10^3$ ; B – Amido black staining after chemiluminescence detection.

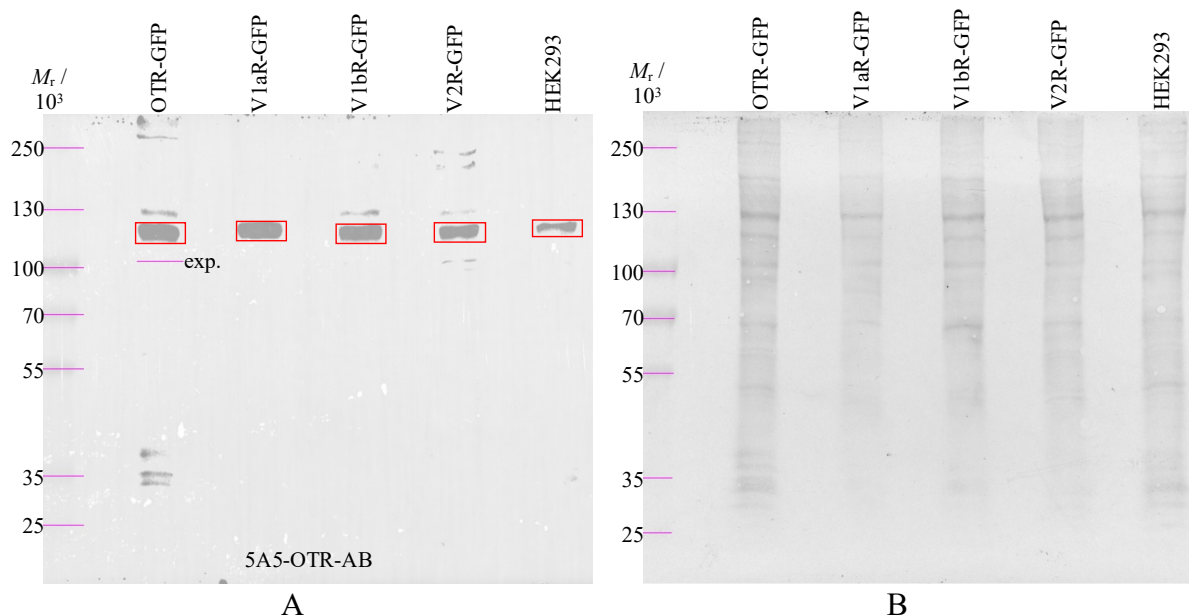


Figure 25. Specificity of primary 5A5 antibody ( $\sim 1:1000$ ) after incubation in secondary DoxRb-HRP antibody (1:10,000) and Clarity Max, 50 s manual exposure, in red  $\sim 115 \times 10^3$ ; B – Amido black staining after chemiluminescence detection.

The strongest band for the 4E3 antibody is not the recurrent one at  $\sim 115 \times 10^3$  (highlighted in red), as can be seen in Figure 26A, but rather slightly higher at  $\sim 125 \times 10^3$ . Figure 26B evidences the protein transfer success. Figure 27B presents a successful transfer for the specificity testing blot. The blot in Figure 27A resulted in band signals after the shortest of all exposure times for the OTR antibodies, after only 15 s. And for such a short exposure time, multiple nonspecific strong bands are present in each sample lane; at  $\sim 185 \times 10^3$ ,  $\sim 125 \times 10^3$ , and  $\sim 67 \times 10^3$ . But being almost equally strong and present in each lane, this would suggest no particular specificity of the tested antibody whatsoever. It could be concluded that the antibody has a strong recognition of the sample proteins, but not necessarily of the target receptors.

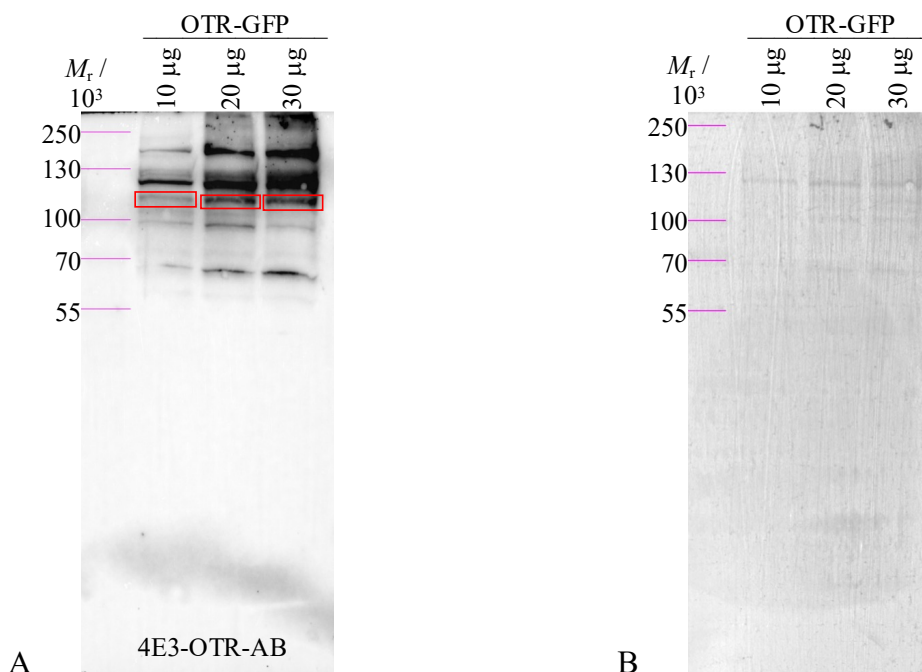


Figure 26. 4E3 antibody ( $\sim 1:1000$ ) signal dependence on OTR-GFP load after incubation in secondary DoxRb-HRP antibody (1:10,000) and Clarity Max, 45.877 s rapid autoexposure, in red  $\sim 115 \times 10^3$ ; B – Amido black staining after chemiluminescence detection.

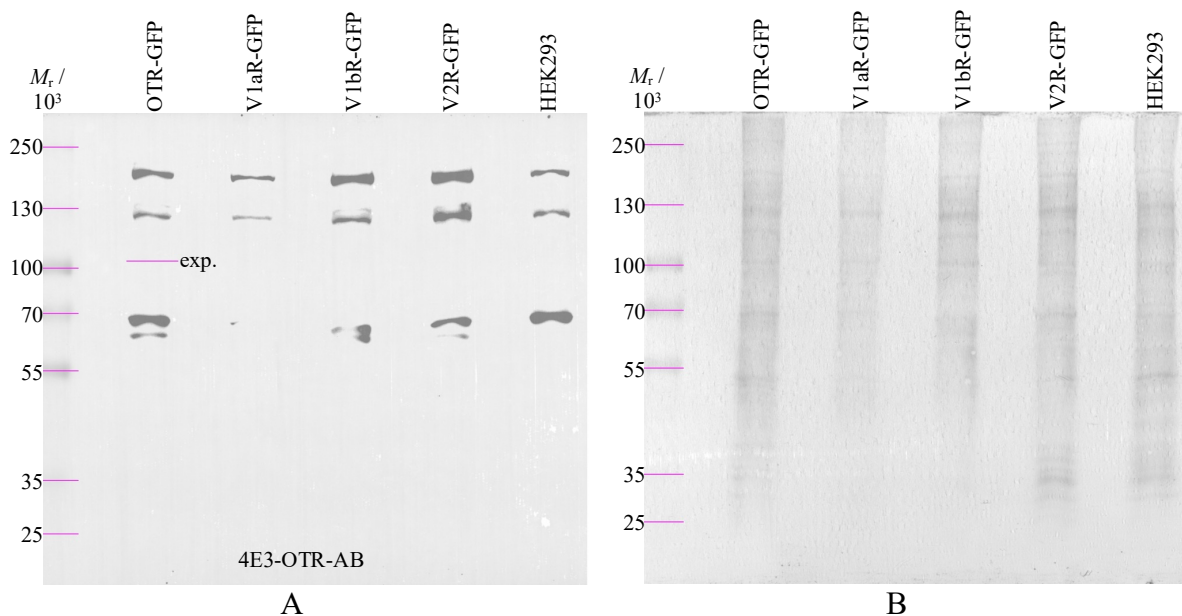


Figure 27. Specificity of primary 4E3 antibody ( $\sim 1:1000$ ) after incubation in secondary DoxRb-HRP antibody (1:10,000) and Clarity Max, 15 s manual exposure; B – Amido black staining after chemiluminescence detection.

For the 1H11 antibody, images were also acquired after a relatively short times of exposure, after  $\sim 39$  s rapid autoexposure and 35 s manual exposure. Figure 28A revealed two fairly strong bands; at  $\sim 115 \times 10^3$  (in red) and somewhat higher at  $\sim 130 \times 10^3$ . Figure 29A displays the same bands, along with additional bands as low as  $\sim 37 \times 10^3$ . However, whatever was recognized by the antibody, no specificity was evident among the receptors. Figure 28B and Figure 29B represent successful transfers.

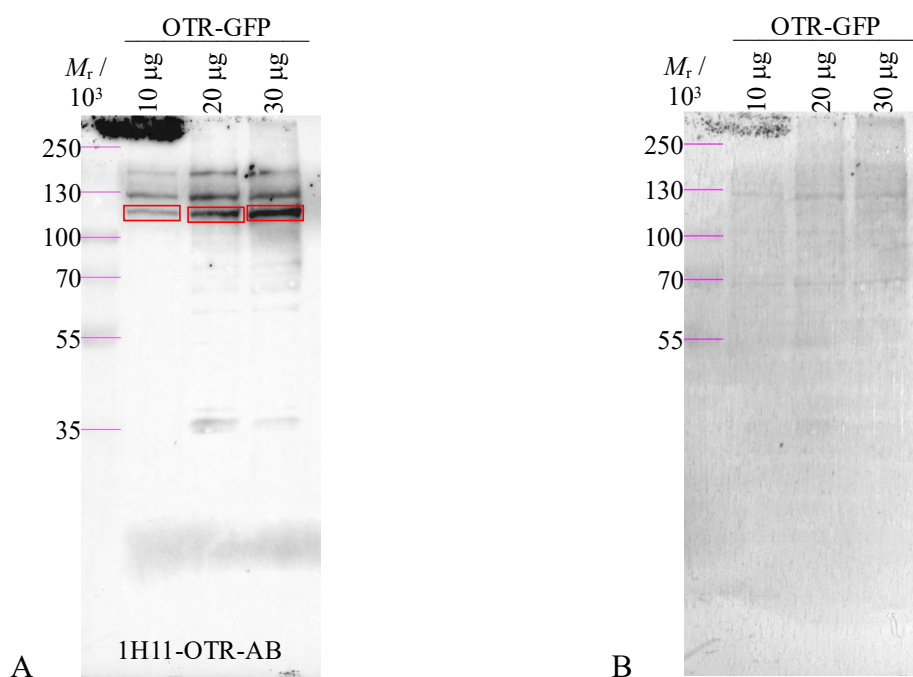


Figure 28. 1H11 antibody ( $\sim 1:1000$ ) signal dependence on OTR-GFP load after incubation in secondary DoxRb-HRP antibody (1:10,000) and Clarity Max, 39.149 s rapid autoexposure, in red  $\sim 115 \times 10^3$ ; B – Amido black staining after chemiluminescence detection.



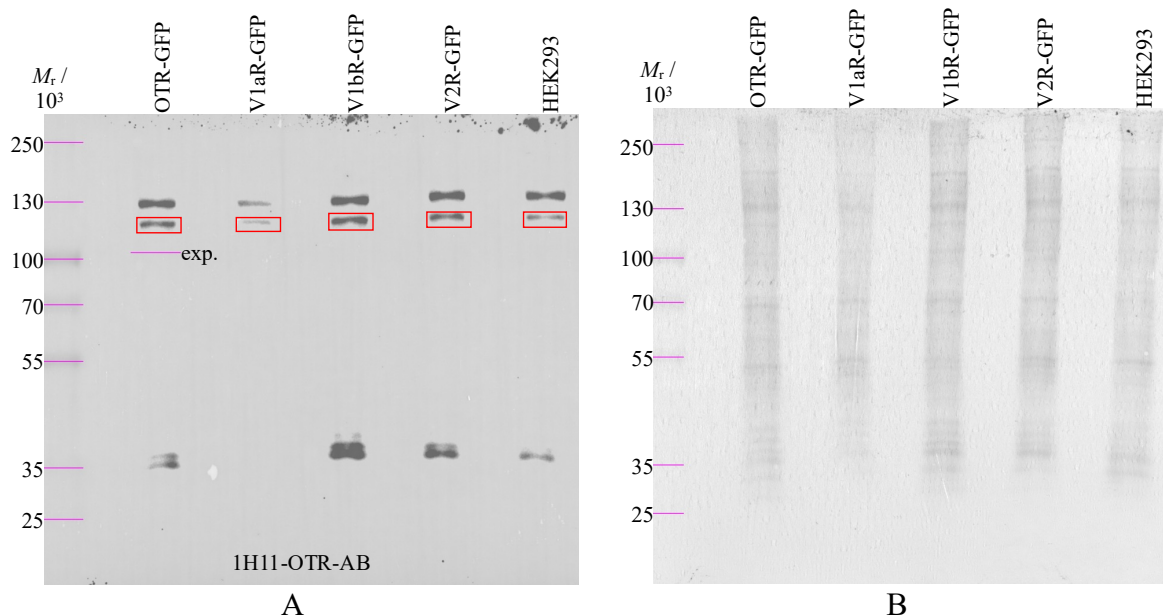


Figure 29. Specificity of primary 1H11 antibody ( $\sim 1:1000$ ) after incubation in secondary DoxRb-HRP antibody (1:10,000) and Clarity Max, 35 s manual exposure, in red  $\sim 115 \times 10^3$ ; B – Amido black staining after chemiluminescence detection.

The rest of the WB images for the antibodies validated against OTR is given in the appendix. WB images for the 1B2 antibody that, later will be shown, delivered positive results in the IP experiment can also be found there as WB did not prove successful for this antibody.

All in all, each of the antibodies validated against V1aR and OTR using WB displayed different, characteristic results. On the anti-GFP blot, bands were observed at the gel entrance and attributed to the possible receptor aggregates. This band also appeared in the 1G1 blot in the respective receptor V1aR-GFP sample lane. Key findings for each of the antibodies discussed above are shortly summarized in Table 12.



Table 12. WB results for antibodies validated against V1aR and OTR; only 1G1 was shown to be specific for the respective recombinant receptor (V1aR-GFP).

Target receptor	Antibody	Epitope region	Observations	Specificity
V1aR	1G1	N-term	- 8–15 s exposure for 20 µg V1aR-GFP load (1:1000 1G1, 1:10,000 DoxRb-HRP) - 1 strong band at gel entrance (receptor aggregates) - 1 faint band at $\sim 115 \times 10^3$ (secondary antibody artefact) - no bands for OTR-GFP, V1bR-GFP, V2R-GFP, and control HEK293	YES
	4G9	ICL-3	- intense band at $\sim 30 \times 10^3$ for all samples (OTR-GFP, V1aR-GFP, V1bR-GFP, V2R-GFP, and control HEK293) - additional non-specific bands	no
	3D2	N-term	- OTR-GFP, V1bR-GFP, V2R-GFP, and control HEK293 displaying non-specific bands, V1aR-GFP no bands at all - non-specific bands for all samples (OTR-GFP, V1aR-GFP,	no
	1H1	C-term	V1bR-GFP, V2R-GFP, and control HEK293) - varying V1aR-GFP loads blot displaying no bands	no
OTR	5A5	ICL-2	- intense band at $\sim 115 \times 10^3$ for all samples (OTR-GFP, V1aR-GFP, V1bR-GFP, V2R-GFP, and control HEK293) - more non-specific bands for all samples	no
	4E3	ICL-2	- non-specific bands for all samples - no $\sim 115 \times 10^3$ band	no
	1H11	C-term	- non-specific bands for all samples (OTR-GFP, V1aR-GFP, V1bR-GFP, V2R-GFP, and control HEK293)	no
- V1aR antibodies (3C1, 3F8, and 4A7) tested, but non-specific				
- OTR antibodies (1A3, 1C10, 1E4, 1F1, 4F3-4, 4F3-5, and 1B2) tested, but non-specific				

## 4.2. Immunoprecipitation

The aim of performing IP-MS was to test the applicability of antibodies in IP. As IP is a technique used to isolate a protein of interest from a complex mixture of proteins, it involves binding the target protein to an antibody that specifically recognizes it. To that end, seven different antibodies against V1aR-GFP and ten antibodies against OTR-GFP were tested following the protocol from Figure 10. Suggesting that the respective receptors were pulled

down, obtained samples were then tryptically digested and the resulting peptides subjected to analysis with MS and to protein identification using different methods and search tools.

Additionally, undigested/intact receptor samples were obtained after elution from the beads that pulled them down, and analysis was conducted using MS. This revealed interesting peaks at around  $73 \times 10^3$ , which were thought to potentially be a small chain of the antibody, or even a large chain, as two peaks were observed at a similar position. The presence of intense CHAPS signals in these samples also motivated us to slightly modify the protocol, to completely remove CHAPS from the final samples for MS analysis, as its' excess in the samples could suppress our signals of interest. For that reason, CHAPS has been removed from the urea buffer in steps for buffer exchange on filter units, and additional washing steps with TEAB were introduced. The size of the protein at around  $73 \times 10^3$  also justified the choice to use filter units with a cut-off value of 30, instead of  $5 \times 10^3$ , as it was anticipated that using a filter with too low of a cut-off value could result in the peptides after digestion becoming stuck and clogging the membrane, given that the peptides bigger than that were expected to be produced with digestion if the receptors with a high proportion of hydrophobicity were present. Apart from that, the analysis of intact samples did not result in receptor detection.

#### 4.2.1. *Antibodies against vassopresin 1a receptor*

Of all the tested antibodies, the 1G1 antibody against the V1aR receptor delivered the most promising results with 6 unique peptides belonging to the V1aR identified by a high-resolution search in Protein Prospector. Five peptides with different sequences were identified (12% sequence coverage), one of which was found in both a modified and unmodified form, with the modified form being oxidized at Met. The same 5 peptides were identified through a high-resolution search in MaxQuant. MaxQuant failed to recognize the special peptide modification detected by the Protein Prospector, justifying the use of the two different protein identification search tools. A Protter illustration<sup>182</sup> of the V1aR protein with the observed peptides highlighted is presented in Figure 30, where the peptide termini correspond to the predicted tryptic digestion sites, suggesting that the identified peptides indeed are the products of the successful digestion of pulled down receptor molecules. As 12% sequence coverage may not seem enough to determine protein in the digested sample, it is important to remember that the protein of interest is a membrane receptor with a large proportion of the sequence belonging to the hydrophobic

transmembrane regions, hence being poorly soluble and consequently unavailable for tryptic digestion. Each detected peptide should be taken into account and given importance.

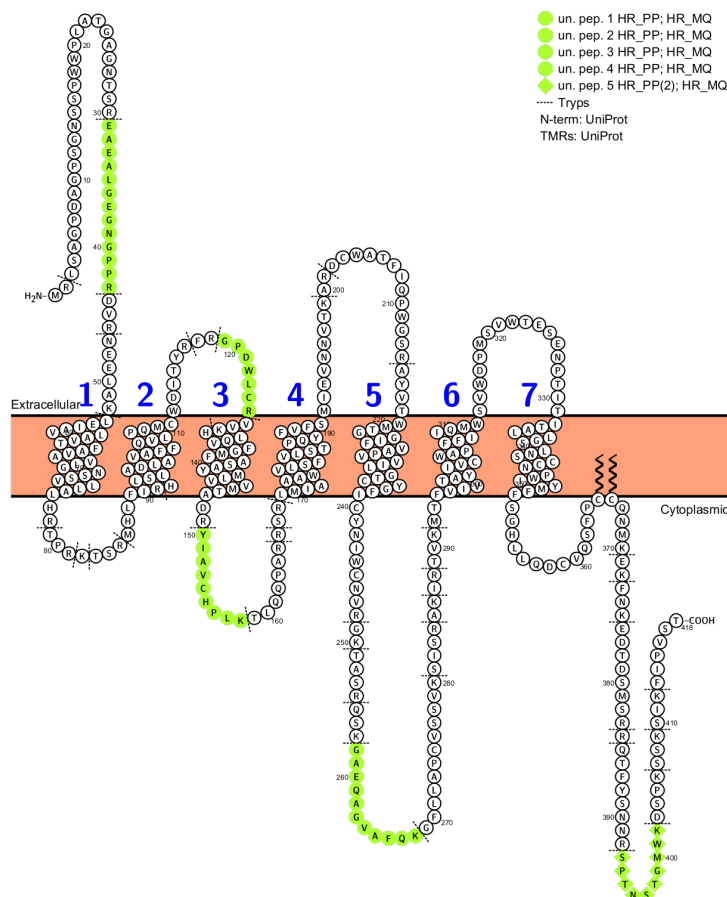


Figure 30. Protter illustrated high-resolution Protein Prospector and high-resolution MaxQuant search results against hV1aR for sample tryptically digested after IP with 1G1 antibody. Identified unique peptide sequences are highlighted in green and predicted tryptic cleavage sites are marked with dashed lines.

Additionally, 5 unique peptides to GFP were identified by performing a high-resolution search in Protein Prospector after IP with 1G1 antibody. Four peptides with different sequences were identified (17.2% sequence coverage), one of which was found in both a modified form oxidized at Met and an unmodified form. This further serves as evidence of the receptor being pulled down by the tested 1G1 antibody, as the receptor carries a GFP tag on its C-terminus. On top of that, ELISA results revealed the highest 1G1 activity towards the other end of the receptor, towards its N-terminus, so the GFP label ideally should not interfere with the

recognition site and the receptor should be perfectly recognizable to the antibody. Observed peptides are portrayed in Figure 31 within the Protter illustration of GFP. Once again, all the peptides produced by tryptic digestion match the peptide sequences and lengths predicted, confirming that both the antibody binding to the target receptor and digestion were successful.

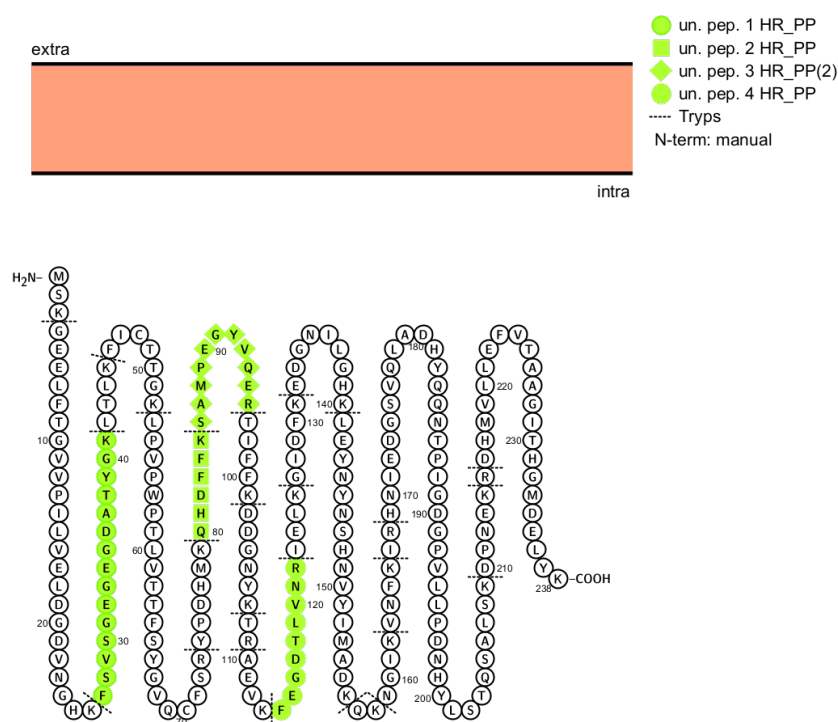


Figure 31. Protter illustrated high-resolution Protein Prospector search result against GFP for sample tryptically digested after IP with 1G1 antibody. Identified unique peptide sequences are highlighted in green and predicted tryptic cleavage sites are marked with dashed lines.

IP-MS results from another antibody demonstrated successful recognition and binding of the V1aR-GFP protein. For the 3D2 antibody, three unique peptides were identified altogether and highlighted in green in Figure 32. One of the peptides was discovered by the low-resolution MaxQuant search, another by the high-resolution MaxQuant search, and the third by the high-resolution Protein Prospector search and the two already mentioned MQ search methods additionally. The overall sequence coverage equals 7.9%. Once again, the employment of multiple search tools and methods was advantageous, as different methods succeeded in recognizing different peptides.

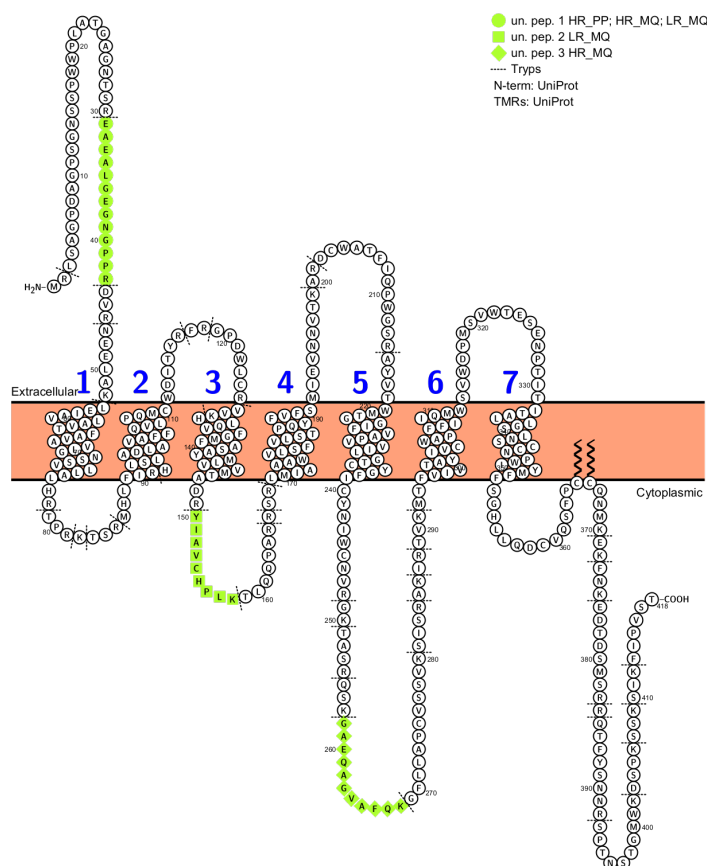


Figure 32. Protter illustrated high-resolution Protein Prospector and high- and low-resolution MaxQuant search results against hV1aR for sample tryptically digested after IP with 3D2 antibody. Identified unique peptide sequences are highlighted in green and predicted tryptic cleavage sites are marked with dashed lines.

1H1 is the final V1aR antibody that led to the receptor fragment recognition. Only one unique peptide was identified with the high-resolution MaxQuant search, equaling 6.7% sequence coverage. Protter illustration with the highlighted peptide is given (Figure 33). All the other V1aR antibodies: 3C1, 3F8, 4A7, and 4G9 did not result in identifying any of the unique peptides to V1aR or GFP after performing IP-MS.

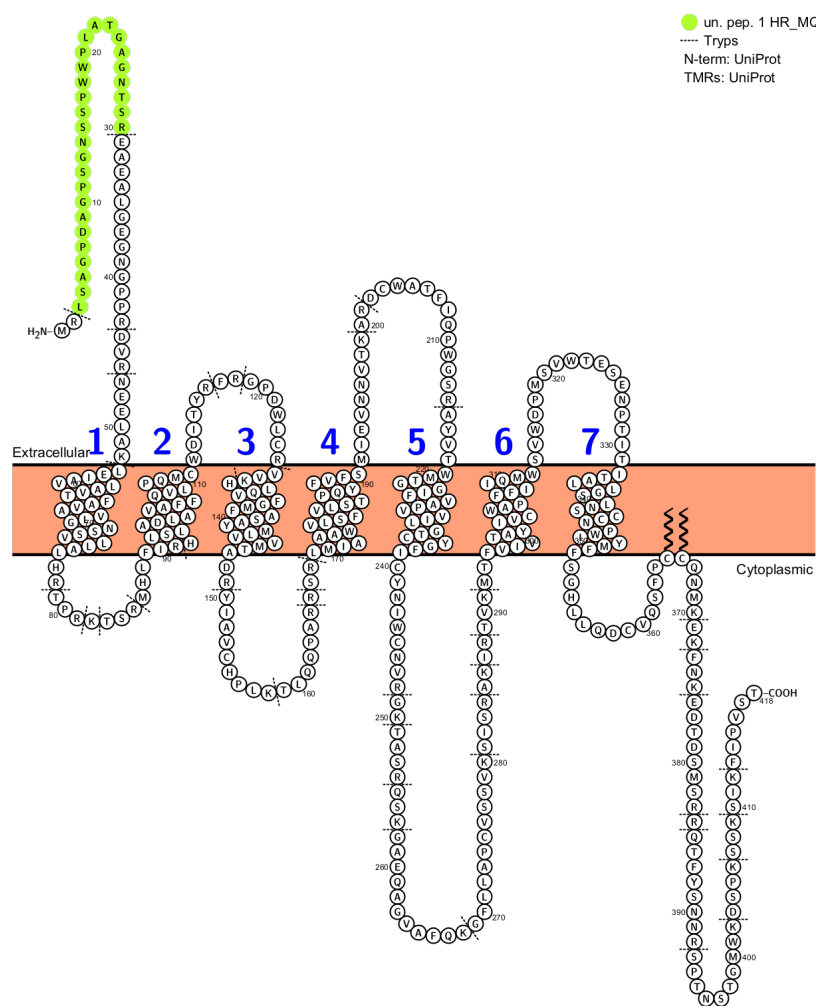


Figure 33. Protter illustrated high-resolution MaxQuant search result against hV1aR for sample tryptically digested after IP with 1H1 antibody. Identified unique peptide sequence is highlighted in green and predicted tryptic cleavage sites are marked with dashed lines.

Controls carried out in conditions without antibody (V1aR\_beads control), and with the non-specific IgG (V1aR\_nsiGg control) did not result in any identified unique peptides belonging to either V1aR or GFP. This indicates that there is no non-specific binding of V1aR-GFP to magnetic beads and suggests that the positive experiment outcomes arise from the specific recognition of the receptor by the antibodies validated.

Another control of the V1aR-GFP tryptic digestion (V1aR control) was also performed and, contrary to expectations, no unique peptides to V1aR or GFP were identified. This control differs from the other experiments in that digestion was performed on the solubilized membrane protein fraction sample and not on the receptor sample purified by IP. Trypsin concentration

---

could have possibly been too low for the number of different proteins present in the sample, which could have potentially had more available sites for trypsin digestion, hence the resulting number of unique peptides in the digested mixture not being enough for detection. Or simply IP step was missing to concentrate the receptors and separate them from the other proteins present in high amounts, whose unique peptides after digestion would mask the detection of receptor's peptides.

#### *4.2.2. Antibodies against oxytocin receptor*

Control of the OTR-GFP tryptic digestion (OTR control) resulted in OTR unique peptides identification. One of the peptides was recognized by HR\_PP, HR\_MQ, and LR\_MQ search methods, and the other which is a two amino acids shorter fragment of the same sequence was only recognized employing HR\_PP. The two amino acids peptides' length difference is because of the two tryptic digestion sites located two amino acids apart, as predicted according to the sequence. Identified peptides are highlighted in the Protter illustration of OTR (Figure 34) together with predicted cleavage sites. It is also visible that the identified unique peptides stem from the 3<sup>rd</sup> intracellular loop, the largest of all the loops with multiple predicted tryptic cleavage sites. Due to the loop size, a certain degree of flexibility could be assumed to facilitate trypsin access, site recognition, and digestion.

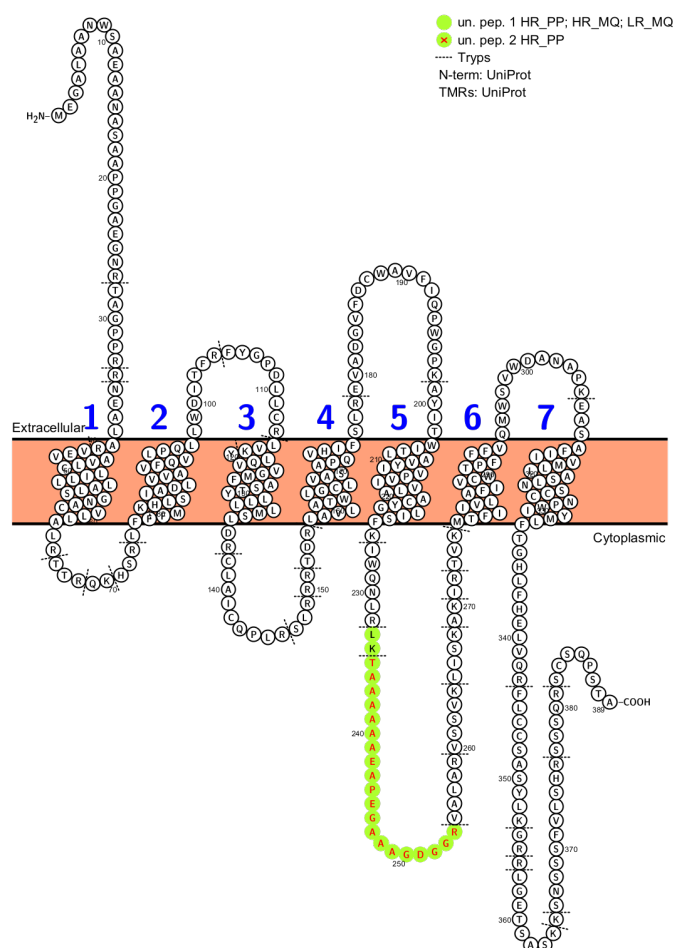


Figure 34. OTR control – Protter illustrated high-resolution Protein Prospector and high- and low-resolution MaxQuant search results against hOTR for tryptically digested OTR-GFP sample. Identified unique peptide sequences are highlighted in green and predicted tryptic cleavage sites are marked with dashed lines.

Control performed with the non-specific IgG (OTR\_nsIgG control) also didn't exhibit any unique peptides to either OTR or GFP, suggesting no non-specific binding to OTR-GFP. HR\_PP search against Immunoglobulin G-binding protein A resulted in identifying four unique peptides, highlighted in the Protter illustration of the protein in Figure 35. The ability to recognize the magnetic beads' coating protein and not discover the target receptor reinforces the argument of non-existent non-specific binding as it indicates that the washing steps were performed thoroughly, and the digestion step was successful. Meaning that if any non-specific protein was present, it should have been detected.



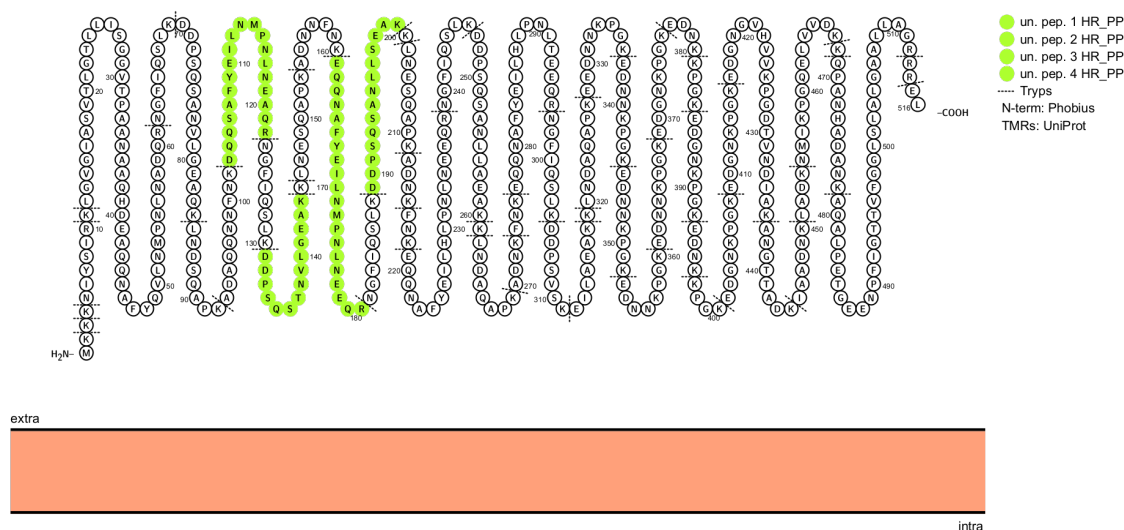


Figure 35. OTR\_beads control – Protter illustrated high-resolution Protein Prospector search result against IgG-binding protein A for sample typically digested after IP without the use of an antibody. Identified unique peptide sequences are highlighted in green and predicted tryptic cleavage sites are marked with dashed lines.

Control without the antibody (OTR\_beads control) also resulted in no identified unique peptides, which was expected and went along with the presumption of the positive experiment outcomes coming from the specific antibody recognition.

Out of the OTR antibodies tested, 1B2 resulted in the identification of the fragment corresponding to the 2<sup>nd</sup> transmembrane region. Two unique peptides were identified by HR\_MQ and LR\_MQ search separately, as demonstrated in the Protter illustration (Figure 36). General sequence coverage equals 14.4%. It is interesting to see the TM region detected as it represents a 34 amino acids big fragment of hydrophobic residues, but it also serves as strong evidence of successful IP where the 1B2 antibody recognized and bound the OTR-GFP from the proteins sample.

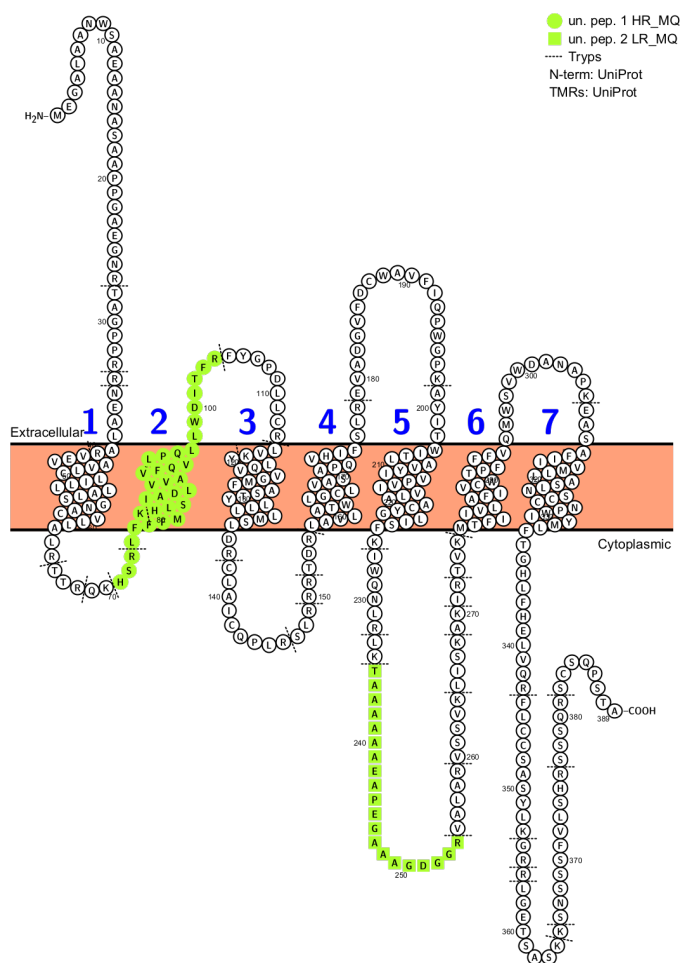


Figure 36. Protter illustrated high- and low-resolution MaxQuant search results against hOTR for the sample tryptically digested after IP with 1B2 antibody. Identified unique peptide sequences are highlighted in green and predicted tryptic cleavage sites are marked with dashed lines.

Antibody 5A5 had one unique peptide to OTR identified by LR\_MQ and one more by both LR\_MQ and HR\_MQ, equaling 12.1% sequence coverage. Peptide fragments and digestion sites are highlighted in the Protter illustration of OTR (Figure 37).

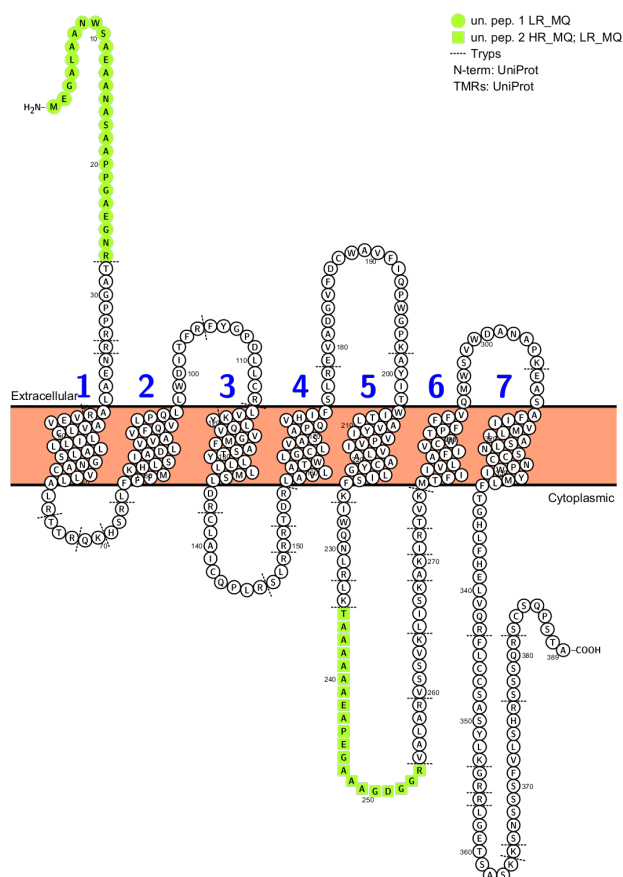


Figure 37. Protter illustrated high- and low-resolution MaxQuant search results against hOTR for sample tryptically digested after IP with 5A5 antibody. Identified unique peptide sequences are highlighted in green and predicted tryptic cleavage sites are marked with dashed lines.

4E3 is the final OTR antibody that led to the receptor fragment recognition. Only one unique peptide was identified with both HR\_MQ and LR\_MQ, equaling 5.1% sequence coverage. Protter illustration with the highlighted peptide is given in Figure 38. All the other OTR antibodies: 1A3, 1C10, 1E4, 1F1, 1H11, 4F3-4, and 4F3-5 did not result in identifying any of the unique peptides to OTR or GFP after performed IP-MS.

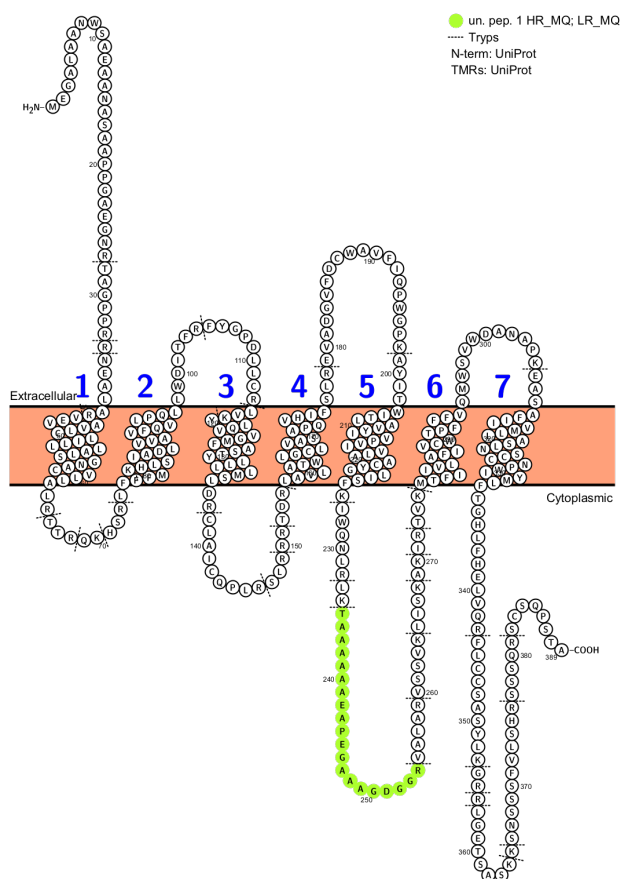


Figure 38. Protter illustrated high- and low-resolution MaxQuant search results against hOTR for sample tryptically digested after IP with 4E3 antibody. Identified unique peptide sequence is highlighted in green and predicted tryptic cleavage sites are marked with dashed lines.

Generally, IP-MS was rather successful in employing validated antibodies for recognizing and binding their respective receptors and identifying their unique peptides after digestion. A shorter summary of all the IP-MS results discussed above for validation of antibodies against V1aR and OTR is given in Table 13.

Table 13. IP-MS results for antibodies validated against V1aR and OTR; showing number of identified respective receptor unique peptides and receptor sequence covered by these peptides.

Target receptor	Antibody	Epitope region	Unique Peptides	Sequence Coverage
V1aR	1G1	N-term	6 (5 + 1)*	12%
	3D2	N-term	3	8%
	1H1	C-term	1	7%
	3C1	C-term		
	3F8	C-term		
	4A7	C-term	0	0%
	4G9	ICL-3		
OTR	1B2	C-term	2**	14%
	5A5	ICL-2	2	12%
	4E3	ICL-2	1	5%
	1A3	C-term		
	1C10	TCL-3		
	1E4	TCL-3		
	1F1	C-term	0	0%
	1H11	C-term		
	4F3-4	C-term		
	4F3-5	C-term		

\* Additional 5 (4 + 1) unique peptides to GFP, with 17% GFP sequence coverage  
\*\* One of the peptides (34 residues) corresponds to entire TM-2 region

Three out of seven antibodies against V1aR, and three out of ten antibodies against OTR resulted in identification of unique peptides corresponding to their respective receptors after performed IP-MS, strongly suggesting efficacy of these antibodies in binding these receptors. The most successful antibody in regard of receptor sequence coverage is 1B2 antibody to OTR with 14% coverage. In regard of number of unique peptides identified, 1G1 antibody for V1aR is the most successful with 6 unique peptides identified. Additionally, 1G1 resulted in 5 unique peptides to GFP identified, accounting for 17% GFP sequence coverage. Two controls by the beads or non-specific IgG demonstrated no non-specific receptor binding, further supporting the success of the IP-MS and the efficacy of antibodies in recognition and pulling down their respective receptors.

## § 5. DISCUSSION AND CONCLUSION

Antibodies are valuable tools for investigating receptors at the protein level and are employed in many fields, including immunology,<sup>183</sup> neuroscience,<sup>184</sup> drug development,<sup>185</sup> and forensics.<sup>186</sup> They detect their target proteins and allow for the evaluation of protein expression, localization, or quantification within investigated biological specimens.<sup>184</sup> Antibodies are particularly valuable in elucidating correlations between receptors and diseases or physiological functions.<sup>17</sup>

OTR and V1aR are two receptors involved in many physiological processes and behaviors, expressed in both the periphery and the CNS.<sup>11</sup> In the CNS, V1aR regulates cognitive functions, sexual behaviors and emotional responses, including memory and learning, partner selection, aggressiveness, and anxiety.<sup>62,187</sup> OTR in the CNS influences sexual behaviors, emotional bonding and maternal connection.<sup>64</sup> In the periphery, their actions include stimulation of lactation and initiation of labor for OTR, or vasoconstrictions for V1aR.<sup>4</sup> Due to their high structural similarity, it is extremely difficult to prepare and validate antibodies specific for only one of these receptors.<sup>11</sup> Furthermore, V1bR and V2R are two additional and very similar receptors that make this task even more challenging. V2R is located only in the periphery regulating fluid homeostasis, and while V1bR is expressed mainly in the brain, it is less important in behavioral regulation than V1aR.<sup>2</sup> For these reasons, the research primarily revolves around V1aR (also express in periphery) and OTR (also expressed in both sites). Due to lack of validated antibodies for OTR and V1aR, their research is hindered, and for that reason there is an immense interest in developing their specific antibodies. For carrying more importance in physiological and behavioral regulation, they have the priority for developing the novel antibodies compared to the other two. The aim of this thesis was to validate recently developed monoclonal antibodies against OTR and V1aR (10 OTR and 7 V1aR antibodies produced by the NIH, USA) against their distinctive peptide fragment epitopes.

WB and IP-MS, two complementary methods, were used for antibody validation. WB separates the proteins based on size and recognizes a target protein under denaturing conditions (SDS-PAGE). IP-MS uses non-denaturing conditions, maintaining the target receptor tertiary structure and displaying epitope within the context of receptor's overall structure. Employing both methods is important to determine the application potential of the

developed antibodies. In this project, OTR-GFP, V1aR-GFP, V1bR-GFP, and V2R-GFP isolated from individual receptor-overexpressing HEK293 cells were used, together with native HEK293 cells' membrane fraction as a control.

## 5.1. Antibody validation results

### 5.1.1. Western blot in validation of antibodies

Due to their high sequence and structural similarity, the production of OTR and V1aR antibodies presents a challenge. Commercially available antibodies targeting these receptors are available, but there have been concerns about their specificity.<sup>16</sup> This raises doubts about the accuracy of the research performed utilizing these antibodies. Polyclonal rabbit antibodies specific for OTR have been successfully developed before and used for investigation of OTR distribution within mouse CNS.<sup>1</sup> In this study, four different peptides corresponding to the mouse OTR were synthesized and used for rabbit immunization. These peptides corresponding to the N-term, ICL-3, and C-term were chosen as their sequences in these regions maximally differed from vasopressin receptors. The resulting immune sera were tested by dot and western blot and immunohistochemistry before OTR antibodies were recovered *via* affinity purification. All four antisera were positive, but the focus for further analysis was put on the one corresponding to the N-terminus with the highest indicated sensitivity. Specificity of antibody was evaluated by western blots on HEK293 OTR-expressing cells and untransfected control cells, and was successful with the purified antibody employed. Immunocytochemistry was also performed on these HEK293 cells expressing OTR-Venus construct by co-labelling for both OTR and Venus, and had a positive outcome. Immunohistochemistry by the antibody was also performed on brain and uterus tissues from wild-type and knock-out mice and proved effective. After the high specificity of the antibody to the OTR was demonstrated, the antibody was employed to examine OTR expression distribution within brain and its subcellular localization. In this thesis, our goal was to validate more sensitive monoclonal antibodies developed by rabbit hybridoma technology, a technology first introduced in 1975.<sup>188</sup> Here the obtained antibodies specifically target antigens and pure antibodies are easily produced in large quantities.<sup>185</sup> Our monoclonal antibodies against OTR and V1aR were also produced based on selected peptides from significantly different receptor regions corresponding to C-term, N-term, TCL-3, ICL-2 and ICL-3. Specificity of the obtained antibodies was tested by western blots on OTR-GFP, V1aR-GFP, V1bR-GFP, and V2R-GFP from individual receptor-overexpressing HEK293 cells, and untransfected HEK293 cell membrane protein fraction as a control.

Five conceptual pillars for antibody validation have been proposed; genetic pillar where the reduction of antibody labelling wants to be observed after target protein expression silencing by RNA interferences or genome editing; orthogonal pillar where the notable correlation between the protein expression estimation by antibody and by antibody-independent method (e.g. MS) wants to be observed; independent antibody pillar where the notable correlation between the protein expression estimation by two distinct antibodies for nonoverlapping epitopes of the same protein wants to be observed; immunocapture with MS pillar where the protein peptides want to be identified by MS after capturing it with the antibody; and tagged protein expression pillar where the notable correlation between antibody labelling and a tag that the protein was expressed with wants to be observed.<sup>21</sup> That last pillar for our antibody validation we have examined with one of our WB experiments employing FITC-labelled antibody against GFP tag fused to our receptor proteins (Figure 11). The idea was to find the band correlation between the position of anti-GFP FITC-labelled antibody fluorescence signal or the secondary chemiluminescent signal and the validated antibody labelling. In our experiment, both FITC fluorescence of anti-GFP antibody labelling and chemiluminescent signal of the secondary antibody were detected to check for the WB positions of tagged receptors. The receptor position was observed at the top of the stacking gel for OTR-GFP and V1aR-GFP, where the strong signal was later observed for one of the V1aR antibodies (1G1, Figure 15), indicating its efficacy in receptor recognition and binding. Another receptor position was observed at  $\sim 102 \times 10^3$  for both OTR-GFP and V1aR-GFP, but our validated antibodies did not result in such signals.

GFP tag is, except for determining position of the receptor on the WB, good as an indicator of successful receptor expression in the cells.<sup>189</sup> And overexpression of such fusion construct aids in testing the antibody specificity since a correlation between evaluated antibody's signal and a GFP signal for examined group of samples indicates the antibody specificity. This can be performed on two separate western blots, but also on a single multiplex blot testing colocalization of two signals, ensuring better accuracy by eliminating mistakes between membranes.<sup>190</sup> One of the issues that could arise with overexpression is the possibility of masking off-target recognition, so it is recommended to have the tag expressed endogenously whenever possible.<sup>21</sup> Furthermore, as GFP at  $27 \times 10^3$  is a rather big protein, there is a worry about GFP altering receptor conformation features in the fusion construct.<sup>191</sup>



Our WB tests for validated antibodies did not completely correlate with the GFP-tag signals, except for 1G1 at the top of the gel. Despite the second GFP-tag signal observed at  $\sim 102 \times 10^3$  for both tagged receptors, many of the antibodies resulted in a recurring band present at  $\sim 115 \times 10^3$ . For these two types of blots, equal percentage gels were used, so the discrepancy shall not arise from different sample running. It could be due to different posttranslational modifications, such as glycosylation, as these receptors have such sites on their N-terminus.<sup>175</sup> This cannot be concluded before conducting further experiments, and in-gel digestion followed by LC-MS/MS should be performed to identify these protein bands.<sup>180</sup> In case these two bands can be correlated to each other, and the one at  $\sim 115 \times 10^3$  is indeed the result of PTMs like phosphorylation or glycosylation, LC-MS/MS could have some problems directly identifying them since the modifications compete with the peptide bonds for a collision-activated dissociation and the resulting MS/MS spectrum of such modified precursor peptides will entirely lack of peptide ion fragment  $m/z$  necessary for peptide identification, so these peptides could be masked by modifications.<sup>192</sup> It would still show a single  $m/z$  corresponding to these peptides with a lost modification if there was one to be lost, and it would also show other unmodified peptides that could be enough for protein identification. The PTM's chemical stability is decisive for its effective MS/MS detection, and the MS/MS is generally useful method for their determination.<sup>193</sup>

For the seven V1aR antibodies the results of the WB experiments indicate that only one of them, 1G1, can be considered specific for V1aR-GFP, as it displayed strong signals in the V1aR-GFP sample lanes and no signals in the lanes consisting other receptors (Figure 15). This antibody demonstrated the strongest ELISA activity towards the N-terminus of V1aR. This value was rather small in comparison to other antibodies' strongest activities (Table 4), where it was actually the lowest activity demonstrated among all 17 validated antibodies (Table 3 and Table 4). This is not as surprising, as the antibodies were raised against specific peptide fragments, where they are out of their structural context. Hence, they are likely to lose their structural determinants, and may possibly present some neoantigenic determinants at the fragment ends. This would suggest that many antibodies could have been raised against epitopes in the linear peptide form, which could be presented differently when part of the receptor structures. In case an antibody recognized linear determinant, this possibly wouldn't pose a problem, but it is worth mentioning that even antibodies binding to linear epitopes will

recognize a specific linear epitope conformation and it might have an effect.<sup>119</sup> Exactly this could be the explanation for most the antibodies that despite demonstrating high ELISA activities displayed no specificity towards respective receptor. Especially the antibodies demonstrating high activities towards multiple epitope regions, for example 1B2 antibody against OTR. It had the highest receptor sequence coverage of all the antibodies after IP-MS, and at the same time provided no useful information after performing WB.

The 1G1 antibody exposed strong band at the entry to the stacking gel, which suggested the presence of V1aR-GFP aggregates. Protein aggregation and immobilization within stacking gel was observed before for another transmembrane protein,<sup>179</sup> where the effect of temperature on membrane protein stability was examined. The protein temperature lability and increased aggregation with increasing temperature was observed for that membrane protein with 12 TM regions. Thermal aggregation was also observed for SARS-CoV membrane protein,<sup>194</sup> and to avoid this issue, heating our membrane receptor samples before loading on lower temperatures for longer times should be considered. Another study demonstrated that heating wasn't even needed for SDS-PAGE sample preparation of two membrane proteins, one of which with 6 TM regions.<sup>195</sup> In fact cold treatment in LSB for 1 h at 4 °C increased the detectable amount of resolved proteins. Trichloroacetic acid treatment without employing heat is another way of tackling the issue of membrane protein aggregation presented in this study, but it is a bit more complicated and could potentially cause a degradation of some membrane proteins.<sup>196</sup> Another paper reported that substitution of LSB with SDS-HEPES buffer with applied 'boiling treatment' did not cause the aggregation of chromaffin granule membrane proteins, but adding the  $\beta$ -mercaptoethanol to SDS-HEPES restored the thermal aggregation.<sup>197</sup> This would further suggest the possible involvement of cysteine oxidation in the aggregation process. This was observed to happen in the stacking gel where the proteins concentrate before their resolution due to presence of oxidizing agent APS used for gel polymerization and is dependent on the amount of loaded protein.<sup>198</sup> Aggregation was found to be preventable by irreversible alkylation with IAA after reduction of thiol groups. Another possible explanation was offered where an SDS could be acting as an organic solvent, since their analysis showed that organic solvents also promote the membrane proteins' aggregation.<sup>197</sup> Different lysis buffers and lysis procedures were tested elsewhere to solve the problem of aggregation, but it was showed that regardless of the lysis condition, only the non-heated samples enabled the resolution, while 'boiled' samples were stuck on top of the gel.<sup>199</sup>

Apart from 1G1, other six V1aR antibodies displayed weak or non-specific bands within the same V1aR-GFP lane and within OTR-GFP, V1bR-GFP, V2R-GFP lanes and receptor non-expressing HEK293 lane, clearly proving these antibodies non-specific. Therefore, these antibodies are not suitable for detecting V1aR in WB experiments.

Of the 10 antibodies tested against OTR-GFP: 5A5, 4E3, and 1H11 resulted strong bands, although the specificity of the antibodies was also not demonstrated, indicating that the WB simply did not work properly for these antibodies. The bands displayed were different for each of the antibodies.

Our WB experiments revealed a lack of specificity in commercially available antibodies against V1aR and OTR towards V1aR-GFP (Figure 12) and OTR-GFP (Figure 13), respectively. Since the experiments were conducted for GFP fused receptors, which do not accurately represent native receptors due to plausible different folding and different structural features, they cannot be regarded as non-specific for their native receptors for which they were validated.<sup>191</sup> Especially since the peptide sequences against which these receptors were raised are not known, as proprietary to Abcam. For V1aR commercial antibody ab124907 was stated, though not the exact information, that the peptide originated somewhere around 350–450 amino acids. This region could correspond to the C-term of 418 amino acids long V1aR, so the GFP tag could indeed influence the recognition of such fused receptor.

### 5.1.2. Immunoprecipitation coupled with mass spectrometry in antibody validation

IP-MS as a method has been used in the antibody validation processes numerous times.<sup>200</sup> This method complements WB and adds another dimension to the validated antibodies and their efficacy in recognizing their respective receptors. After receptors are pulled down in IP and tryptically digested, tandem MS separates the resulting ions based on their  $m/z$  values.<sup>201</sup> In the first MS scan, all the precursor ions with the intensity/abundance above the set minimum signal threshold are during data dependent acquisition automatically selected for sequential fragmentation, starting from the most abundant.<sup>202</sup> These peptides, typically fragmented at the amide bonds, are then analyzed using a second MS.<sup>203</sup> And while mainly used for qualitative determination of peptides and proteins, this method also allows for protein quantification by quantifying the identified peptides unique for these proteins.<sup>204</sup> And despite being highly specific and accurate, LC-MS/MS due to its performance complexity lacks reproducibility and

can face a multitude of potential issues from sample preparation, over choosing the corresponding parameters, to appropriate database searching algorithms for matching obtained data with peptide sequences.<sup>205</sup> A large number of false positive protein identifications has been reported in the literature so stringent quality control measures must be taken.<sup>206</sup>

Results obtained after IP-MS offer valuable evidence of the successful binding and recognition of the V1aR-GFP and OTR-GFP proteins by the validated antibodies, as peptides corresponding to the expected tryptic digestion sites of the receptors were identified and their sequences confirmed, demonstrating the potential of this technique for helping to detect and analyze membrane proteins. Moreover, in one study this method was used for a phosphorylation analysis and enabled discovery of a novel phosphorylation site in the ICL-3 of V2R.<sup>207</sup>

Of all V1aR antibodies, 1G1 demonstrated the highest activity in IP-MS with 6 unique peptides to V1aR detected and a sequence coverage of 12% (Figure 30), along with 5 unique peptides to GFP (17.2%, Figure 31). To present the meaning of these 12%, we must remember that these receptors are membrane proteins with seven transmembrane regions, which accounts for the big part of their structure estimated at around 40%, somewhat less than for the other members of rhodopsin class GPCRs.<sup>208</sup> Due to hydrophobic nature of these regions, there is a lack of sites being recognized by trypsin, so these proteins are hardly digested, leading to lower sequence coverages.<sup>209</sup> It is encouraging to find peptides unique for GFP, since GFP protein is part of the fusion construct, confirming the antibody's efficacy in pulling down the target receptor. Combining the 1G1 results from WB with IP-MS results makes this antibody a very good candidate for further investigation and potential validation.

The 3D2 V1aR antibody was the second most successful with 3 unique peptides to V1aR identified and 7.9% sequence coverage (Figure 32). The 1H1 antibody yielded the least successful result with only one unique peptide to V1aR identified and 6.7% sequence coverage (Figure 33). The remaining four antibodies were not successful in binding the V1aR-GFP, as they did not result in identifying any of the unique peptides to V1aR or GFP after performed IP-MS. Reason for this could simply be the antibodies not being able to bind the receptor, but it could also be due to tryptic digestion difficulties, as explained earlier.

The antibodies against OTR tested in this research have varying success in terms of recognizing and binding the OTR-GFP from the protein sample. Antibodies 1B2, 5A5, and 4E3 have successfully recognized and bound the receptor, as demonstrated by sequence coverage of 14.4% with 2 unique peptides (Figure 36), 12.1% with 2 unique peptides (Figure 37), and

5.1% with 1 unique peptide detected (Figure 38), respectively. The 1B2 antibody, despite failing to produce any significant information on WB was the most successful of all the OTR antibodies tested by IP-MS, with one of the transmembrane regions identified, and the potential reasonings for this observation were explained in the previous section.

Controls carried out including no antibody conditions, non-specific IgG and fused receptor sample digestion suggested the efficacy of the validated antibodies in binding their respective receptors, since no non-specific binding was observed in the first two control types for both receptor samples, as was expected. Digestion of V1aR-GFP sample, contrary to expectations, did not result in receptor identification. This could be because of too low trypsin to target protein ratio since these samples were not IP purified prior digestion, or if not, because of the presence of other proteins in the mixture whose precursor peptides after digestion could have been more abundant and prevented the selection of target protein peptides for fragmentation, and so disabled their recognition on MS/MS spectra.<sup>202</sup> Digestion of OTR-GFP, as expected, resulted in receptor identification, with recognized peptides originating from ICL-3 (Figure 34). This loop is the biggest of all and has many predicted cleavage sites, so the identification could be possible due to loop flexibility enabling easier trypsin access and enhancing cleavage.<sup>210</sup> Maybe another positive control to think of, same as the GFP tag was employed as a control in the WB, would be to employ it in IP to pull down these receptors using an anti-GFP antibody.<sup>154</sup> This would concentrate these receptors based on a tag we know is there, separate them from off-target proteins whose resulting peptides after digestion might have masked the detection, and facilitate their identification.<sup>211</sup> A specific GFP-binding protein has been engineered that can almost quantitatively isolate GFP-tagged fusion proteins from complex protein mixtures, and can be used in IP step followed by MS analysis.<sup>212</sup>

## 5.2. Limitations and future directions

The anti-V1aR 1G1 antibody was the most promising antibody for further research. Suggestions for future experiments include different sample preparation or electrophoresis running conditions, such as omitting SDS, decreasing protein and antibody concentrations, or using lower percentage gels.<sup>198</sup> Using lower temperatures, different sample loading buffers, detergents, or sonication could help with the receptor aggregation problem.<sup>194,197,213</sup>

For IP-MS, the same procedure should be performed for each antibody against the three other closely related receptors to confirm IP-MS receptor specificity. Furthermore, all four

receptors should be mixed together to confirm receptor specificity. Besides that, for WB experiments in-gel or on-membrane digestion followed by MS should be performed to characterize the observed aggregates and recurring bands at  $\sim 115 \times 10^3$ .

Subsequent research for this project will focus on producing the receptors without a GFP label, which will be of particular interest for antibodies 4F3-5, 1B2, 1A3, 4F3-4, 1F1, 1H11, 4A3, 5A5, 1H1, 3C1, 3F8, 4A7, and 4G9 that target the intracellular parts of the receptors. For that, new plasmid construct carrying sequences for native V1aR or OTR overexpression should be synthesized. Such plasmids could be constructed following the Gibson assembly from DNA fragments with overlapping ends for V1aR/OTR and GFP that would serve as a marker of successful transfection, IRES sequence that would enable the V1aR/OTR and GFP translation from a single promoter, antibiotic resistance sequence as a selectable marker, and some other components for normal plasmid replication.<sup>214,215</sup> For combining these sequences into a single plasmid, DNA exonuclease, DNA polymerase and DNA ligase would be required.<sup>216</sup> With constructed plasmids, HEK293 cells would be transfected to generate stable cell lines overexpressing unfused receptors.<sup>217,218</sup> The use of these receptors for conducting WB and IP-MS experiments would eliminate the potential negative side effects of GFP on antibody recognition and provide results that are more applicable for validating the antibodies, especially those targeting C-terminus and intracellular loops of the receptors.

Antibodies that proved successful and demonstrated potential for future development (1G1 and 1B2) could also be evaluated by immunohistochemistry on receptors-rich tissue regions, such as uterus or brain specimens, or more accessible brain surrogates tissues.<sup>219</sup> In another study after validating antibodies against dopamine receptors by WB and immunohistochemistry, the validation process was followed with IP-MS for the antibodies specific in these two tests.<sup>20</sup> Receptor-knock out mice should be used as a control in such experiments.

### 5.3. Conclusion

Overall, this research has provided valuable insights into the specificity of newly raised monoclonal antibodies for both V1aR and OTR, and their efficacy in methods such as WB and IP-MS by recognizing and binding to their respective targets. Out of 10 antibodies validated against OTR, the most promising was 1B2. This antibody in the IP-MS experiment resulted in the highest receptor sequence coverage of 14.4% among all 17 tested receptors. Out of two

unique peptides identified by this antibody, one corresponded to 34 amino acids long 2<sup>nd</sup> TM region. Out of 7 antibodies validated against V1aR, antibody 1G1 is the only one with V1aR specificity. This antibody in the WB experiment distinguished V1aR from all other structurally similar receptor samples and the negative control, but also identified six unique peptides to V1aR by the IP-MS. In addition to that, as V1aR-GFP constructs were employed, 1G1 yielded 5 unique peptides to GFP, which amounts to 17.2% GFP sequence coverage. These two antibodies have a promising potential for further investigation, and the future work will show their true efficacy.

## § 6. LIST OF ABBREVIATIONS AND SYMBOLS

3D	three-dimensional
3V	third ventricle
7TM	seven-transmembrane
ALP	alkaline phosphatase
APS	ammonium persulfate
BCA	bicinchoninic acid
BSA	bovine serum albumin
C18	octadecylsilane
C4	butylsilane
cAMP	cyclic adenosine monophosphate
CCD	charge-coupled device
cGMP	cyclic guanosine monophosphate
CHAPS	3-[(3-cholamidopropyl)dimethylammonio]-1-propanesulfonate
CTX	cortex
DAG	diacylglycerol
DoxGoat	donkey anti-goat
DoxRb	donkey anti-rabbit
DTT	dithiothreitol
E	eluate fraction
ECL	enhanced chemiluminescence
EDTA	ethylenediamine tetraacetic acid
EL	extracellular loop
ELISA	enzyme-linked immunosorbent assay
Fc	fragment crystallizable
FITC	fluorescein isothiocyanate
FT	flow-through fraction
FWHM	full width at half maximum
GDP	guanosine diphosphate



---

GFP / eGFP	green fluorescent protein / enhanced green fluorescent protein
GPCR	G protein-coupled receptor
GRAFS	glutamate, rhodopsin, adhesion, frizzled/taste2, secretin
GRKs	G protein-coupled receptor kinase
GTP	guanosine triphosphate
HEK293	human embryonic kidney 293
HEPES	4-(2-hydroxyethyl)-1-piperazineethanesulfonic acid
HPLC	high-performance liquid chromatography
HR	high-resolution
HRP	horseradish peroxidase
IAA	iodoacetamide
IgG / nsIgG	immunoglobulin G / non-specific immunoglobulin G
ICL	intracellular loop
IP	immunoprecipitation
IP3	inositol-1,4,5-trisphosphate
$K_i$	inhibitory constant
LC-MS/MS	liquid chromatography tandem mass spectrometry
LR	low-resolution
LSB	Laemmli sample buffer
LTQ	linear trap quadrupole
m/z	mass-to-charge ratio
MALDI-MS	matrix-assisted laser desorption/ionization mass spectrometry
MLCK	myosin light chain kinase
MQ	MaxQuant
MQW	Milli-Q water
MS	mass spectrometry
NC	nitrocellulose
NFDM	non-fat dried milk
NIH	National Institutes of Health
OD	optical density
OT	oxytocin
OTR / hOTR	oxytocin receptor / human oxytocin receptor

---

PAGE	polyacrylamide gel electrophoresis
PBS	phosphate-buffered saline
PBS-T	phosphate-buffered saline with Tween 20
PFC	prefrontal cortex
PIP2	phosphatidylinositol-4,5-bisphosphate
PIR	piriform cortex
PKA	protein kinase A
PKC	protein kinase C
PP	Protein Prospector
PTM	posttranslational modification
PVDF	polyvinylidene difluoride
rpm	revolutions per minute
RT	room temperature
scFv16	single-chain variable fragment 16
SDS	sodium dodecyl sulfate
TBS	Tris-buffered saline
TBS-T	Tris-buffered saline with Tween 20
TCL-3	transcellular loop 3
TEAB	triethylammonium bicarbonate
TEMED	tetramethylethylenediamine
TM	transmembrane helix
UPW	ultra-pure water
V1aR / hV1aR	vasopressin 1a receptor / human vasopressin 1a receptor
V1bR / hV1bR	vasopressin 1b receptor / human vasopressin 1b receptor
V2R / hV2R	vasopressin 2 receptor / human vasopressin 2 receptor
VOCC	voltage-operated calcium channel
VP	vasopressin
W	washing fraction
WB	western blot

## § 7. REFERENCES

1. M. Mitre, B. J. Marlin, J. K. Schiavo, E. Morina, S. E. Norden, T. A. Hackett, C. J. Aoki, M. V. Chao and R. C. Froemke, A Distributed Network for Social Cognition Enriched for Oxytocin Receptors, *J. Neurosci.* **36** (2016) 2517–2535.
2. Z. R. Donaldson and L. J. Young, Oxytocin, vasopressin, and the neurogenetics of sociality, *Science* **322** (2008) 900–904.
3. G. Bussolati, P. Cassoni, G. Ghisolfi, F. Negro and A. Sapino, Immunolocalization and gene expression of oxytocin receptors in carcinomas and non-neoplastic tissues of the breast, *Am. J. Pathol.* **148** (1996) 1895–1903.
4. H. H. Zingg, Vasopressin and oxytocin receptors, *Baillieres Clin. Endocrinol. Metab.* **10** (1996) 75–96.
5. E. Szczepanska-Sadowska, A. Wsol, A. Cudnoch-Jedrzejewska and T. Żera, Complementary Role of Oxytocin and Vasopressin in Cardiovascular Regulation, *Int. J. Mol. Sci.* **22**, 11465 (2021) 1–24.
6. S. Arrowsmith, Oxytocin and vasopressin signalling and myometrial contraction, *Curr. Opin. Physiol.* **13** (2020) 62–70.
7. F. Hernando, O. Schoots, S. J. Lolait and J. P. H. Burbach, Immunohistochemical localization of the vasopressin V1b receptor in the rat brain and pituitary gland: anatomical support for its involvement in the central effects of vasopressin, *Endocrinology* **142** (2001) 1659–1668.
8. A. Gupta, A. S. Heimann, I. Gomes and L. A. Devi, Antibodies against G-protein coupled receptors: novel uses in screening and drug development, *Comb. Chem. High Throughput Screen.* **11** (2008) 463–467.
9. N. C. Danbolt, Y. Zhou, D. N. Furness and S. Holmseth, Strategies for immunohistochemical protein localization using antibodies: What did we learn from neurotransmitter transporters in glial cells and neurons, *Glia* **64** (2016) 2045–2064.
10. M. G. Di Giglio, M. Muttenthaler, K. Harpsøe, Z. Liutkeviciute, P. Keov, T. Eder, T. Rattei, S. Arrowsmith, S. Wray, A. Marek, T. Elbert, P. F. Alewood, D. E. Gloriam and C. W. Gruber, Development of a human vasopressin V1a-receptor antagonist from an evolutionary-related insect neuropeptide, *Sci. Rep.* **7**, 41002 (2017) 1–15.
11. Z. Song and H. E. Albers, Cross-talk among oxytocin and arginine-vasopressin receptors: Relevance for basic and clinical studies of the brain and periphery, *Front. Neuroendocrinol.* **51** (2018) 14–24.
12. B. Chini and M. Manning, Agonist selectivity in the oxytocin/vasopressin receptor family: new insights and challenges, *Biochem. Soc. Trans.* **35** (2007) 737–741.
13. D. Ocampo Daza, M. Lewicka and D. Larhammar, The oxytocin/vasopressin receptor family has at least five members in the gnathostome lineage, including two distinct V2 subtypes, *Gen. Comp. Endocrinol.* **175** (2012) 135–143.
14. Y. Waltenspühl, J. Ehrenmann, S. Vacca, C. Thom, O. Medalia and A. Plückthun, Structural basis for the activation and ligand recognition of the human oxytocin receptor, *Nat. Commun.* **13**, 4153 (2022) 1–9.

15. C. J. W. Smith, B. T. DiBenedictis and A. H. Veenema, Comparing vasopressin and oxytocin fiber and receptor density patterns in the social behavior neural network: Implications for cross-system signaling, *Front. Neuroendocrinol.* **53**, 100737 (2019) 1–43.
16. M. Yoshida, Y. Takayanagi, K. Inoue, T. Kimura, L. J. Young, T. Onaka and K. Nishimori, Evidence that oxytocin exerts anxiolytic effects via oxytocin receptor expressed in serotonergic neurons in mice, *J. Neurosci.* **29** (2009) 2259–2271.
17. M. Meyer, B. Jurek, M. Alfonso-Prieto, R. Ribeiro, V. M. Milenkovic, J. Winter, P. Hoffmann, C. H. Wetzel, A. Giorgetti, P. Carloni and I. D. Neumann, Structure–function relationships of the disease-linked A218T oxytocin receptor variant, *Mol. Psychiatry* **27** (2022) 907–917.
18. Polyclonal vs. monoclonal antibodies | proteintech, <https://www.ptglab.com/news/blog/polyclonal-vs-monoclonal-antibodies/> (Date accessed: 08/05/2023)
19. J. Bordeaux, A. Welsh, S. Agarwal, E. Killiam, M. Baquero, J. Hanna, V. Anagnostou and D. Rimm, Antibody validation, *Biotechniques* **48** (2010) 197–209.
20. T. Stojanovic, M. Orlova, F. J. Sialana, H. Höger, S. Stuchlik, I. Milenkovic, J. Aradska and G. Lubec, Validation of dopamine receptor DRD1 and DRD2 antibodies using receptor deficient mice, *Amino Acids* **49** (2017) 1101–1109.
21. M. Uhlen, A. Bandrowski, S. Carr, A. Edwards, J. Ellenberg, E. Lundberg, D. L. Rimm, H. Rodriguez, T. Hiltke, M. Snyder and T. Yamamoto, A proposal for validation of antibodies, *Nat. Methods* **13** (2016) 823–827.
22. R. J. Lefkowitz, Historical review: a brief history and personal retrospective of seven-transmembrane receptors, *Trends Pharmacol. Sci.* **25** (2004) 413–422.
23. L. M. Wingler and R. J. Lefkowitz, Conformational basis of G protein-coupled receptor signaling versatility, *Trends Cell Biol.* **30** (2020) 736–747.
24. E. Jacoby, R. Bouhelal, M. Gerspacher and K. Seuwen, The 7 TM G-protein-coupled receptor target family, *ChemMedChem* **1** (2006) 760–782.
25. R. Fredriksson, M. C. Lagerström, L. G. Lundin and H. B. Schiöth, The G-protein-coupled receptors in the human genome form five main families. Phylogenetic analysis, paralogon groups, and fingerprints, *Mol. Pharmacol.* **63** (2003) 1256–1272.
26. C. S. Odoemelam, B. Percival, H. Wallis, M. W. Chang, Z. Ahmad, D. Scholey, E. Burton, I. H. Williams, C. L. Kamerlin and P. B. Wilson, G-Protein coupled receptors: structure and function in drug discovery, *RSC Adv.* **10** (2020) 36337–36348.
27. P. S. H. Park, D. T. Lodowski and K. Palczewski, Activation of G Protein–Coupled Receptors: Beyond Two-State Models and Tertiary Conformational Changes, *Annu. Rev. Pharmacol. Toxicol.* **48** (2008) 107–141.
28. K. Sriram and P. A. Insel, G Protein-Coupled Receptors as Targets for Approved Drugs: How Many Targets and How Many Drugs?, *Mol. Pharmacol.* **93** (2018) 251–258.
29. R. A. Hall, R. T. Premont and R. J. Lefkowitz, Heptahelical Receptor Signaling: Beyond the G Protein Paradigm, *J. Cell Biol.* **145** (1999) 927–932.
30. J. Bockaert and J. P. Pin, Molecular tinkering of G protein-coupled receptors: an evolutionary success, *EMBO J.* **18** (1999) 1723–1729.

31. E. Neumann, K. Khawaja and U. Müller-Ladner, G protein-coupled receptors in rheumatology, *Nat. Rev. Rheumatol.* **10** (2014) 429–436.
32. K. Palczewski, T. Kumasaka, T. Hori, C. A. Behnke, H. Motoshima, B. A. Fox, I. Le Trong, D. C. Teller, T. Okada, R. E. Stenkamp, M. Yamamoto and M. Miyano, Crystal structure of rhodopsin: A G protein-coupled receptor, *Science* **289** (2000) 739–745.
33. M. Wheatley, D. Wootten, M. T. Conner, J. Simms, R. Kendrick, R. T. Logan, D. R. Poyner and J. Barwell, Lifting the lid on GPCRs: the role of extracellular loops, *Br. J. Pharmacol.* **165** (2012) 1688–1703.
34. O. B. Sanchez-Reyes, A. L. G. Cooke, D. B. Tranter, D. Rashid, M. Eilers, P. J. Reeves and S. O. Smith, G Protein-Coupled Receptors Contain Two Conserved Packing Clusters, *Biophys. J.* **112** (2017) 2315–2326.
35. G. M. Hu, T. L. Mai and C. M. Chen, Visualizing the GPCR Network: Classification and Evolution, *Sci. Rep.* **7**, 15495 (2017) 1–15.
36. F. Horn, E. Bettler, L. Oliveira, F. Campagne, F. E. Cohen and G. Vriend, GPCRDB information system for G protein-coupled receptors, *Nucleic Acids Res.* **31** (2003) 294–297.
37. T. K. Attwood and J. B. C. Findlay, Fingerprinting G-protein-coupled receptors, *Protein Eng.* **7** (1994) 195–203.
38. M. C. Lagerström, A. R. Hellström, D. E. Gloriam, T. P. Larsson, H. B. Schiöth and R. Fredriksson, The G Protein-Coupled Receptor Subset of the Chicken Genome, *PLoS Comput. Biol.* **2**, e54 (2006) 0493–0507.
39. H. B. Schiöth and R. Fredriksson, The GRAFS classification system of G-protein coupled receptors in comparative perspective, *Gen. Comp. Endocrinol.* **142** (2005) 94–101.
40. K. Kochman, Superfamily of G-protein coupled receptors (GPCRs)—extraordinary and outstanding success of evolution, *Postepy Hig. Med. Dosw. (Online)* **68** (2014) 1225–1237.
41. A. Sarkar, S. Kumar, D. Sundar, The G protein-coupled receptors in the pufferfish *Takifugu rubripes*, *BMC Bioinformatics* **12** (Suppl 1), S3 (2011) 1–9.
42. M. Rinne, Z. U. R. Tanoli, A. Khan and H. Xhaard, Cartography of rhodopsin-like G protein-coupled receptors across vertebrate genomes, *Sci. Rep.* **9**, 7058 (2019) 1–16.
43. K. Palczewski, G protein-coupled receptor rhodopsin, *Annu. Rev. Biochem.* **75** (2006) 743–767.
44. J. M. Baldwin, Structure and function of receptors coupled to G proteins, *Curr. Opin. Cell Biol.* **6** (1994) 180–190.
45. V. Cherezov, E. Abola and R. C. Stevens, Toward drug design: recent progress in the structure determination of GPCRs, a membrane protein family with high potential as pharmaceutical targets, *Methods Mol. Biol.* **654** (2010) 141–168.
46. E. W. Sutherland, Studies on the mechanism of hormone action, *Science* **177** (1972) 401–408.
47. P. Sassone-Corsi, The Cyclic AMP Pathway, *Cold Spring Harb. Perspect. Biol.* **4**, a011148 (2012) 1–3.
48. A. C. Newton, M. D. Bootman and J. D. Scott, Second Messengers, *Cold Spring Harb. Perspect. Biol.* **8**, a005926 (2016) 1–14.
49. M. J. Marinissen and J. S. Gutkind, G-protein-coupled receptors and signaling networks: emerging paradigms, *Trends Pharmacol. Sci.* **22** (2001) 368–376.
50. R. J. Stanley and G. M. H. Thomas, Activation of G Proteins by Guanine Nucleotide Exchange Factors Relies on GTPase Activity, *PLoS One* **11**, e0151861 (2016) 1–12.

51. W. I. Weis and B. K. Kobilka, The Molecular Basis of G Protein–Coupled Receptor Activation, *Annu. Rev. Biochem.* **87** (2018) 897–919.
52. H. E. Hamm, The many faces of G protein signaling, *J. Biol. Chem.* **273** (1998) 669–672.
53. P. A. Insel, K. Sriram, M. W. Gorr, S. Z. Wiley, A. Michkov, C. Salmerón and A. M. Chinn, GPCRomics: An Approach to Discover GPCR Drug Targets, *Trends Pharmacol. Sci.* **40** (2019) 378–387.
54. T. Laeremans, Z. A. Sands, P. Claes, A. De Blicke, S. De Cesco, S. Triest, A. Busch, D. Felix, A. Kumar, V. P. Jaakola and C. Menet, Accelerating GPCR Drug Discovery With Conformation-Stabilizing VHHs, *Front. Mol. Biosci.* **9**, 863099 (2022) 1–21.
55. A. P. Davenport, C. C. G. Scully, C. de Graaf, A. J. H. Brown and J. J. Maguire, Advances in therapeutic peptides targeting G protein-coupled receptors, *Nat. Rev. Drug Discov.* **19** (2020) 389–413.
56. M. Congreve, C. de Graaf, N. A. Swain and C. G. Tate, Impact of GPCR Structures on Drug Discovery, *Cell* **181** (2020) 81–91.
57. Y. Waltenspühl, J. Schöppe, J. Ehrenmann, L. Kummer and A. Plückthun, Crystal structure of the human oxytocin receptor, *Sci. Adv.* **6**, eabb5419 (2020) 1–11.
58. C. Barberis, B. Mouillac and T. Durroux, Structural bases of vasopressin/oxytocin receptor function, *J. Endocrinol.* **156** (1998) 223–229.
59. A. Glukhova, C. J. Draper-Joyce, R. K. Sunahara, A. Christopoulos, D. Wootten and P. M. Sexton, Rules of Engagement: GPCRs and G Proteins, *ACS Pharmacol. Transl. Sci.* **1** (2018) 73–83.
60. A. Meyer-Lindenberg, G. Domes, P. Kirsch and M. Heinrichs, Oxytocin and vasopressin in the human brain: social neuropeptides for translational medicine, *Nat. Rev. Neurosci.* **12** (2011) 524–538.
61. A. K. Mitra, Oxytocin and vasopressin: the social networking buttons of the body, *AIMS Mol. Sci.* **8** (2021) 32–50.
62. C. Brunnie, G. Nave, C. F. Camerer, S. Schosser, B. Vogt, T. F. Münte and M. Heldmann, Vasopressin increases human risky cooperative behavior, *Proc. Natl. Acad. Sci. U. S. A.* **113** (2016) 2051–2056.
63. S. Jard, R. C. Gaillard, G. Guillon, J. Marie, P. Schoenberg, A. F. Muller, M. Manning and W. H. Sawyer, Vasopressin antagonists allow demonstration of a novel type of vasopressin receptor in the rat adenohypophysis, *Mol. Pharmacol.* **30** (1986) 171–177.
64. A. Argiolas and G. L. Gessa, Central functions of oxytocin, *Neurosci. Biobehav. Rev.* **15** (1991) 217–231.
65. L. Wang, J. Xu, S. Cao, D. Sun, H. Liu, Q. Lu, Z. Liu, Y. Du and C. Zhang, Cryo-EM structure of the AVP–vasopressin receptor 2–Gs signaling complex, *Cell Res.* **31** (2021) 932–934.
66. U. Gether and B. K. Kobilka, G protein-coupled receptors. II. Mechanism of agonist activation, *J. Biol. Chem.* **273** (1998) 17979–17982.
67. L. M. Luttrell, 'Location, location, location': activation and targeting of MAP kinases by G protein-coupled receptors, *J. Mol. Endocrinol.* **30** (2003) 117–126.
68. F. M. Heydenreich, B. Plouffe, A. Rizk, D. Milić, J. Zhou, B. Breton, C. le Gouill, A. Inoue, M. Bouvier and D. B. Veprintsev, Vasopressin V2 is a promiscuous G protein-coupled receptor that is biased by its peptide ligands, *bioRxiv* (2021) doi: <https://doi.org/10.1101/2021.01.28.427950>

69. M. Busnelli, A. Saulière, M. Manning, M. Bouvier, C. Galés and B. Chini, Functional selective oxytocin-derived agonists discriminate between individual G protein family subtypes, *J. Biol. Chem.* **287** (2012) 3617–3629.
70. G. Innamorati, H. Sadeghi and M. Birnbaumer, Transient phosphorylation of the V1a vasopressin receptor, *J. Biol. Chem.* **273** (1998) 7155–7161.
71. F. L. Tan, S. J. Lolait, M. J. Brownstein, N. Saito, V. Macleod, D. A. Baeyens, P. R. Mayeux, S. M. Jones and L. E. Cornett, Molecular cloning and functional characterization of a vasotocin receptor subtype that is expressed in the shell gland and brain of the domestic chicken, *Biol. Reprod.* **62** (2000) 8–15.
72. M. M. Rinschen, B. Schermer and T. Benzing, Vasopressin-2 Receptor Signaling and Autosomal Dominant Polycystic Kidney Disease: From Bench to Bedside and Back Again, *J. Am. Soc. Nephrol.* **25** (2014) 1140–1147.
73. S. Arrowsmith and S. Wray, Oxytocin: its mechanism of action and receptor signalling in the myometrium, *J. Neuroendocrinol.* **26** (2014) 356–369.
74. K. D. Gada and D. E. Logothetis, PKC regulation of ion channels: The involvement of PIP2, *J. Biol. Chem.* **298**, 102035 (2022) 1–19.
75. U. Klein, G. Gimpl and F. Fahrenholz, Alteration of the myometrial plasma membrane cholesterol content with beta-cyclodextrin modulates the binding affinity of the oxytocin receptor, *Biochemistry* **34** (1995) 13784–13793.
76. G. Gimpl, K. Burger and F. Fahrenholz, Cholesterol as modulator of receptor function, *Biochemistry* **36** (1997) 10959–10974.
77. J. J. Hulce, A. B. Cognetta, M. J. Niphakis, S. E. Tully and B. F. Cravatt, Proteome-wide mapping of cholesterol-interacting proteins in mammalian cells, *Nat. Methods* **10** (2013) 259–264.
78. F. A. Antoni and S. E. Chadio, Essential role of magnesium in oxytocin-receptor affinity and ligand specificity, *Biochem. J.* **257** (1989) 611–614.
79. A. F. Pearlmutter and M. S. Soloff, Characterization of the metal ion requirement for oxytocin-receptor interaction in rat mammary gland membranes, *J. Biol. Chem.* **254** (1979) 3899–3906.
80. R. J. Lefkowitz, G protein-coupled receptors. III. New roles for receptor kinases and beta-arrestins in receptor signaling and desensitization, *J. Biol. Chem.* **273** (1998) 18677–18680.
81. P. C. Gwee, C. T. Amemiya, S. Brenner and B. Venkatesh, Sequence and organization of coelacanth neurohypophysial hormone genes: Evolutionary history of the vertebrate neurohypophysial hormone gene locus, *BMC Evol. Biol.* **8**, 93 (2008) 1–12.
82. R. Acher, Molecular evolution of biologically active polypeptides, *Proc. R. Soc. Lond. B Biol. Sci.* **210** (1980) 21–43.
83. V. du Vigneaud, C. Ressler and S. Trippett, The sequence of amino acids in oxytocin, with a proposal for the structure of oxytocin, *J. Biol. Chem.* **205** (1953) 949–957.
84. M. Manning, A. Misicka, A. Olma, K. Bankowski, S. Stoev, B. Chini, T. Durroux, B. Mouillac, M. Corbani and G. Guillon, Oxytocin and vasopressin agonists and antagonists as research tools and potential therapeutics, *J. Neuroendocrinol.* **24** (2012) 609–628.

85. D. A. Baribeau and E. Anagnostou, Oxytocin and vasopressin: Linking pituitary neuropeptides and their receptors to social neurocircuits, *Front. Neurosci.* **9**, 335 (2015) 1–21.
86. H. K. Caldwell, Oxytocin and Vasopressin: Powerful Regulators of Social Behavior, *Neuroscientist* **23** (2017) 517–528.
87. G. J. de Vries and G. C. Panzica, Sexual differentiation of central vasopressin and vasotocin systems in vertebrates: different mechanisms, similar endpoints, *Neuroscience* **138** (2006) 947–955.
88. A. R. Fuchs, F. Fuchs, P. Husslein, M. S. Soloff and M. J. Fernström, Oxytocin receptors and human parturition: a dual role for oxytocin in the initiation of labor, *Science* **215** (1982) 1396–1398.
89. K. Uvnäs-Moberg, A. M. Widström, S. Werner, A. S. Matthiesen and J. Winberg, Oxytocin and prolactin levels in breast-feeding women. Correlation with milk yield and duration of breast-feeding, *Acta Obstet. Gynecol. Scand.* **69** (1990) 301–306.
90. V. Grinevich and I. D. Neumann, Brain oxytocin: how puzzle stones from animal studies translate into psychiatry, *Mol. Psychiatry* **26** (2020) 265–279.
91. J. Gupta, R. J. Russell, C. P. Wayman, D. Hurley and V. M. Jackson, Oxytocin-induced contractions within rat and rabbit ejaculatory tissues are mediated by vasopressin V1A receptors and not oxytocin receptors, *Br. J. Pharmacol.* **155** (2008) 118–126.
92. T. R. Insel and L. J. Young, Neuropeptides and the evolution of social behavior, *Curr. Opin. Neurobiol.* **10** (2000) 784–789.
93. L. J. Young, Oxytocin and vasopressin receptors and species-typical social behaviors, *Horm. Behav.* **36** (1999) 212–221.
94. J. L. Goodson and A. H. Bass, Social behavior functions and related anatomical characteristics of vasotocin/vasopressin systems in vertebrates, *Brain Res. Rev.* **35** (2001) 246–265.
95. M. Maggi, P. del Carlo, G. Fantoni, S. Giannini, C. Torrisi, D. Casparis, G. Massi and M. Serio, Human myometrium during pregnancy contains and responds to V1 vasopressin receptors as well as oxytocin receptors, *J. Clin. Endocrinol. Metab.* **70** (1990) 1142–1154.
96. S. E. McCormack, J. E. Blevins and E. A. Lawson, Metabolic Effects of Oxytocin, *Endocr. Rev.* **41** (2020) 121–145.
97. J. Kruse, Oxytocin: pharmacology and clinical application, *J. Fam. Pract.* **23** (1986) 473–479.
98. C. S. Ejekam, I. P. Okafor, C. Anyakora, E. A. Ozomata, K. Okunade, S. E. Oridota and J. Nwokike, Clinical experiences with the use of oxytocin injection by healthcare providers in a southwestern state of Nigeria: A cross-sectional study, *PLoS One* **14**, e0208367 (2019) 1–15.
99. E. MacDonald, M. R. Dadds, J. L. Brennan, K. Williams, F. Levy and A. J. Cauchi, A review of safety, side-effects and subjective reactions to intranasal oxytocin in human research, *Psychoneuroendocrinology* **36** (2011) 1114–1126.
100. A. E. Taylor, H. E. Lee and F. T. A. Buisman-Pijlman, Oxytocin treatment in pediatric populations, *Front. Behav. Neurosci.* **8**, 360 (2014) 1–8.
101. F. J. Theunissen, L. Chinery and Y. V. Pujar, Current research on carbetocin and implications for prevention of postpartum haemorrhage, *Reprod. Health* **15** (Suppl 1), 94 (2018) 55–59.



102. X. H. Jin, D. Li and X. Li, Carbetocin vs oxytocin for prevention of postpartum hemorrhage after vaginal delivery: A meta-analysis, *Medicine* **98**, e17911 (2019) 1–7.
103. M. Busnelli and B. Chini, Molecular Basis of Oxytocin Receptor Signalling in the Brain: What We Know and What We Need to Know, *Curr. Top. Behav. Neurosci.* **35** (2018) 3–29.
104. I. Passoni, M. Leonzino, V. Gigliucci, B. Chini and M. Busnelli, Carbetocin is a Functional Selective Gq Agonist That Does Not Promote Oxytocin Receptor Recycling After Inducing  $\beta$ -Arrestin-Independent Internalisation, *J. Neuroendocrinol.* **28** (2016) 1–10.
105. T. M. Goodwin, R. Paul, H. Silver, W. Spellacy, M. Parsons, R. Chez, R. Hayashi, G. Valenzuela, G. W. Creasy and R. Merriman, The effect of the oxytocin antagonist atosiban on preterm uterine activity in the human, *Am. J. Obstet. Gynecol.* **170** (1994) 474–478.
106. A. Reversi, V. Rimoldi, T. Marrocco, P. Cassoni, G. Bussolati, M. Parenti and B. Chini, The oxytocin receptor antagonist atosiban inhibits cell growth via a “biased agonist” mechanism, *J. Biol. Chem.* **280** (2005) 16311–16318.
107. V. Tsatsaris, B. Carbonne and D. Cabrol, Atosiban for preterm labour, *Drugs* **64** (2004) 375–382.
108. B. S. Coler, O. Shynlova, A. Boros-Rausch, S. Lye, S. McCartney, K. B. Leimert, W. Xu, S. Chemtob, D. Olson, M. Li, E. Huebner, A. Curtin, A. Kachikis, L. Savitsky, J. W. Paul, R. Smith and K. M. A. Waldorf, Landscape of Preterm Birth Therapeutics and a Path Forward, *J. Clin. Med.* **10**, 2912 (2021) 1–34.
109. M. Åkerlund, T. Bossmar, R. Brouard, A. Kostrzewska, T. Laudanski, A. Lemancewicz, C. S. le Gal and M. Steinwall, Receptor binding of oxytocin and vasopressin antagonists and inhibitory effects on isolated myometrium from preterm and term pregnant women, *Br. J. Obstet. Gynaecol.* **106** (1999) 1047–1053.
110. H. Helmer, L. Saleh, L. Petricevic, M. Knöfler and T. M. Reinheimer, Barusiban, a selective oxytocin receptor antagonist: placental transfer in rabbit, monkey, and human, *Biol. Reprod.* **103** (2020) 135–143.
111. L. Nilsson, T. Reinheimer, M. Steinwall and M. Åkerlund, FE 200 440: A selective oxytocin antagonist on the term-pregnant human uterus, *BJOG* **110** (2003) 1025–1028.
112. A. D. Borthwick and J. Liddle, The design of orally bioavailable 2, 5-diketopiperazine oxytocin antagonists: from concept to clinical candidate for premature labor, *Med. Res. Rev.* **31** (2011) 576–604.
113. A. A. Moraitis, Y. Cordeaux, D. S. Charnock-Jones and G. C. S. Smith, The Effect of an Oxytocin Receptor Antagonist (Retosiban, GSK221149A) on the Response of Human Myometrial Explants to Prolonged Mechanical Stretch, *Endocrinology* **156** (2015) 3511–3516.
114. S. Thornton, H. Miller, G. Valenzuela, J. Snidow, B. Stier, M. J. Fossler, T. H. Montague, M. Powell and K. J. Beach, Treatment of spontaneous preterm labour with retosiban: a phase 2 proof-of-concept study, *Br. J. Clin. Pharmacol.* **80** (2015) 740–749.
115. Difference between antibody specificity and selectivity | Aeonian Biotech, <https://aeonianbiotech.com/difference-between-antibody-specificity-and-selectivity/> (Date accessed: 15/05/2023)
116. D. J. MacPhee, Methodological considerations for improving Western blot analysis, *J. Pharmacol. Toxicol. Methods* **61** (2010) 171–177.
117. A. K. Abbas, A. H. Lichtman and S. Pillai, *Cellular & Molecular Immunology, 7th Edition*, Saunders, Philadelphia, 2011, pp. 101–103.

118. Y. T. Lo, T. C. Shih, T. W. Pai, L. P. Ho, J. L. Wu and H. Y. Chou, Conformational epitope matching and prediction based on protein surface spiral features, *BMC Genomics* **22** (Suppl 2), 116 (2021) 1–16.
119. B. Forsström, B. Bisławska Axnäs, J. Rockberg, H. Danielsson, A. Bohlin and M. Uhlen, Dissecting antibodies with regards to linear and conformational epitopes, *PLoS One* **10**, e0121673 (2015) 1–11.
120. L. Berglund, J. Andrade, J. Odeberg and M. Uhlén, The epitope space of the human proteome, *Protein Sci.* **17** (2008) 606–613.
121. S. F. Beresten, B. I. Rubikaite and L. L. Kisselev, A general approach to the localization of antigenic determinants of a linear type in proteins of unknown primary structure, *J. Immunol. Methods* **113** (1988) 247–254.
122. Z. Zhang, M. Lu, Y. Qin, W. Gao, L. Tao, W. Su and J. Zhong, Neoantigen: A New Breakthrough in Tumor Immunotherapy, *Front. Immunol.* **12**, 672356 (2021) 1–9.
123. T. MacNeil, I. A. Vathiotis, S. Martinez-Morilla, V. Yaghoobi, J. Zugazagoitia, Y. Liu and D. L. Rimm, Antibody validation for protein expression on tissue slides: a protocol for immunohistochemistry, *Biotechniques* **69** (2020) 461–468.
124. T. Mahmood and P. C. Yang, Western blot: technique, theory, and trouble shooting, *N. Am. J. Med. Sci.* **4** (2012) 429–434.
125. K. Martínez-Flores, Á. T. Salazar-Anzures, J. Fernández-Torres, C. Pineda, C. A. Aguilar-González and A. López-Reyes, Western blot: a tool in the biomedical field, *Investigación discapac.* **6** (2017) 128–137.
126. P. Grayson and J. Rex, The Process of Western Blotting, *Eureka Methods* **1**, e03 (2018) 1–6.
127. E. C. Jensen, The basics of western Blotting, *Anat. Rec. (Hoboken)* **295** (2012) 369–371.
128. R. Ghosh, J. E. Gilda and A. V. Gomes, The necessity of and strategies for improving confidence in the accuracy of western blots, *Expert Rev. Proteomics* **11** (2014) 549–560.
129. S. M. Sandrini, R. D. Haigh and P. P. E. Freestone, Fractionation by Ultracentrifugation of Gram Negative Cytoplasmic and Membrane Proteins, *Bio-Protoc.* **4**, e1287 (2014) 1–4.
130. J. Lebowitz, M. S. Lewis and P. Schuck, Modern analytical ultracentrifugation in protein science: A tutorial review, *Protein Sci.* **11** (2002) 2067–2079.
131. R. Matar-Merheb, M. Rhimi, A. Leydier, F. Huché, C. Galián, E. Desuzinges-Mandon, D. Ficheux, D. Flot, N. Aghajari, R. Kahn, A. di Pietro, J. M. Jault, A. W. Coleman and P. Falson, Structuring detergents for extracting and stabilizing functional membrane proteins, *PLoS One* **6**, e18036 (2011) 1–10.
132. J. J. Bass, D. J. Wilkinson, D. Rankin, B. E. Phillips, N. J. Szewczyk, K. Smith and P. J. Atherton, An overview of technical considerations for Western blotting applications to physiological research, *Scand. J. Med. Sci. Sports* **27** (2017) 4–25.
133. S. C. Taylor, T. Berkelman, G. Yadav and M. Hammond, A defined methodology for reliable quantification of western blot data, *Mol. Biotechnol.* **55** (2013) 217–226.
134. J. E. Noble and M. J. A. Bailey, Quantitation of protein, *Methods Enzymol.* **463** (2009) 73–95.
135. J. P. D. Goldring, Protein quantification methods to determine protein concentration prior to electrophoresis, *Methods Mol. Biol.* **869** (2012) 29–35.
136. O. H. Lowry, N. J. Rosebrough, A. L. Farr and R. J. Randall, Protein measurement with the Folin phenol reagent, *J. Biol. Chem.* **193** (1951) 265–275.

137. S. J. Compton and C. G. Jones, Mechanism of dye response and interference in the Bradford protein assay, *Anal. Biochem.* **151** (1985) 369–374.
138. M. M. Bradford, A rapid and sensitive method for the quantitation of microgram quantities of protein utilizing the principle of protein-dye binding, *Anal. Biochem.* **72** (1976) 248–254.
139. B. O. Fanger, Adaptation of the Bradford protein assay to membrane-bound proteins by solubilizing in glucopyranoside detergents, *Anal. Biochem.* **162** (1987) 11–17.
140. P. K. Smith, R. I. Krohn, G. T. Hermanson, A. K. Mallia, F. H. Gartner, M. D. Provenzano, E. K. Fujimoto, N. M. Goeke, B. J. Olson and D. C. Klenk, Measurement of protein using bicinchoninic acid, *Anal. Biochem.* **150** (1985) 76–85.
141. J. M. Walker, The bicinchoninic acid (BCA) assay for protein quantitation, *Methods Mol. Biol.* **32** (1994) 5–8.
142. Bicinchoninic Acid Protein Assay Kit, Catalog Numbers BCA1 AND B9643, TECHNICAL BULLETIN | Sigma-Aldrich, <https://www.sigmaaldrich.com/deepweb/assets/sigmaaldrich/product/documents/322/296/bca1bul.pdf> (Date accessed: 05/03/2023)
143. H. Begum, P. Murugesan and A. D. Tangutur, Western blotting: A powerful staple in scientific and biomedical research, *Biotechniques* **73** (2022) 59–69.
144. J. L. Tonkinson and B. A. Stillman, Nitrocellulose: a tried and true polymer finds utility as a post-genomic substrate, *Front. Biosci.* **7** (2002) c1–12.
145. B. T. Kurien and R. H. Scofield, Western Blotting: An Introduction, *Methods Mol. Biol.* **1312** (2015) 17–30.
146. P. Matsudaira, Sequence from picomole quantities of proteins electroblotted onto polyvinylidene difluoride membranes, *J. Biol. Chem.* **262** (1987) 10035–10038.
147. B. T. Kurien and R. H. Scofield, Protein blotting: A review, *J. Immunol. Methods* **274** (2003) 1–15.
148. H. Towbin, T. Staehelin and J. Gordon, Electrophoretic transfer of proteins from polyacrylamide gels to nitrocellulose sheets: procedure and some applications, *Proc. Natl. Acad. Sci. U. S. A.* **76** (1979) 4350–4354.
149. E. R. Tovey and B. A. Baldo, Protein binding to nitrocellulose, nylon and PVDF membranes in immunoassays and electroblotting, *J. Biochem. Biophys. Methods* **19** (1989) 169–183.
150. J. M. Gershoni and G. E. Palade, Electrophoretic transfer of proteins from sodium dodecyl sulfate-polyacrylamide gels to a positively charged membrane filter, *Anal. Biochem.* **124** (1982) 396–405.
151. S. W. Lallier, C. L. Hill, D. P. Nichols and S. D. Reynolds, Protein Abundance Determination: An Optimized Western Blot Workflow, *Ann. Clin. Lab. Sci.* **49** (2019) 507–512.
152. R. J. Ober, C. G. Radu, V. Ghetie and E. S. Ward, Differences in promiscuity for antibody-FcRn interactions across species: implications for therapeutic antibodies, *Int. Immunol.* **13** (2001) 1551–1559.
153. Clarity and Clarity Max Western ECL Substrates | Bio-Rad, Instruction Manual, <https://www.bio-rad.com/webroot/web/pdf/lsr/literature/D085075.pdf> (Date accessed: 05/03/2023)
154. E. van Andel, M. Roosjen, S. van der Zanden, S. C. Lange, D. Weijers, M. M. J. Smulders, H. F. J. Savelkoul, H. Zuilhof and E. J. Tijhaar, Highly Specific Protein Identification by Immunoprecipitation-Mass Spectrometry Using Antifouling Microbeads, *ACS Appl. Mater. Interfaces* **14** (2022) 23102–23116.

155. J. S. Bonifacino, D. C. Gershlick and E. C. Dell'Angelica, Immunoprecipitation, *Curr. Protoc. Cell Biol.* **71** (2016) 7.2.1–7.2.24.
156. B. Kaboord and M. Perr, Isolation of proteins and protein complexes by immunoprecipitation, *Methods Mol. Biol.* **424** (2008) 349–364.
157. J. S. K. Chan, Z. Q. Teo, M. K. Sng and N. S. Tan, Probing for protein-protein interactions during cell migration: limitations and challenges, *Histol. Histopathol.* **29** (2014) 965–976.
158. Affinity of Protein A/G for IgG Types from Different Species | NEB, <https://international.neb.com/tools-and-resources/selection-charts/affinity-of-protein-ag-for-igg-types-from-different-species> (Date accessed: 08/03/2023)
159. Protein A vs Protein G | sepmag, <https://www.sepmag.eu/blog/protein-a-vs-protein-g> (Date accessed: 08/03/2023)
160. Comparison of Antibody IgG Binding Proteins | Thermo Fisher Scientific – ES, <https://www.thermofisher.com/es/es/home/life-science/antibodies/antibodies-learning-center/antibodies-resource-library/antibody-methods/comparison-antibody-igg-binding-proteins.html> (Date accessed: 08/03/2023)
161. Optimize elution conditions for immunoaffinity purification | Thermo Fisher Scientific, TECH TIP # 27, <https://assets.thermofisher.com/TFS-Assets/LSG/Application-Notes/TR0027-Elution-conditions.pdf> (Date accessed: 06/03/2023))
162. J. DeCaprio and T. O. Kohl, Immunoprecipitation, *Cold Spring Harb. Protoc.* **2017** (2017) 1003–1008.
163. T. Dau, G. Bartolomucci and J. Rappsilber, Proteomics Using Protease Alternatives to Trypsin Benefits from Sequential Digestion with Trypsin, *Anal. Chem.* **92** (2020) 9523–9527.
164. L. Tsiatsiani and A. J. R. Heck, Proteomics beyond trypsin, *FEBS J.* **282** (2015) 2612–2626.
165. E. di Cera, Serine Proteases, *IUBMB Life* **61** (2009) 510–515.
166. T. M. Maia, A. Staes, K. Plasman, J. Pauwels, K. Boucher, A. Argentini, L. Martens, T. Montoye, K. Gevaert and F. Impens, Simple Peptide Quantification Approach for MS-Based Proteomics Quality Control, *ACS Omega* **5** (2020) 6754–6762.
167. Scientific Image and Illustration Software | BioRender, <https://www.biorender.com>
168. Pierce BCA Protein Assay Kit | Thermo Fisher Scientific, Instructions, [https://www.urmc.rochester.edu/MediaLibraries/URMCMedia/labs/ritchlin-lab/documents/MAN0011430\\_Pierce\\_BCA\\_Protein\\_Asy\\_UG.pdf](https://www.urmc.rochester.edu/MediaLibraries/URMCMedia/labs/ritchlin-lab/documents/MAN0011430_Pierce_BCA_Protein_Asy_UG.pdf) (Date accessed: 08/03/2023)
169. J. L. Luque-Garcia and T. A. Neubert, On-Membrane Tryptic Digestion of Proteins for Mass Spectrometry Analysis, *Methods Mol. Biol.* **536** (2009) 331–341.
170. D. D. Mruk and C. Y. Cheng, Enhanced chemiluminescence (ECL) for routine immunoblotting: An inexpensive alternative to commercially available kits, *Spermatogenesis* **1** (2011) 121–122.
171. H. Sander, S. Wallace, R. Plouse, S. Tiwari and A. V. Gomes, Ponceau S Waste: Ponceau S Staining for Total Protein Normalization, *Anal. Biochem.* **575** (2019) 44–53.
172. D. Racusen, Stoichiometry of the amido black reaction with proteins, *Anal. Biochem.* **52** (1973) 96–101.
173. Western Blotting | BioLegend, <https://www.biolegend.com/en-ie/western-blot> (Date accessed: 27/03/2023)

174. R. L. Gundry, M. Y. White, C. I. Murray, L. A. Kane, Q. Fu, B. A. Stanley and J. E. Van Eyk, Preparation of proteins and peptides for mass spectrometry analysis in a bottom-up proteomics workflow, *Curr. Protoc. Mol. Biol.* (2009) 10.25.1–10.25.29.
175. S. R. Hawtin, A. R. L. Davies, G. Matthews and M. Wheatley, Identification of the glycosylation sites utilized on the V1a vasopressin receptor and assessment of their role in receptor signalling and expression, *Biochem. J.* **357** (2001) 73–81.
176. E. C. McKay and S. E. Counts, Oxytocin Receptor Signaling in Vascular Function and Stroke, *Front. Neurosci.* **14**, 574499 (2020) 1–18.
177. F. Wang, X. S. Yin, J. Lu, C. Cen and Y. Wang, Phosphorylation-dependent positive feedback on the oxytocin receptor through the kinase PKD1 contributes to long-term social memory, *Sci. Signal.* **15**, eabd0033 (2022)
178. C. R. Lee, Y. H. Park, Y. R. Kim, A. Peterkofsky and Y. J. Seok, Phosphorylation-Dependent Mobility Shift of Proteins on SDS-PAGE is Due to Decreased Binding of SDS, *Bull. Korean Chem. Soc.* **34** (2013) 2063–2066.
179. E. Selcuk Unal, R. Zhao, A. Qiu and I. D. Goldman, N-linked glycosylation and its impact on the electrophoretic mobility and function of the human proton-coupled folate transporter (HsPCFT), *Biochim. Biophys. Acta Biomembr.* 1778 (2008) 1407–1414.
180. A. Shevchenko, H. Tomas, J. Havliš, J. V. Olsen and M. Mann, In-gel digestion for mass spectrometric characterization of proteins and proteomes, *Nat. Protoc.* **1** (2007) 2856–2860.
181. J. Fernandez and S. M. Mische, Enzymatic Digestion of Proteins on PVDF Membranes, *Curr. Protoc. Protein Sci.* (2001) 11.2.1–11.2.10.
182. U. Omasits, C. H. Ahrens, S. Müller and B. Wollscheid, Protter: interactive protein feature visualization and integration with experimental proteomic data, *Bioinformatics* **30** (2014) 884–886.
183. S. Milling, Using monoclonal antibodies to investigate molecular immunology: there's more to know!, *Immunology* 157 (2019) 281–282.
184. K. J. Rhodes and J. S. Trimmer, Antibodies as Valuable Neuroscience Research Tools versus Reagents of Mass Distraction, *J. Neurosci.* **26** (2006) 8017–8020.
185. R. M. Lu, Y. C. Hwang, I. J. Liu, C. C. Lee, H. Z. Tsai, H. J. Li and H. C. Wu, Development of therapeutic antibodies for the treatment of diseases, *J. Biomed. Sci.* **27** (2020) 1–30.
186. B. Baldari, S. Vittorio, F. Sessa, L. Cipolloni, G. Bertozzi, M. Neri, S. Cantatore, V. Fineschi and M. Aromatario, Forensic Application of Monoclonal Anti-Human Glycophorin A Antibody in Samples from Decomposed Bodies to Establish Vitality of the Injuries. A Preliminary Experimental Study, *Healthcare* **9**, 514 (2021) 1–10.
187. N. Egashira, A. Tanoue, T. Matsuda, E. Koushi, S. Harada, Y. Takano, G. Tsujimoto, K. Mishima, K. Iwasaki and M. Fujiwara, Impaired social interaction and reduced anxiety-related behavior in vasopressin V1a receptor knockout mice, *Behav. Brain Res.* **178** (2007) 123–127.
188. G. Köhler and C. Milstein, Continuous cultures of fused cells secreting antibody of predefined specificity, *Nature* **256** (1975) 495–497.

189. M. Chalfie, Y. Tu, G. Euskirchen, W. W. Ward and D. C. Prasher, Green fluorescent protein as a marker for gene expression, *Science* **263** (1994) 802–805.
190. L. Pillai-Kastoori, S. Heaton, S. D. Shiflett, A. C. Roberts, A. Solache and A. R. Schutz-Geschwender, Antibody validation for Western blot: By the user, for the user, *J. Biol. Chem.* **295** (2020) 926–939.
191. G. Milligan, Exploring the dynamics of regulation of G protein-coupled receptors using green fluorescent protein, *Br. J. Pharmacol.* **128** (1999) 501–510.
192. J. J. Coon, J. E. P. Syka, J. Shabanowitz and D. F. Hunt, Tandem mass spectrometry for peptide and protein sequence analysis, *Biotechniques* **38** (2005) 519–523.
193. M. R. Larsen, M. B. Trelle, T. E. Thingholm and O. N. Jensen, Analysis of posttranslational modifications of proteins by tandem mass spectrometry, *Biotechniques* **40** (2006) 790–798.
194. Y. N. Lee, L. K. Chen, H. C. Ma, H. H. Yang, H. P. Li and S. Y. Lo, Thermal aggregation of SARS-CoV membrane protein, *J. Virol. Methods* **129** (2005) 152–161.
195. K. Miyano, S. Okamoto, M. Kajikawa, C. Kawai, T. Kanagawa, S. Tominaga, A. Yamauchi, F. Kiribayashi, The efficient detection of membrane protein with immunoblotting: lessons from cold-temperature denaturation, *Kawasaki Med. J.* **47** (2021) 13–19.
196. J. P. Hennessey and G. A. Scarborough, An optimized procedure for sodium dodecyl sulfate-polyacrylamide gel electrophoresis analysis of hydrophobic peptides from an integral membrane protein, *Anal. Biochem.* **176** (1989) 284–289.
197. C. Sagné, M. F. Isambert, J. P. Henry and B. Gasnier, SDS-resistant aggregation of membrane proteins: application to the purification of the vesicular monoamine transporter, *Biochem. J.* **316** (1996) 825–831.
198. M. K. Crow, N. Karasavvas and A. H. Sarris, Protein aggregation mediated by cysteine oxidation during the stacking phase of discontinuous buffer SDS-PAGE, *Biotechniques* **30** (2001) 311–316.
199. Y. Tsuji, Transmembrane protein western blotting: Impact of sample preparation on detection of SLC11A2 (DMT1) and SLC40A1 (ferroportin), *PLoS One* **15**, e0235563 (2020) 1–18.
200. H. Persson, C. Preger, E. Marcon, J. Lengqvist and S. Gräslund, Antibody Validation by Immunoprecipitation Followed by Mass Spectrometry Analysis, *Methods Mol. Biol.* **1575** (2017) 175–187.
201. S. N. Thomas, 'Mass spectrometry', in Ed. W. Clarke and M. A. Marzinke, *Contemporary Practice in Clinical Chemistry, Fourth Edition*, Academic Press, 2020, pp. 171–185.
202. A. Kalli, G. T. Smith, M. J. Sweredoski and S. Hess, Evaluation and optimization of mass spectrometric settings during data-dependent acquisition mode: focus on LTQ-Orbitrap mass analyzers, *J. Proteome Res.* **12** (2013) 3071–3086.
203. D. M. Cox, M. Du and J. C. McDermott, 'Proteomic Analysis of MEF2 Post-Translational Regulation in the Heart', in Ed. N. Rosenthal and R. P. Harvey, *Heart Development and Regeneration*, Vol. 1, Academic Press, 2010, pp. 805–824.
204. J. G. Meyer, Qualitative and Quantitative Shotgun Proteomics Data Analysis from Data-Dependent Acquisition Mass Spectrometry, *Methods Mol. Biol.* **2259** (2021) 297–308.
205. G. Lubec and L. Afjehi-Sadat, Limitations and pitfalls in protein identification by mass spectrometry, *Chem. Rev.* **107** (2007) 3568–3584.

206. T. Köcher, P. Pichler, R. Swart and K. Mechtler, Quality control in LC-MS/MS, *Proteomics* **11** (2011) 1026–1030.
207. S. Wu, M. Birnbaumer and Z. Guan, Phosphorylation Analysis of G Protein-coupled Receptor by Mass Spectrometry: Identification of a Novel Phosphorylation Site in V2 Vasopressin Receptor, *Anal. Chem.* **80** (2008) 6034–6037.
208. S. Pal and A. Chattopadhyay, Extramembranous Regions in G Protein-Coupled Receptors: Cinderella in Receptor Biology?, *J. Membr. Biol.* **252** (2019) 483–497.
209. H.-C. Yang, W. Li, J. Sun and M. L. Gross, Advances in Mass Spectrometry on Membrane Proteins, *Membranes* **13**, 457 (2023) 1–15.
210. S. Grutsch, J. E. Fuchs, L. Ahammer, A. S. Kamenik, K. R. Liedl and M. Tollinger, Conformational Flexibility Differentiates Naturally Occurring Bet v 1 Isoforms, *Int. J. Mol. Sci.* **18**, 1192 (2017) 1–15.
211. L. Trinkle-Mulcahy, S. Boulon, Y. W. Lam, R. Urcia, F. M. Boisvert, F. Vandermoere, N. A. Morrice, S. Swift, U. Rothbauer, H. Leonhardt and A. Lamond, Identifying specific protein interaction partners using quantitative mass spectrometry and bead proteomes, *J. Cell Biol.* **183** (2008) 223–239.
212. U. Rothbauer, K. Zolghadr, S. Muyldermans, A. Schepers, M. C. Cardoso and H. Leonhardt, A versatile nanotrap for biochemical and functional studies with fluorescent fusion proteins, *Mol. Cell. Proteomics* **7** (2008) 282–289.
213. S. M. Moore, S. M. Hess and J. W. Jorgenson, Extraction, Enrichment, Solubilization, and Digestion Techniques for Membrane Proteomics, *J. Proteome Res.* **15** (2016) 1243–1252.
214. H. Bouabe, R. Fässler and J. Heesemann, Improvement of reporter activity by IRES-mediated polycistronic reporter system, *Nucleic Acids Res.* **36**, e28 (2008) 1–9.
215. M. Iwamoto, C. Mori, Y. Hiraoka and T. Haraguchi, Puromycin resistance gene as an effective selection marker for ciliate Tetrahymena, *Gene*. **534** (2014) 249–255.
216. D. G. Gibson, L. Young, R. Y. Chuang, J. C. Venter, C. A. Hutchison and H. O. Smith, Enzymatic assembly of DNA molecules up to several hundred kilobases, *Nat. Methods* **6** (2009) 343–345.
217. J. A. Powers, B. Skinner, B. S. Davis, B. J. Biggerstaff, L. Robb, E. Gordon, W. M. de Souza, M. J. Fumagalli, A. E. Calvert and G.-J. Chang, Development of HEK-293 Cell Lines Constitutively Expressing Flaviviral Antigens for Use in Diagnostics, *Microbiol. Spectr.* **10**, e00592-22 (2022) 1–16.
218. E. Tan, C. S. H. Chin, Z. F. S. Lim and S. K. Ng, HEK293 Cell Line as a Platform to Produce Recombinant Proteins and Viral Vectors, *Front. Bioeng. Biotechnol.* **9**, 796991 (2021) 1–9.
219. N. A. Farahany, S. Hyman, C. Koch, C. Grady, S. P. Paşca, N. Sestan, P. Arlotta, J. L. Bernat, J. Ting, J. E. Lunshof, E. P. R. Iyer, I. Hyun, B. H. Capestany, G. M. Church, H. Huang and H. Song, The ethics of experimenting with human brain tissue, *Nature* **556** (2018) 429–432.

## § 8. APPENDIX

Predicted and partially confirmed sequences of two plasmids for overexpression of recombinant proteins hOTR-eGFP and hV1aR-eGFP are given below. Plasmids were sent for sequencing, but the information obtained was limited.

>hOTR-eGFP fused

```

ATGGAGGGCGCGCTCGCAGCCAACCTGGAGCGCCGAGGCAGCCAACGCCAGCGCCGCGCCGGGGGCCGAGGGC
AACCGCACCCGCCGGACCCCGCGGGCGCAACGAGGCCCTGGCGCGCGTGGAGGTGGCGGTGCTGTGTCTCATCCTG
CTCCTGGCGCTGAGCGGGAACGCGTGTGTGCTGCTGGCGCTGCGCACACGCCAGAAGCACTCGCGCCTCTTC
TTCTTCATGAAGCACCTAAGCATCGCCGACCTGGTGGTGGCAGTGTTCAGGTGCTGCCGAGTTGCTGTGGGAC
ATCACCTTCCGCTTCTACGGGCCCGACCTGCTGTGCCGCTGGTCAAGTACTTGCAGGTGGTGGGCATGTTCCGCC
TCCACCTACCTGCTGCTGCTCATGTCCCTGGACCGCTGCCTGGCCATCTGCCAGCCGCTGCGCTCGCTGCGCCGC
CGCACCCGACCGCCTGGCAGTGCTCGCCACGTGGCTCGGCTGCCTGGTGGCCAGCGCGCCGAGGTGCACATCTTC
TCTCTGCGCGAGGTGGCTGACGGCGTCTTCGACTGCTGGGCCGTCTTCATCCAGCCCTGGGGACCCAAGGCCAC
ATCACATGGATCACGCTAGCTGTCTACATCGTGCCGGTTCATCGTGCTCGCTGCCTGCTACGGCCTTATCAGCTTC
AAGATCTGGCAGAACTTGGCGCTCAAGACCGCTGCAGCGGCGGGCCGAGGGCGCCAGAGGGCGCGGGCGGTGGC
GATGGGGGGCGCGTGGCCCTGGCGCGTGTGASCAGCGTCAAGCTCATCTCCAAGGCCAAGATCCGCACGGTCAAG
ATGACTTTCATCATCGTGCTGCTGGCCTTCATCGTGTGCTGGACGCCTTCTTCTTCGTGCAGATGTGGAGCGTCTGG
GATGCCAACCGCGCCCAAGGAAGCCTCGGCCTTCATCATCGTTCATGCTCCTGGCCAGCCTCAACAGCTGCTGCAAC
CCCTGGATCTACATGCTGTTACGGGCCACCTCTTCCACRAACTCGTGCAGCGCTTCTGTGCTGCTCCGCCAGC
TACCTGAAGGGCAGACGCCTGGGAGAGACGAGTGCCAGCAAAAAAGAGCAACTCGTCCTCCTTTGTCTGAGCCAT
CGCAGCTCCAGCCAGAGGAGCTGCTCCCAGCCATCCACGATCCACCGGATCCAGGATGGTGAGCAAGGGCGAG
GAGCTGTTACCGGGGTGGTGCCATCCTGGTCGAGCTGGACGGCGACGTAAACGGCCACAAGTTCAGCGTGTCC
GGCGAGGGCGAGGGCGATGCCACCTACGGCAAGCTGACCCTGAAGTTCATCTGCACCACCGGCAAGCTGCCCGTG
CCCTGGCCACCCTCGTGACCACCCTGACCTACGGCGTGCAGTGCTTCAGCCGCTACCCCGACCACATGAAGCAG
CACGACTTCTTCAAGTCCGCCATGCCCCAAGGCTACGTCCAGGAGCGCACCATCTTCTTCAAGGACGACGGCAAC
TACAAGACCCGCGCCGAGGTGAAGTTCGAGGGCGACACCCTGGTGAACCGCATCGAGCTGAAGGGCATCGACTTC
AAGGAGGACGGCAACATCCTGGGGCACAAGCTGGAGTACAACAGCCACAACGTCTATATCATGGCCGAC
AAGCAGAAGAACGGCATCAAGGTGAAGTTCAGATCCGCCACAACATCGAGGACGGCAGCGTGCAGCTCGCCGAC
CACTACCAGCAGAACACCCCATCGGCGACGGCCCCGTGCTGCTGCCCCGACAACCACTACCTGAGCACCAGTCC
GCCCTGAGCAAAGACCCCAACGAGAAGCGCGATCACATGGTCTGCTGGAGTTTCGTGACCGCCGCCGGGATCACT
CTCGGCATGGACGAGCTGTACAAGTAA

```

\_ hOTR – not sequenced part, assuming it is correct

\_ hOTR – sequenced part

**Linker**

\_ eGFP



>hV1aR-eGFP fused

```

ATGCGTCTCTCCGCCGGTCCCGACGCGGGGCCCTCGGGCAACTCCAGCCCATGGTGGCCTCTGGCCACCGGCGCT
GGCAACACAAGCCGGGAGGCCGAAGCCCTCGGGGAGGGCAACGGCCACCGAGGGACGTGCGCAACGAGGAGCTG
GCCAAACTGGAGATCGCCGTGCTGGCGGTGACTTTTCGCGGTGGCCGTGCTGGGCAACAGCAGCGTACTGCTGGCT
CTGCACCGGACGCCGCGCAAGACGTCCCGCATGCACCTCTTCATCCGACACCTCAGCCTGGCCGACCTGGCCGTG
GCATTCTTCCAGGTGCTGCCGCAAATGTGCTGGGACATCACCTACCGCTTCCGCGGGCCCCGACTGGCTGTGCCGC
GTGGTGAAGCACCTGCAGGTGTTTCGGCATGTTTTCGCTCGGCCTACATGCTGGTAGTCATGACAGCCGACCGCTAC
ATCGCGGTGTGCCACCCGCTCAAGACTCTGCAACAGCCCGCGCGCCGCTCGCGCCTCATGATCGCGGCCGCTGG
GTGCTGAGCTTCGTGCTGAGCACGCCGACGTACTTCGTCTTCTCCATGATCGAGGTGAACAATGTCACCAAGGCC
CGCGACTGCTGGGCCACCTTCATCCAGCCCTGGGGTTCTCGTGCCTACGTGACCTGGATGACGGGCGGCATCTTT
GTGGCGCCCGTGGTCACTTTGGGTACCTGCTACGGCTTCATCTGCTACAACATCTGGTGAACGTCCGCGGGAAG
ACGGCGTCCGCGCAGAGCAAGGTGCAGAGCAAGCGGTGTGGCCTTCCAAAAGGGGTTCTGCTCGCACCTGT
GTCAGCAGCGTGAAGTCCATTTCCCGGGCCAAGATCCGACCGGTGAAGATGACTTTTGTGATCGTGACGGCTTAC
ATCGTCTGCTGGGCGCCTTTCTTCATCATCCAGATGTGGTCTGTCTGGGATCCCATGTCCGTCTGGACCGAATCG
GAAAACCCTACCATCACCATCACTGCATTACTGGGTTCCCTTGAATAGCTGCTGTAATCCCTGGATATACATGTTT
TTTAGTGGCCATCTCCTTCAAGACTGTGTTCAAAGCTTCCCATGCTGCCAAAAACATGAAGGAAAAAATCAACAAA
GAAGATACTGACAGTATGAGCAGAAGACAGACTTTTTATTCTAACAATCGAAGCCCAACAAAACAGTACGGGTATG
TGGAAGGACTCGCCTAAATCTTCCAAGTCCATCAAATTCATTCCTGTTTCAACTGATCCACCGGTTCGCCACCATG
GTGAGCAAGGGCGAGGAGCTGTTTACCAGGGGTGGTGCCATCCTGGTCGAGCTGGACGGCGACGTAAACGGCCAC
AAGTTCAGCGTGTCCGGCGAGGGCGAGGGCGATGCCACCTACGGCAAGCTGACCTGAAGTTCATCTGCACCACC
GGCAAGCTGCCCGTGCCTGGCCACCCTCGTGACCACCTGACCTACGGCGTGCAGTGTTCAGCCGCTACCCC
GACCACATGAAGCAGCACGACTTCTTCAAGTCCGCCATGCCCGAAGGCTACGTCCAGGAGCGCACCATCTTCTTC
AAGGACGACGGCAACTACAAGACCCGCGCCGAGGTGAAGTTCGAGGGCGACACCCTGGTGAACCGCATCGAGCTG
AAGGGCATCGACTTCAAGGAGGACGGCAACATCCTGGGGCACAAGCTGGAGTACAACACTACAACAGCCACAACGTC
TATATCATGGCCGACAAGCAGAAGAACGGCATCAAGGTGAACTTCAAGATCCGCCACAACATCGAGGACGGCAGC
GTGCAGCTCGCCGACCACTACCAGCAGAACACCCCATCGGCGACGGCCCCGTGCTGCTGCCGACAACCACTAC
CTGAGCACCCAGTCCGCCCTGAGCAAAGACCCCAACGAGAAGCGCGATCACATGGTCTGCTGGAGTTCGTGACC
GCCCGGGGATCACTCTCGGCATGGACGAGCTGTACAAGTAA

```

\*(this sequence is purely theoretical, as it was not sequenced successfully)

\_ hV1aR – ref seq

**Linker** (assuming the same as in hOTR-eGFP fused)

\_ eGFP

WB images and corresponding amido black stained membranes for the antibodies validated against V1aR: 3C1, 3F8, and 4A7, are presented in Figure A1–Figure A6.

WB images and corresponding amido black stained membranes for the antibodies validated against OTR: 1A3, 1C10, 1E4, 1F1, 4F3-4, 4F3-5, and 1B2, are presented in Figure A7–Figure A20.

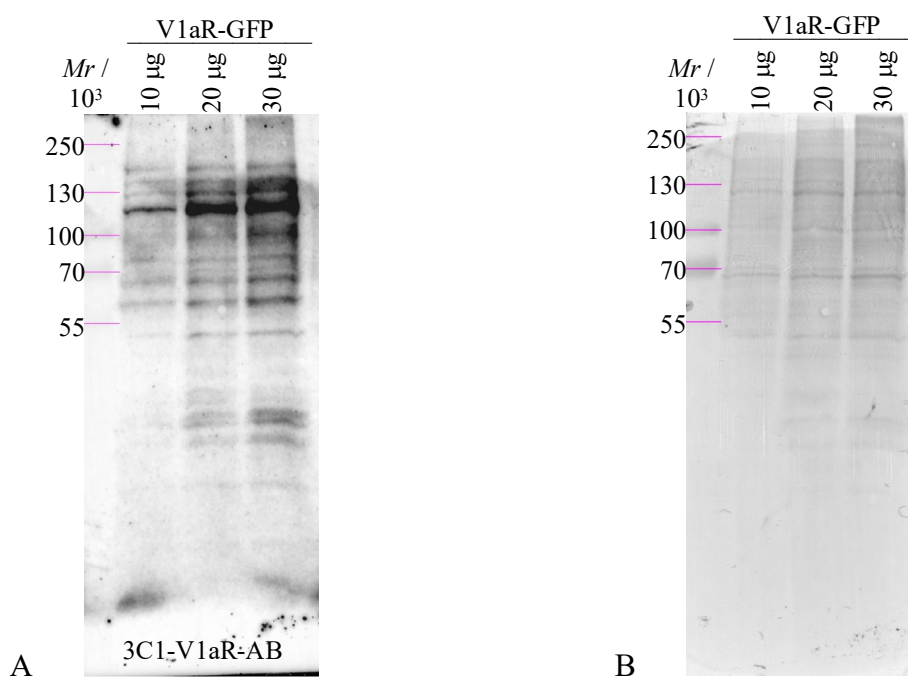


Figure A1. 3C1 antibody (~1:1000) signal dependence on V1aR-GFP load after incubation in secondary DoxRb-HRP antibody (1:10,000) and Clarity Max, 173.118 s rapid autoexposure; B – Amido black staining after chemiluminescence detection.

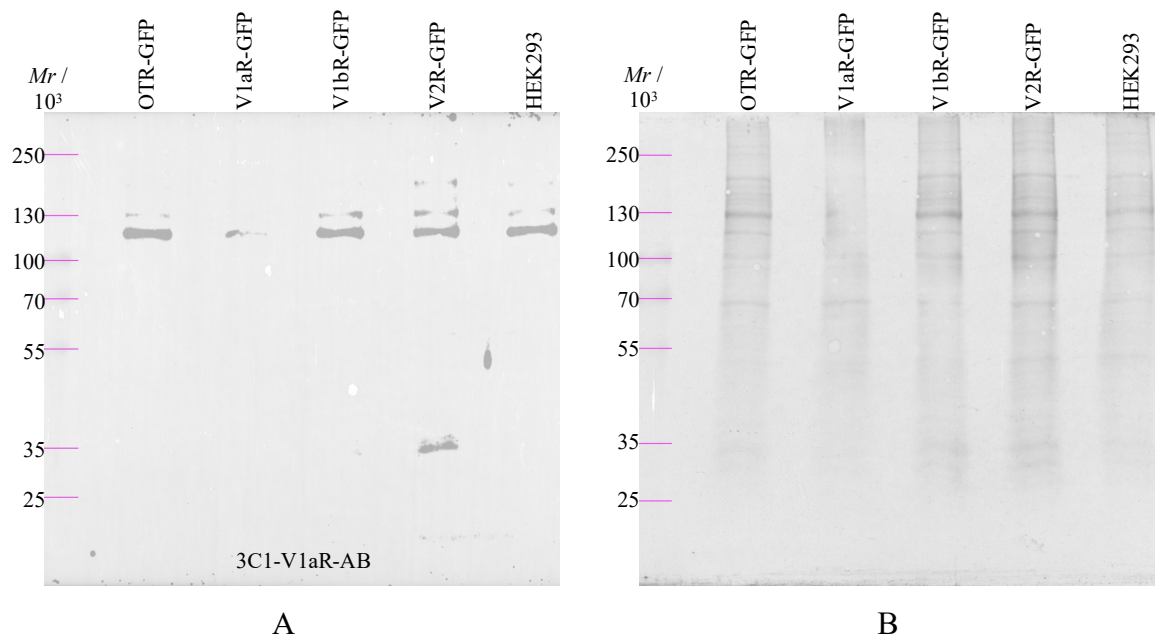


Figure A2. Specificity of primary 3C1 antibody (~1:1000) after incubation in secondary DoxRb-HRP antibody (1:10,000) and Clarity Max, 200 s manual exposure; B – Amido black staining after chemiluminescence detection.

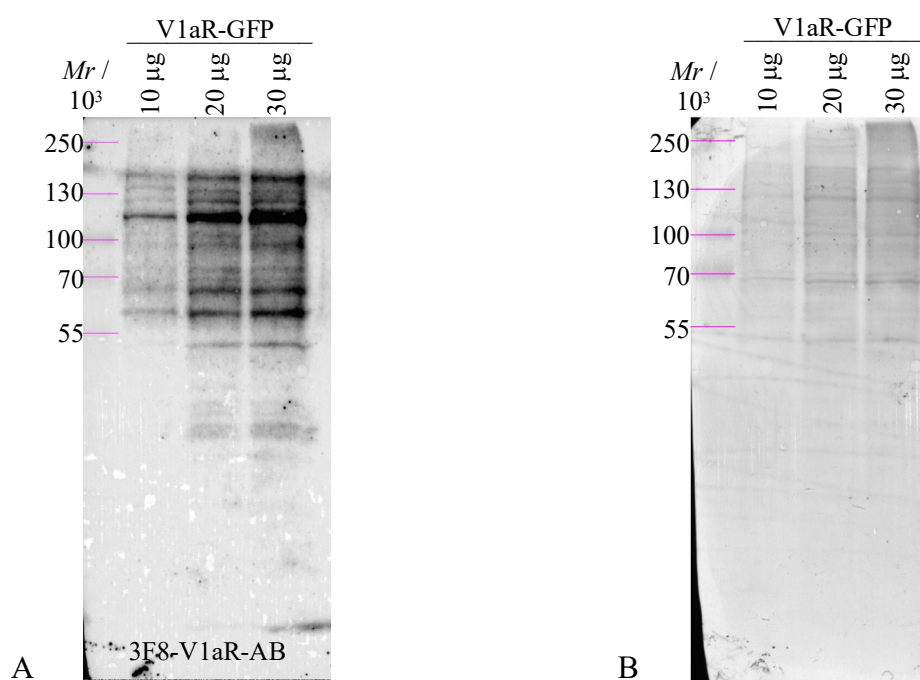


Figure A3. 3F8 antibody (~1:1000) signal dependence on V1aR-GFP load after incubation in secondary DoxRb-HRP antibody (1:10,000) and Clarity Max, 268.826 s rapid autoexposure; B – Amido black staining after chemiluminescence detection.

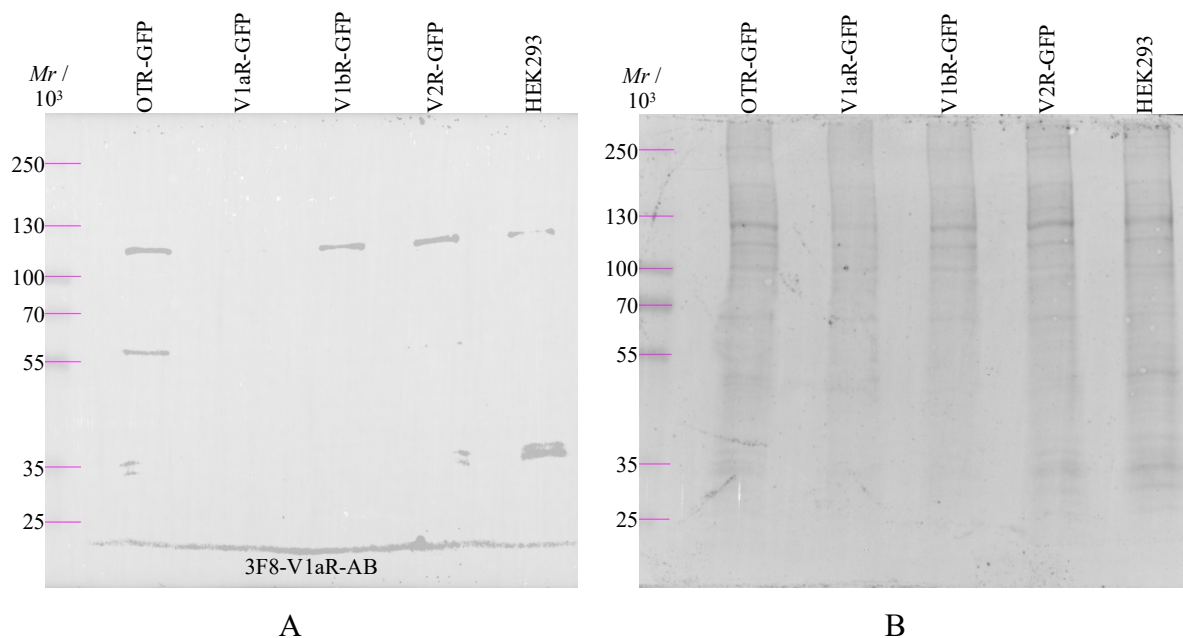


Figure A4. Specificity of primary 3F8 antibody (~1:1000) after incubation in secondary DoxRb-HRP antibody (1:10,000) and Clarity Max, 90 s manual exposure; B – Amido black staining after chemiluminescence detection.

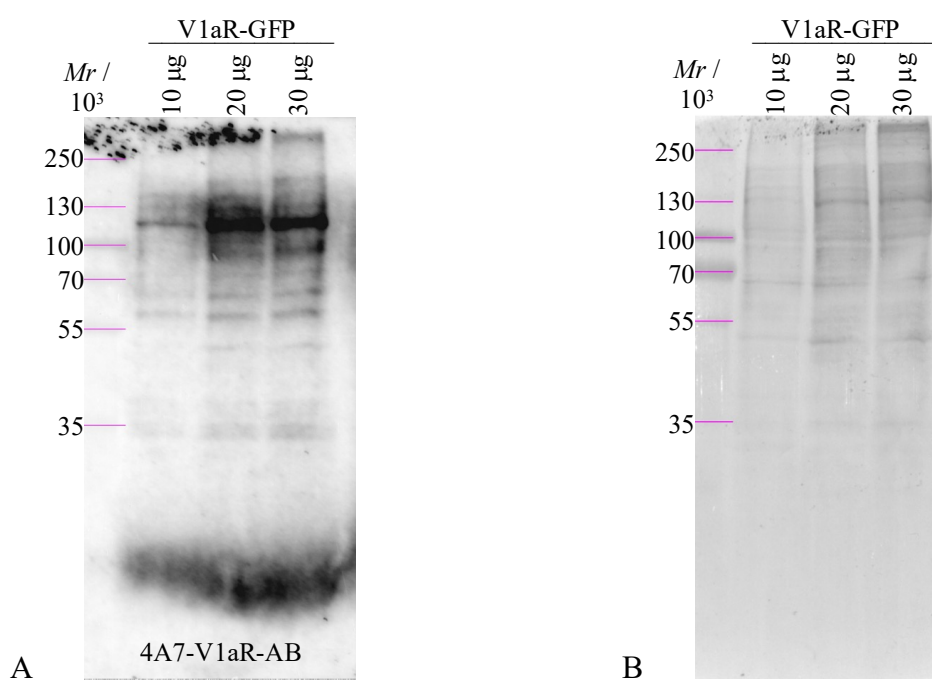


Figure A5. 4A7 antibody (~1:1000) signal dependence on V1aR-GFP load after incubation in secondary DoxRb-HRP antibody (1:10,000) and Clarity Max, 301.865 s rapid autoexposure; B – Amido black staining after chemiluminescence detection.

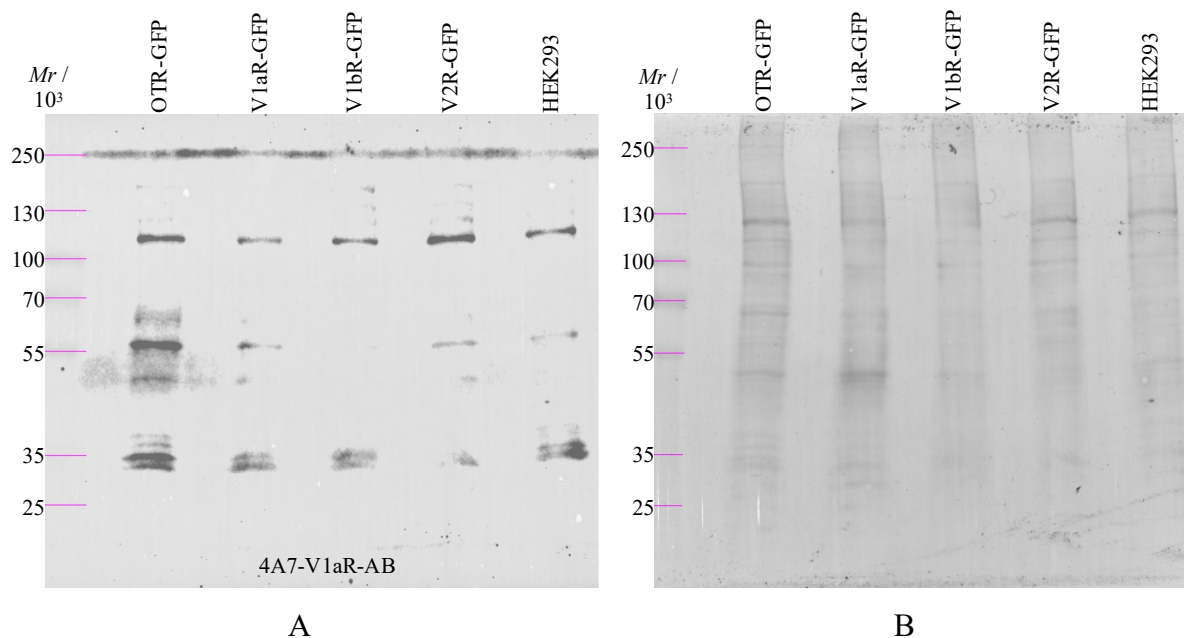


Figure A6. Specificity of primary 4A7 antibody (~1:1000) after incubation in secondary DoxRb-HRP antibody (1:10,000) and Clarity Max, 150 s manual exposure; B – Amido black staining after chemiluminescence detection.

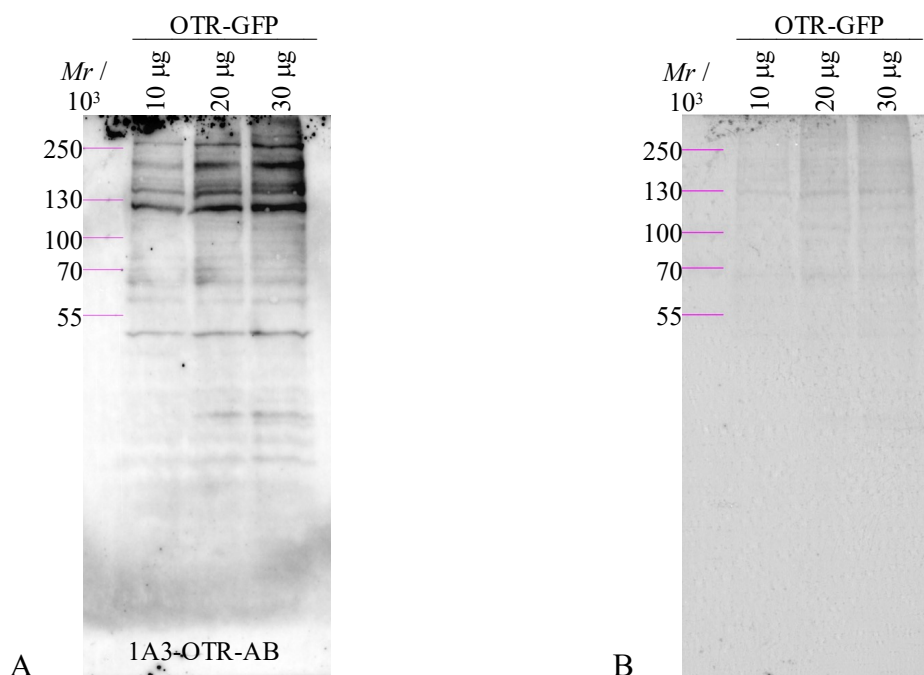


Figure A7. 1A3 antibody (~1:1000) signal dependence on OTR-GFP load after incubation in secondary DoxRb-HRP antibody (1:10,000) and Clarity Max, 471.973 s rapid autoexposure; B – Amido black staining after chemiluminescence detection.

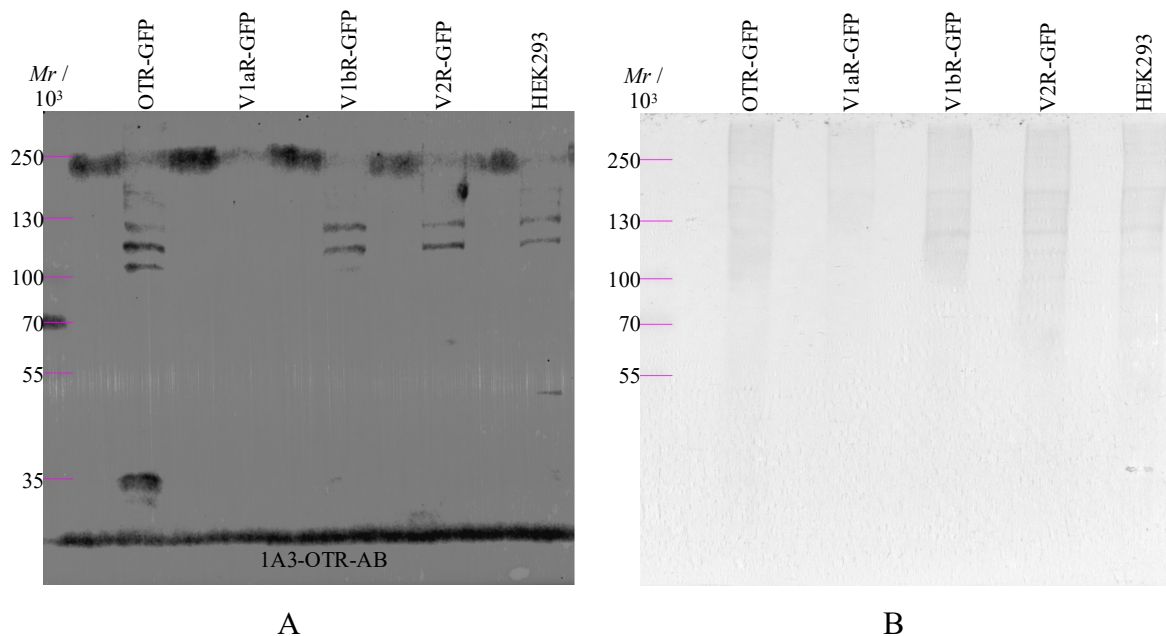


Figure A8. Specificity of primary 1A3 antibody (~1:1000) after incubation in secondary DoxRb-HRP antibody (1:10,000) and Clarity Max, 120 s manual exposure; B – Amido black staining after chemiluminescence detection.

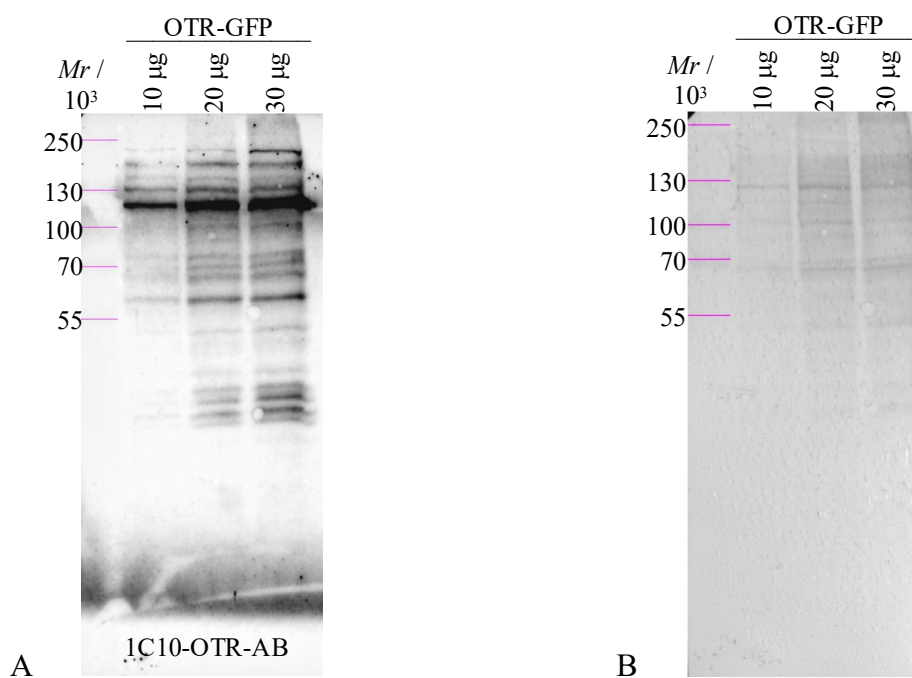


Figure A9. 1C10 antibody (~1:1000) signal dependence on OTR-GFP load after incubation in secondary DoxRb-HRP antibody (1:10,000) and Clarity Max, 189.130 s rapid autoexposure; B – Amido black staining after chemiluminescence detection.

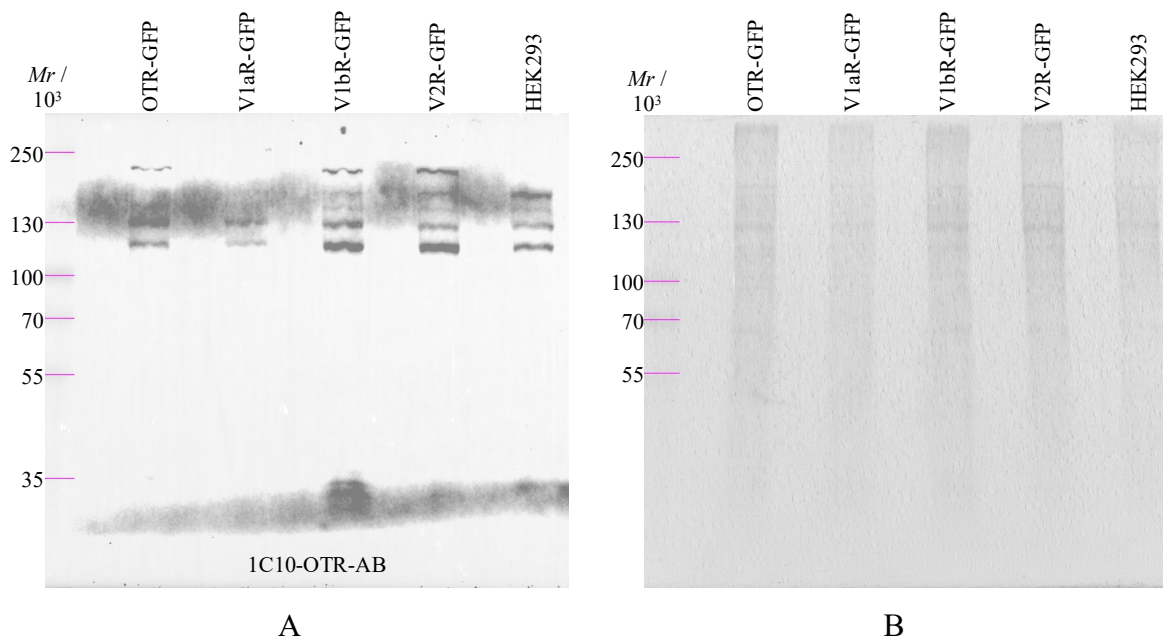


Figure A10. Specificity of primary 1C10 antibody (~1:1000) after incubation in secondary DoxRb-HRP antibody (1:10,000) and Clarity Max, 80 s manual exposure; B – Amido black staining after chemiluminescence detection.



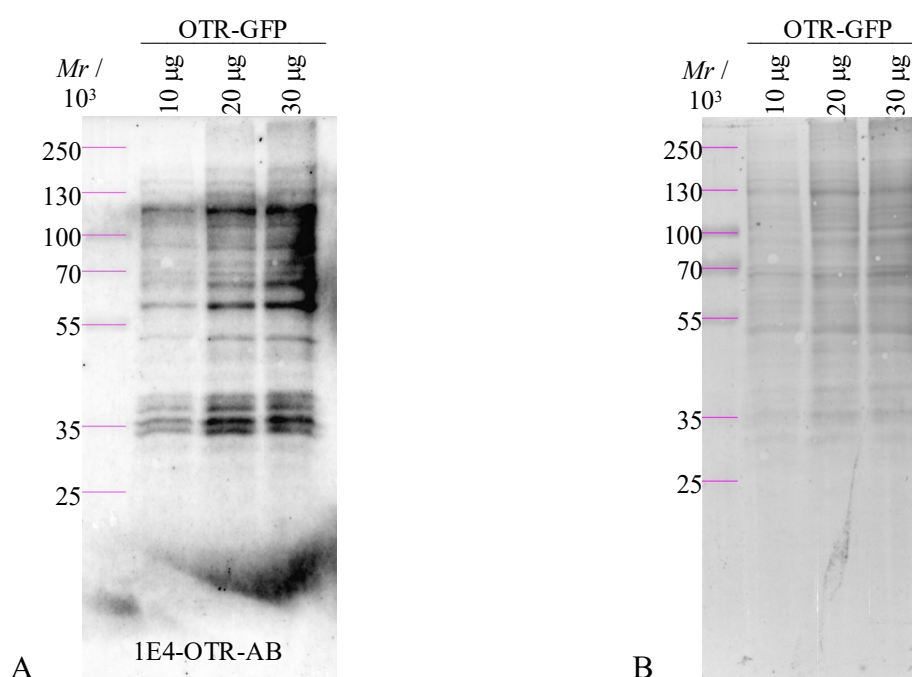


Figure A11. 1E4 antibody (~1:1000) signal dependence on OTR-GFP load after incubation in secondary DoxRb-HRP antibody (1:10,000) and Clarity Max, 338.204 s rapid autoexposure; B – Amido black staining after chemiluminescence detection.

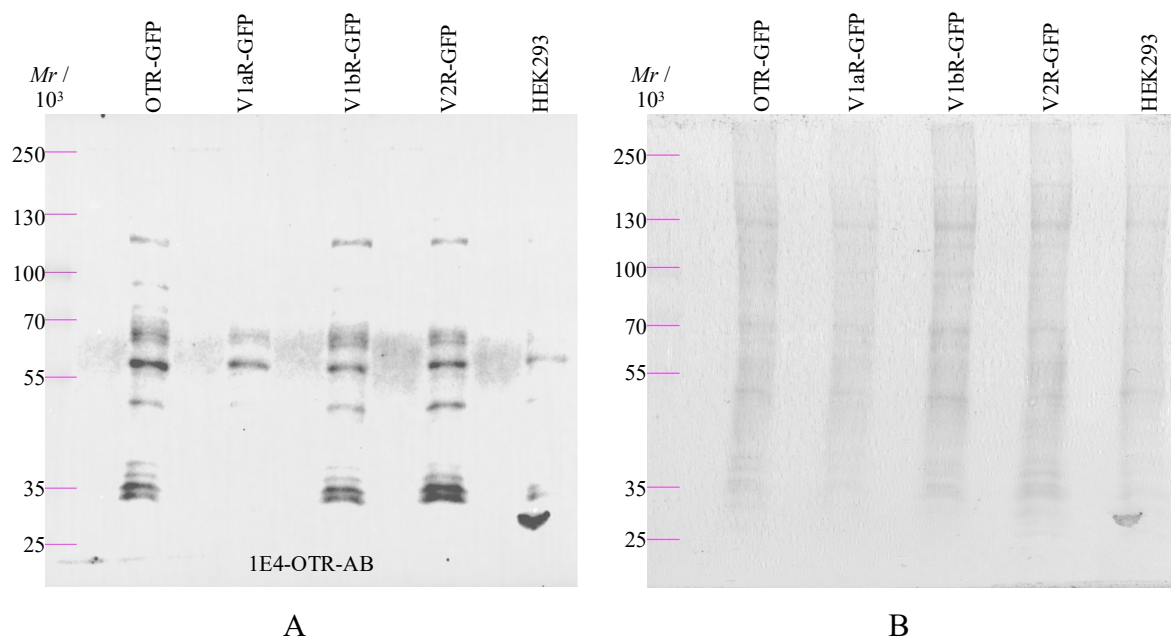


Figure A12. Specificity of primary 1E4 antibody (~1:1000) after incubation in secondary DoxRb-HRP antibody (1:10,000) and Clarity Max, 150 s manual exposure; B – Amido black staining after chemiluminescence detection.

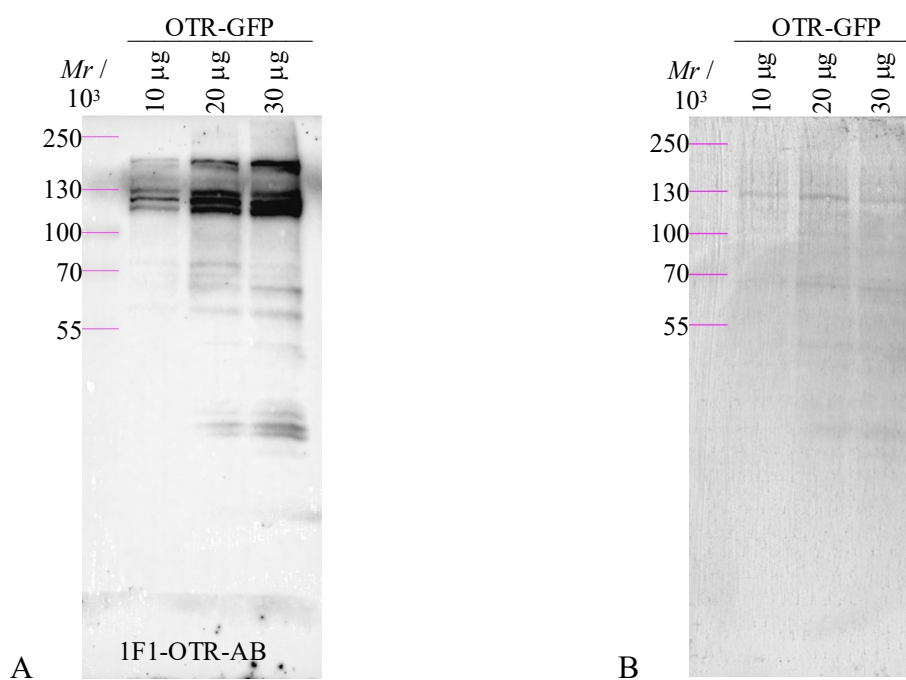


Figure A13. 1F1 antibody (~1:1000) signal dependence on OTR-GFP load after incubation in secondary DoxRb-HRP antibody (1:10,000) and Clarity Max, 77.773 s rapid autoexposure; B – Amido black staining after chemiluminescence detection.

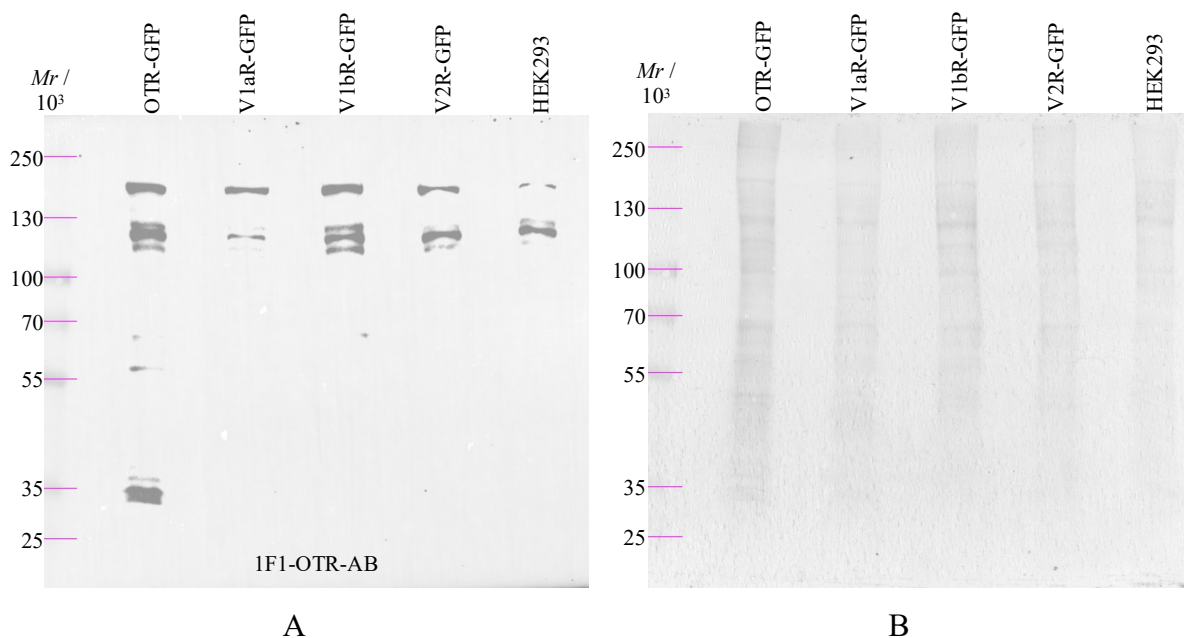


Figure A14. Specificity of primary 1F1 antibody (~1:1000) after incubation in secondary DoxRb-HRP antibody (1:10,000) and Clarity Max, 120 s manual exposure; B – Amido black staining after chemiluminescence detection.



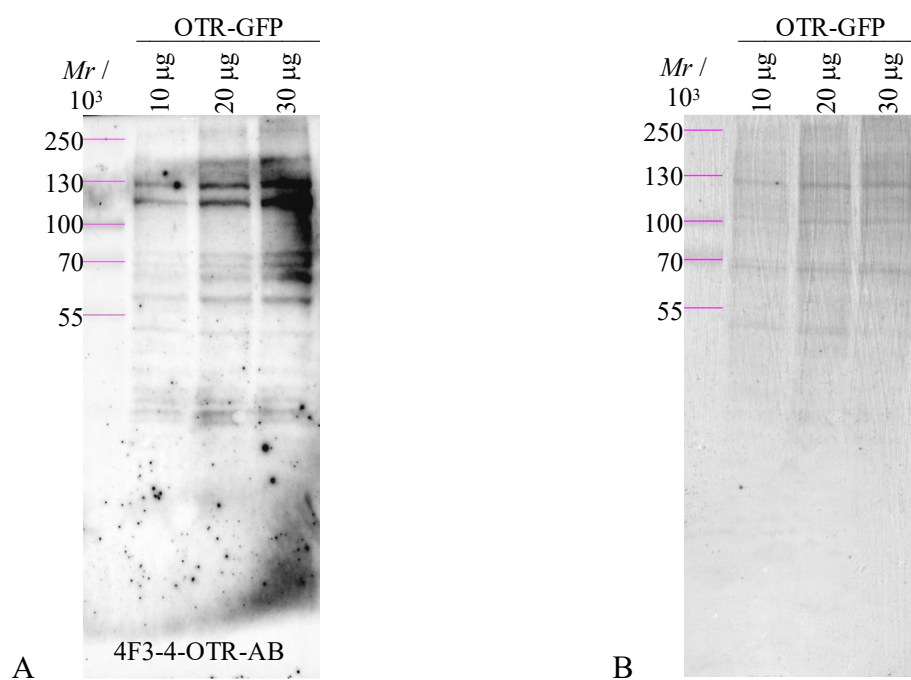


Figure A15. 4F3-4 antibody (~1:1000) signal dependence on OTR-GFP load after incubation in secondary DoxRb-HRP antibody (1:10,000) and Clarity Max, 145.701 s rapid autoexposure; B – Amido black staining after chemiluminescence detection.

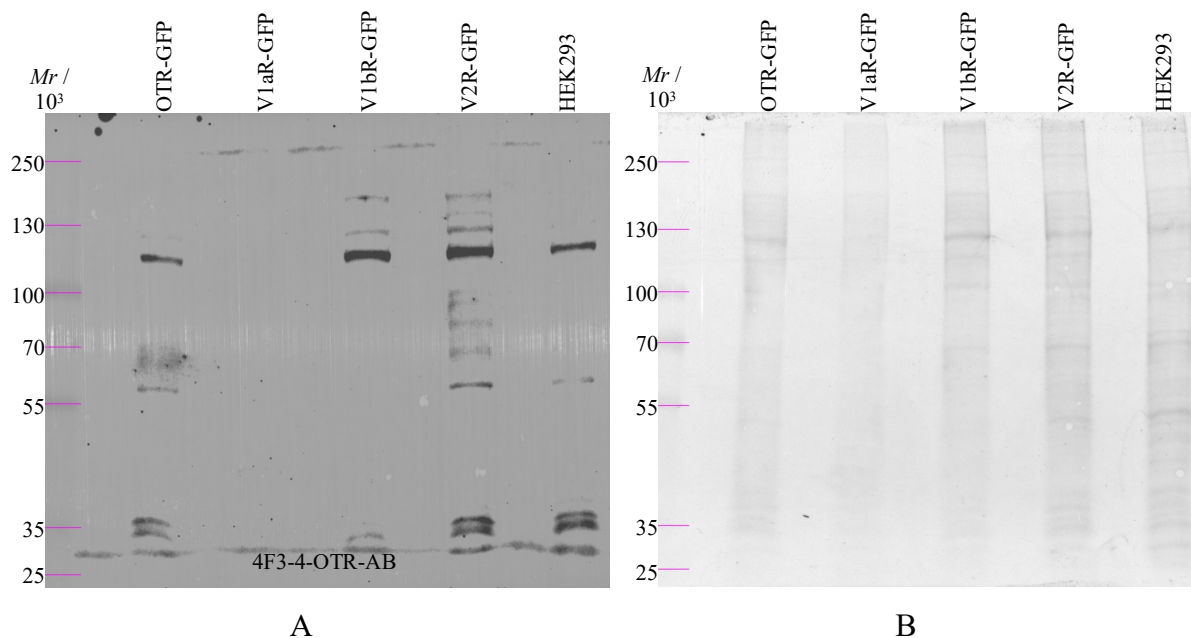


Figure A16. Specificity of primary 4F3-4 antibody (~1:1000) after incubation in secondary DoxRb-HRP antibody (1:10,000) and Clarity Max, 50 s manual exposure; B – Amido black staining after chemiluminescence detection.

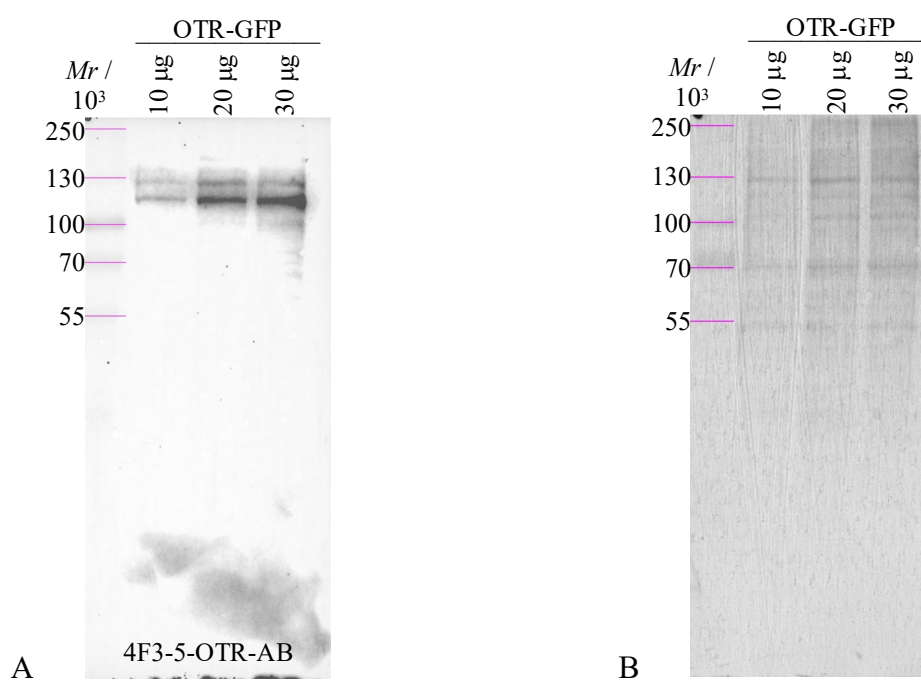


Figure A17. 4F3-5 antibody (~1:1000) signal dependence on OTR-GFP load after incubation in secondary DoxRb-HRP antibody (1:10,000) and Clarity Max, 40.509 s rapid autoexposure; B – Amido black staining after chemiluminescence detection.

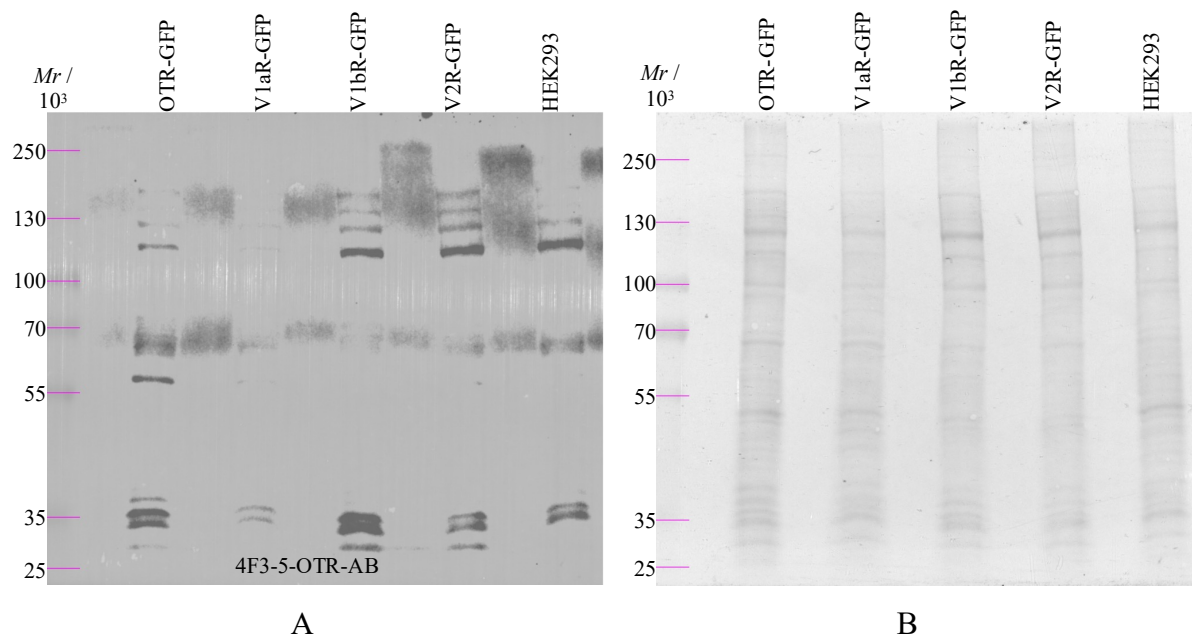


Figure A18. Specificity of primary 4F3-5 antibody (~1:1000) after incubation in secondary DoxRb-HRP antibody (1:10,000) and Clarity Max, 40 s manual exposure; B – Amido black staining after chemiluminescence detection.

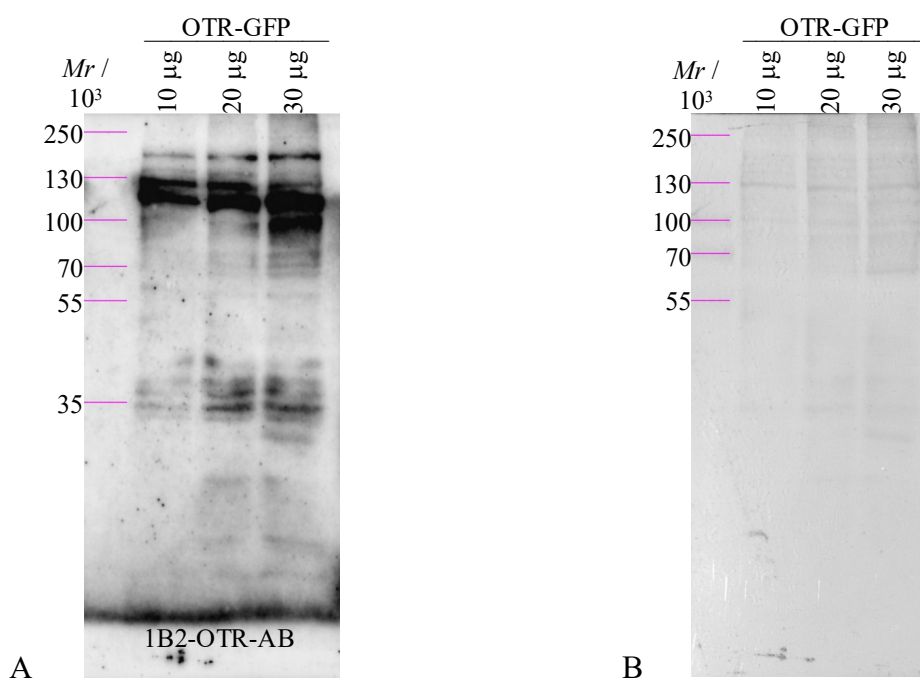


Figure A19. 1B2 antibody (~1:1000) signal dependence on OTR-GFP load after incubation in secondary DoxRb-HRP antibody (1:10,000) and Clarity Max, 218.506 s rapid autoexposure; B – Amido black staining after chemiluminescence detection.

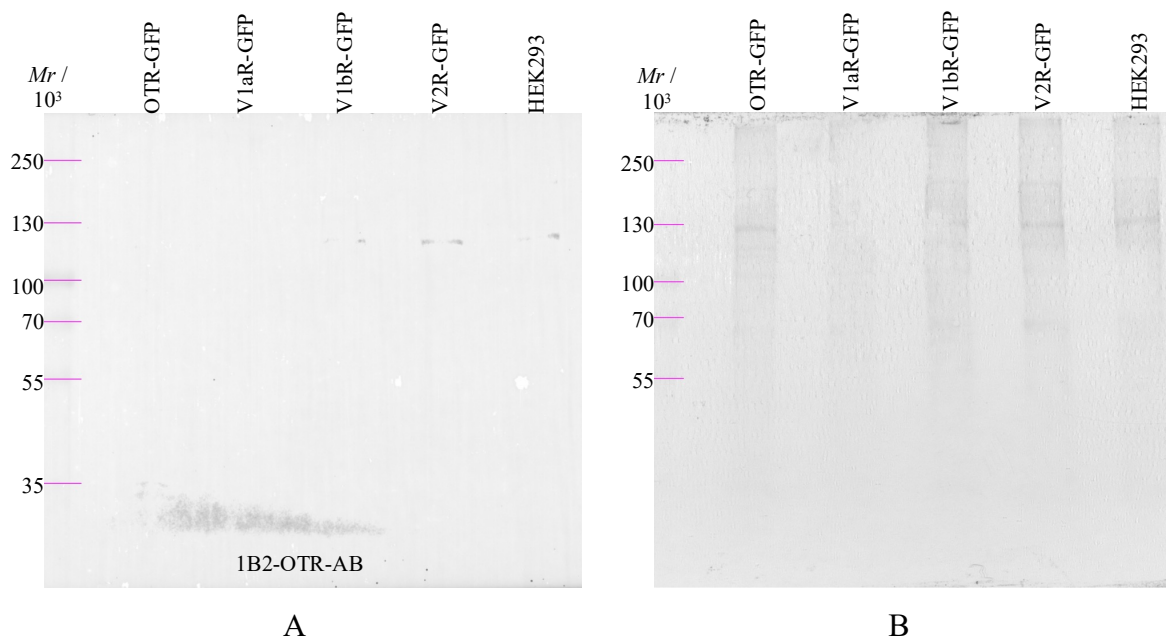


Figure A20. Specificity of primary 1B2 antibody (~1:1000) after incubation in secondary DoxRb-HRP antibody (1:10,000) and Clarity Max, 120 s manual exposure; B – Amido black staining after chemiluminescence detection.

## § 9. CURRICULUM VITAE

### Personal Information

Name and surname: Bojan Kuridža

Date of birth: 30 November 1998

Place of birth: Sisak, Croatia

### Education

2005–2013	Mate Lovrak Primary School – Kutina, Croatia
2013–2017	Tin Ujević High School – Kutina, Croatia
2017–2020	Undergraduate Study in Chemistry, Faculty of Science, University of Zagreb – Zagreb, Croatia
2022	Erasmus+ Studies, University of Vienna – Vienna, Austria
2022/2023	Erasmus+ Traineeship, Center for Biological Research Margarita Salas – Madrid, Spain
2023	Erasmus+ Traineeship, Institute of Parasitology and Biomedicine "López-Neyra" – Granada, Spain

### Honours and Awards

2022	Department of Chemistry Medal for excellent achievement during Studies in Chemistry
2022	Department of Chemistry Award for scientific research conducted by students in academic year 2021/2022

### Activities in Popularization of Science

2018	Day and Night at the Faculty of Science
2019	Day and Night at the Faculty of Science
2021	Day and Night at the Faculty of Science

### Scientific Publications

1. V. Rep, R. Štulić, S. Koštrun, B. Kuridža, I Crnolatac, M. Radić Stojković, H. Čipčić Paljetak, M. Perić, M. Matijašić, S. Raić-Malić, Novel tetrahydropyrimidinyl-substituted benzimidazoles and benzothiazoles: synthesis, antibacterial activity, DNA interactions and ADME profiling, *RSC Med. Chem.* **13** (2022) 1504–1525.